Studying the promotional effects of different metals on Pd catalysts for the selective hydrogenation of 1,3-butadiene

Master Thesis

S.M.J. (Sonja) Wilms

Daily supervisor:

MSc. Oscar Brandt Corstius

Examiners:

Prof. dr. Petra de Jongh

Dr. Jessi van der Hoeven

Date:

November 2021 - February 2023

Materials Chemistry and Catalysis

Debye Institute for Nanomaterials Science

Utrecht University

MCC Materials Chemistry and Catalysis

Utrecht University

Abstract

The current demand for mono-unsaturated hydrocarbons is large and it is expected that it will keep growing. To produce these alkenes more purely, selective hydrogenation is needed to remove small amounts of alkadiene or alkyne impurities in the stream. This is done by using supported Pd catalysts, which are very active for this reaction, but not as selective. To improve the selectivity of the catalyst, the Pd metal can be promoted or alloyed with other metals. The aim of this research is to study the effects of K, Mn, Cu, Zn and Ag promoters on Pd catalysts in the selective hydrogenation of poly-unsaturated hydrocarbons. To investigate this, the selective hydrogenation of a 1,3-butadiene impurity in a propylene feed is used as a model reaction.

A synthesis method has been established to prepare comparable promoted catalysts, namely sequential incipient wetness impregnation with a subsequent reduction. Promoted Pd catalysts are obtained with the desired mol ratio of promoter metal to Pd of 1:10. Electron Microscopy (EM) analysis showed that the metal nanoparticles have an uniform distribution over the support and the particles have a surface averaged particle size between 6 and 11 nm. With Temperature Programmed Reduction (TPR) analysis it was determined that Pd promotes the reduction of ZnO and possibly CuO, hence ZnO and potentially CuO are probably in close proximity to Pd. X-ray Diffraction (XRD) characterisation showed that there was a lattice contraction for the Mn, Ag, Zn and Cu promoted catalysts of 0.46, 0.51, 0.91 and 0.97%, respectively. This suggests that the metals might be incorporated into the Pd crystal lattice.

Overall, the monometallic Pd catalyst yielded the highest activity and total butene selectivity in the selective hydrogenation of butadiene. Only at room temperature, the K-Pd/C catalyst exhibited an increase in Turnover Frequency (TOF) from 25 to 41 s^{-1} compared to the Pd/C catalyst. Nevertheless, all catalysts still displayed a high activity (>100 s^{-1} at 90 °C) for the hydrogenation of butadiene in comparison to other metals. The Ag promoted catalyst exhibited the highest total butene selectivity among the promoted catalysts, which was just a little bit lower than the monometallic Pd catalyst. The Ag promoted Pd catalyst also showed a higher 1-butene selectivity than the monometallic Pd catalyst, both at low and high conversion levels. The Zn and Cu promoted samples also exhibit a higher 1-butene selectivity, in contrast to the K and Mn promoted samples, which showed a decrease at higher conversion. This effect on the 1-butene selectivity is explained by the isomerisation activity of the catalysts. The Pd catalyst displays a high isomerisation activity, while the Ag and Zn promoted catalysts show a significant lower 1-butene TOF over the whole temperature range (22-150 °C).

The (isomerisation) activity and selectivity were compared to the relative electronegativity (ΔEN), van der Waals radius (r_{vdw}) of the promoter metals and the XRD derived lattice contraction of each catalyst. The butadiene and 1-butene TOF did not seem to correlate with the ΔEN or the lattice contraction. However, when the promoter metal has a smaller r_{vdw}, both the butadiene and 1-butene TOF seem to increase. The r_{vdw} did also seem to have an influence on the selectivity to all butenes and 1-butene; the larger the promoter atom, the higher the selectivity. Using a promoter metal with a lower electronegativity seemed to increase the total and 1-butene selectivity. No distinct correlation is found between the lattice contraction and the selectivity.

Oxidation (O), reduction (R), oxidation-reduction (OR) and reduction-oxidation-reduction (ROR) pre-treatments (PTs) are performed before the catalytic test of the Mn promoted Pd catalyst. All PTs decreased the temperature that was needed to reach full conversion, compared to the catalyst that was not pre-treated. The ROR PT increased the butadiene conversion of the Mn-Pd/C catalyst at 25 °C from 20% to 50%. When an O or R PT was performed before catalysis, the catalyst activated during heating under reaction conditions. Finally, performing a R or ROR PT increased the total selectivity and a reducing PT as last step increased the selectivity towards 1-butene.

Table of contents

1. Introduction

Catalysis, especially heterogeneous catalysis, plays an important role in the chemical industry.[1–5] In approximately 90% of chemical processes a catalyst is required for at least one step in the process.[2,3] Furthermore, the majority of catalysts used in industry are heterogeneous catalysts. Therefore, heterogeneous catalysis is viewed as one of the pillars of the chemical and energy industry. Moreover, it will be important in the transition towards a more sustainable and carbon neutral chemical industry.[4,5] The production of chemicals accounts for about 25% of the industrial energy use and heterogeneous catalysts play a large role in these energy-intensive processes.[4] Accordingly, increasing the efficiency of heterogeneous catalysts will also lead to less energy consumption and reduction of the environmental impact of these large chemical processes.

One large process in chemical industry is the production of mono-unsaturated hydrocarbons. Currently, there is a significant demand for mono-unsaturated hydrocarbons, and this demand is still growing as well.[6–8] For example, propylene and ethylene are the two most important starting materials in petrochemical industry.[6–12] In 2021, the world consumption of propylene was 100 million tonnes and it is expected to grow to 135 million tonnes in 2025.[8] The produced chemicals ethylene and propylene are mainly used for the production of polyethylene and polypropylene plastics.[8–11,13–15] These plastics are used in a large variety of products such as, bottle caps, furniture, toys, diapers, tampons and more.[7,16] Moreover, ethylene and propylene are the building blocks for many other chemicals. Ethylene is used to produce polyvinyl-chloride, ethylene oxide, ethanol, acetaldehyde, vinyl acetate, ethylbenzene and propylene for propylene oxide, acrylonitrile and isopropyl alcohol.[7,13] The monomers are synthesized during the steam cracking of petroleum hydrocarbons, such as Naphta or LPG. This oil fraction is converted to a mixture of unsaturated hydrocarbons and small amounts of poly-unsaturated hydrocarbon impurities, like alkadienes and alkynes.[7–9,13–15,17–19] These impurities form during the cracking due to the harsh conditions, more specifically high temperature and high pressure.[7–9,13] The formation of these poly-unsaturated hydrocarbons is unfavourable since they irreversibly deactivate the catalysts needed for the downstream polymerization process, for example the Ziegler-Natta catalyst.[7,9–15,17,18,20–25] To minimize the catalyst deactivation in processes downstream, the alkadiene levels should be decreased to well below 10 ppm in the stream.[7,11,13,15,18,20,24] To remove the small amount of impurity from the main alkene stream, there are multiple solutions; remove the impurities by fractional distillation, extract the impurities with solvent extraction or with a zeolite or metal-organic framework.[7,9,11,13,17] Besides these solutions, the one that is applied the most because it is the most efficient, is selective hydrogenation.[7,9,11,13,15,24] In addition to the chemical industry, selective hydrogenation is also important in the pharmaceutical, agrochemical and food industry.[9,15,24,26] In selective hydrogenation, a catalyst will selectively convert the poly-unsaturated hydrocarbon impurities in the olefin mixture to mono-unsaturated hydrocarbons, without fully hydrogenating the alkenes towards alkanes, thereby removing the unwanted impurities from the olefin stream. There are two main side reactions in selective hydrogenation reactions: the over hydrogenation to alkanes and oligomerisation reactions.[9,11,13,15,27] The over hydrogenation to alkanes is unwanted because it will decrease the selectivity towards alkenes. Oligomerisation reactions are responsible for the formation of green oil, which is a precursor for solid coke. This coke will lead to activity loss because it will block the active sites on a catalyst, therefore the oligomerisation reaction is also an undesired side reaction of selective hydrogenation reactions.[7,9,11,27]

Palladium (Pd) based catalysts are known to have high activity and selectivity for selective hydrogenation reactions and are therefore widely used in industry.[6,12,22,28–30] However, these Pd catalysts usually have a poor long-term stability and show a limited selectivity,[9,14,28,31–33] especially at higher conversion levels.[7,24] To increase the selectivity of the catalyst, the Pd metal can be promoted or alloyed with other metals.[6,7,9,17,21,22,34] This will likely increase the selectivity, however most of the time also decrease the catalyst activity.[15,35] Therefore finding a catalyst for selective hydrogenation with both high activity and selectivity, is still of great interest in research today.[12,15,28,36] Two examples of Pd based alloyed catalysts are the Pd-Ag/Al_2O_3 and Lindlar Pd-Pb/$CaCO_3$ catalysts that are still widely used in industry, because they improve the alkene selectivity of Pd catalysts.[6,7,9,18,24,31,37] However, suitable alternatives for the Lindlar catalyst are being explored due to catalyst poisoning by lead and low Pd atom utilization efficiency.[15,31] Besides Ag and Pb, many components may be used to promote the Pd, for instance Na, K, C, Si, Fe, Mn, Co, Ni, Cu, Zn, B, S, Cr, Sn, Sb, Bi, Au, Ga, Ge and Tl have been reported to improve the Pd catalyst in some way.[6,9,21,24,28,38]

In this study we will focus on five promoter metals, K, Mn, Cu, Zn and Ag, and their effect on carbon supported Pd catalysts in a model selective hydrogenation reaction. The research will solely be focused on promoting effects, hence the molar ratio of metal to Pd will be kept constant at 1 to 10. The model reaction that is used, is the selective hydrogenation of 1,3-butadiene towards butenes in an excess of propylene, which is displayed in Figure 1. This reaction is not only an industrially relevant process, but also an interesting model-reaction for the study of catalysts in selective hydrogenation reactions.[19,34,39–41] It is desired to selectively hydrogenate 1,3-butadiene towards butenes without the over hydrogenation of the butenes to n-butane or the propylene to propane. Butenes that might form are 1-butene and its isomers cis-2-butene and trans-2-butene. An application of 2-butenes is the use as an alkylating agent for the production of high octane fuel.[6,7,10,13] However, 1-butene is the most desired butene specie, for instance as a monomer for the production of polybutene, as a co-monomer for the production of polyethylene and as a reagent in the synthesis of butyl alcohol and maleic anhydride.[6,7,10,11,13,42] Therefore, it is not only relevant to improve the overall selectivity of this reaction towards butenes instead of butanes, but also to look at the selectivity to 1-butenes versus 2-butenes and among the latter the selectivity towards cis-2-butene versus trans-2-butene. Besides the selectivity, it is also important to retain the high activity of Pd in this reaction.

In this work, first a theoretical background will be given on the selective hydrogenation of butadiene and the role of the catalyst support and Pd in this reaction. Additionally, the different promoting effects of K, Mn, Cu, Zn and Ag that are already known will be discussed. After this, the research aim and approach will be stated. Next, the experimental details of the synthesis method, characterisation techniques and catalytic tests will be given. In the results and discussion section, the promoting effect on selectivity, activity and isomerisation properties will be studied. Furthermore, correlations are made between the obtained catalyst activity and selectivity to promoter metal properties, such as the electronegativity and van der Waals radius. Additionally, the effect of performing a reducing or oxidizing pre-treatment on the promoted catalysts is looked into. Finally, the conclusion of the study and ideas for further research are stated in the outlook.

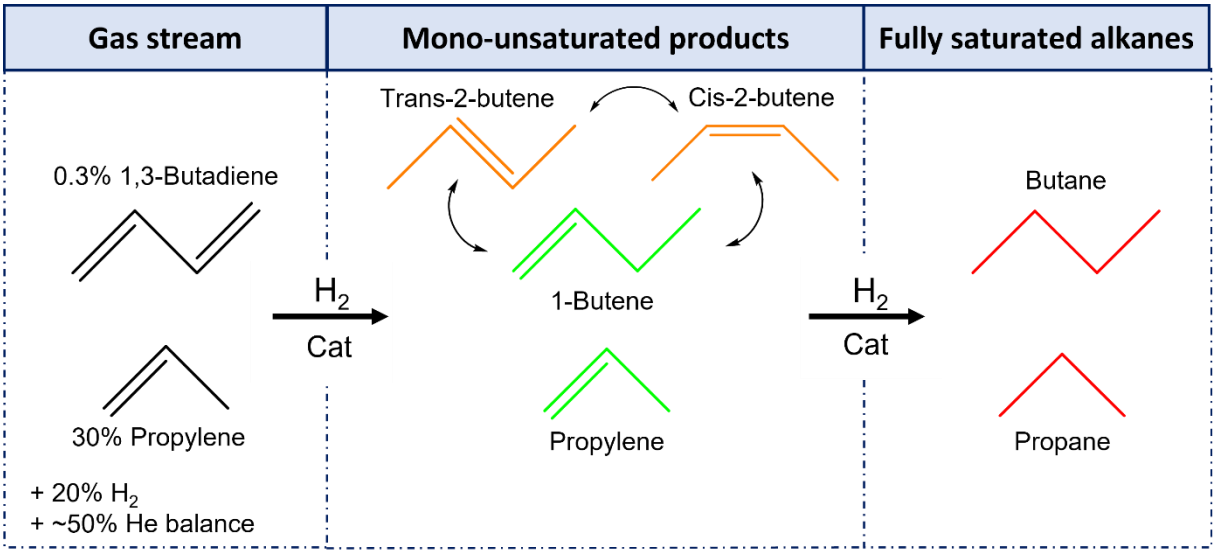

Figure 1: Model reaction used for this research; The selective hydrogenation of 1,3-butadiene to butenes in an excess of propylene. The gas stream consists of a small impurity of 1,3-butadiene, hydrogen, an excess of propylene and a helium balance. It is desired to produce the mono-unsaturated products; 1-butene and its isomers, trans- and cis-2-butene. The over hydrogenation of the alkenes to fully saturated alkanes is undesired.

2. Background

2.1 Selective hydrogenation of 1,3-butadiene

As stated in the introduction and displayed in Figure 1, in the selective or semi-hydrogenation of 1,3-butadiene it desired to selectively hydrogenate 1,3-butadiene to butenes without the hydrogenation of unsaturated hydrocarbons towards fully hydrogenated alkanes.[11,20,23,43] It was found that the activation energies for the hydrogenation of 1,3-butadiene to butenes by Pd is approximately 40-85 kJ/mol.[19,23,43] Three butene isomers might form during this reaction; 1-butene, cis-2-butene and trans-2-butene. The composition of the isomers is usually unchanged until 1,3-butadiene is fully consumed, which indicates that the reactant 1,3-butadiene is more strongly adsorbed on the catalyst surface than the butene products. This leads to reaction orders close to zero in 1,3-butadiene and first order in hydrogen.[23,43,44]

The selective hydrogenation of an alkadiene over a Pd catalyst follows the Horiuti-Polanyi mechanism, of which the mechanism of the hydrogenation of butadiene is displayed in Figure 2.[7,15,43,45,46] Butadiene species can exist in two conformations, syn and anti, and can also interconvert between these conformations. However, after the anti- or syn-butadiene is adsorbed on the surface, it is conformationally non-interconvertible. Therefore, the ratio of anti- and syn-butadiene in the gas mixture is the determining factor for the final ratio of cis- to trans-2-butene. In the gas phase and at room temperature, the preferred conformation of butadiene is anti, this conformation is 20 times more likely than the syn-conformation.[43,46] The 1,4-addition of hydrogen to the anti-conformation will lead to trans-2-butene and the syn-conformation to cis-2-butene.[7,43,45,46] Besides the 1,4-addition, the 1,2-addition of hydrogen to the anti- and syn-conformation will yield 1-butene. All butene species are primary products and isomerisation of the species on the catalyst surface does not occur. Moreover, the butene composition was not affected by the formation of butane.[43,46] Since the preferred conformation of gaseous butadiene at room temperature is anti, trans-2-butene formation will be dominant over cis-2-butene formation. The ratio of trans- to cis-2-butene can even be as high as 20 for Pd catalysts, but this ratio is expected to drop at higher temperatures. [7,43,45,46]

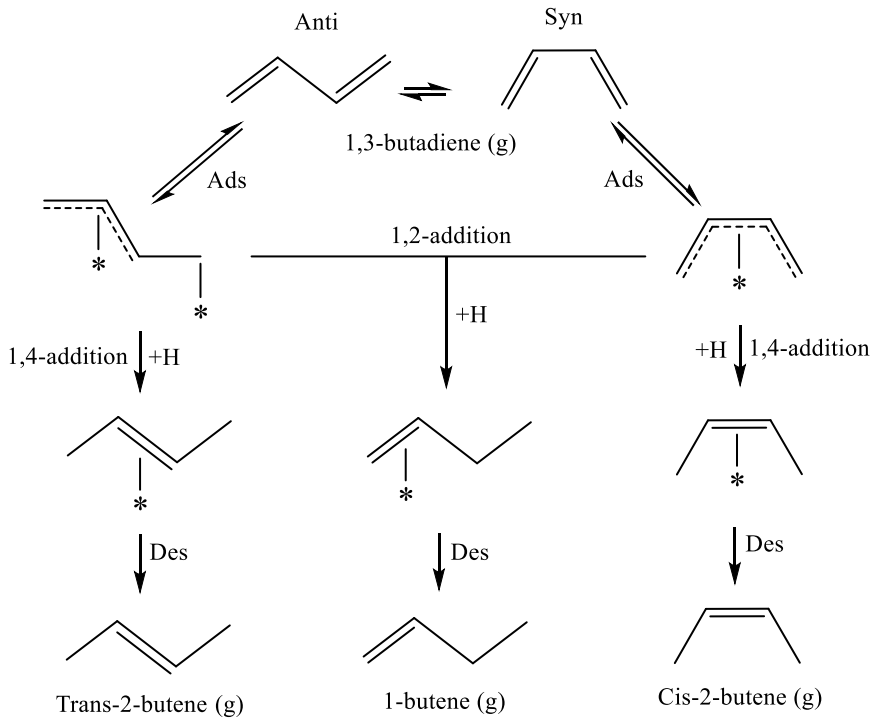

Figure 2: Mechanism of the selective hydrogenation of 1,3-butadiene on a Pd catalyst. Gaseous 1,3-butadiene exists in the anti- and syn-conformation. The 1,2- and 1,4-addition of hydrogen to the adsorbed anti-butadiene will lead to 1-butene and trans-2-butene formation, respectively. The 1,2- and 1,4-addition of hydrogen to the adsorbed syn-butadiene will lead to 1-butene and cis-2-butene formation, respectively. Adsorption is abbreviated as Ads and desorption as Des.

2.2 Pd as catalyst for selective hydrogenation

Pd has been widely applied in catalysts for selective hydrogenation reactions due to its high activity and relatively high selectivity in this process.[6,12,22,28–30] However, the selectivity of Pd catalysts in these reactions could still be improved,[9,14,28,31–33] especially at higher conversion levels.[7,24] Therefore, the possibility of promoting the Pd catalysts with other metals to improve the catalyst selectivity has been explored since the 1970s.[11,47] Besides adjusting the Pd catalyst, the use of a poison, like CO, in the feedstock may also increase the selectivity of the catalyst.[9,13,15]

Pd has been studied extensively in selective hydrogenation reactions and it was found that Pd could form both Pd hydrides (PdH_x) and Pd carbides (PdC_x).[9,11,27,48,49] Pd is able to absorb large amounts of hydrogen, even in Pd nanoparticles. Two phases of Pd hydrides have been reported, with α-PdH_x observed at low hydrogen pressures and β-PdH_x observed at high hydrogen pressures. In hydrogenation reactions, the β-PdH_x phase does show a higher activity, but also a lower selectivity to alkenes than α-PdH_x due to more over hydrogenation. Smaller Pd particles show less formation of hydrides and therefore higher selectivity as well.[9,11,27,35,48,49] The Pd carbide phase (PdC_x, where x is between 0 and 0.13) can be formed as well during the hydrogenation reactions with a hydrocarbon gas feeds around 100 °C. The phase decomposes again in hydrogen or oxygen atmosphere above 100 °C.[50] The formation of the PdC_x phase suppresses hydrogen absorption and therefore also PdH_x formation, which is favourable for the selectivity. However, the carbide phase has been correlated with a decrease in activity and stability of the Pd catalysts. This is probably because the carbon atoms in the PdC_x phase are able to involve in certain reactions and the phase was not favourable in the suppression of oligomerisation reactions.[11,27,48]

2.3 Choice of catalyst support

Pd nanoparticles are often deposited on a support to improve the dispersion of the Pd particles. Besides that, a support may influence the electronic structure of the Pd particles.[51] Therefore, the use of different catalyst supports may have an important influence on the catalyst performance.[9,15,51–53] In literature, inorganic oxides like titania, silica and alumina and carbonous supports are listed as good supports for Pd nanoparticles in selective hydrogenation reactions.[9,13,51] The support should not contain tiny pores as these might lead to the full hydrogenation towards alkanes and therefore a lower alkene selectivity. Furthermore, the support should be inert to products and reactants, to prevent side reactions from occurring. Finally, acidic groups on the support are unfavourable since these will result in more polymerisation reactions, which will decrease the catalyst selectivity and stability.[9,13]

In this research, Graphene Nanoplatelets (GNP) will be used as a support for the Pd catalysts. GNP is known for its high surface area and high pore volume, which is favourable for the synthesis method. Additionally, the carbon support has a high electrical and thermal conductivity and is chemically inert.[9,18,54] Besides that, research has shown that GNP is able to intercalate hydrogen, which resulted in a higher activity for the hydrogenation of ethylene. This was explained by the additional supply of hydrogen from GNP to the Pd particles. Moreover, the Pd hydride phase seemed to be more stable on a GNP support than on an activated carbon support.[55] Finally, the carbon support is easy to analyse with XRD and gives a good contrast in TEM making the catalyst characterisation easier.

2.4 Promotional effects on Pd

The selectivity of a Pd catalyst may be improved by three effects: a geometric, an electronic and a kinetic effect. A geometric effect may occur due to active site isolation, for example in a single atom alloy catalyst. By increasing the distance between Pd atoms and decreasing the Pd-coordination numbers, the adsorption of the alkene species is altered, leading to a different selectivity. An electronic effect might be obtained by alloying or promoting the Pd metal with other metals. This will lead to a modified electronic structure of the surface, which will change the properties of adsorption and desorption of the catalyst during a selective hydrogenation reaction. Alkenes are replaced by gaseous polyunsaturated hydrocarbons on the catalyst surface, before it will have the possibility to hydrogenate fully to alkanes. This will increase selectivity towards monosaturated hydrocarbons. Finally, there is the kinetic effect, which can be caused by alloying or promoting the Pd catalyst. This alloyed or promoted catalyst will dilute the Pd concentration and therefore restrain the Pd hydride formation, consequently

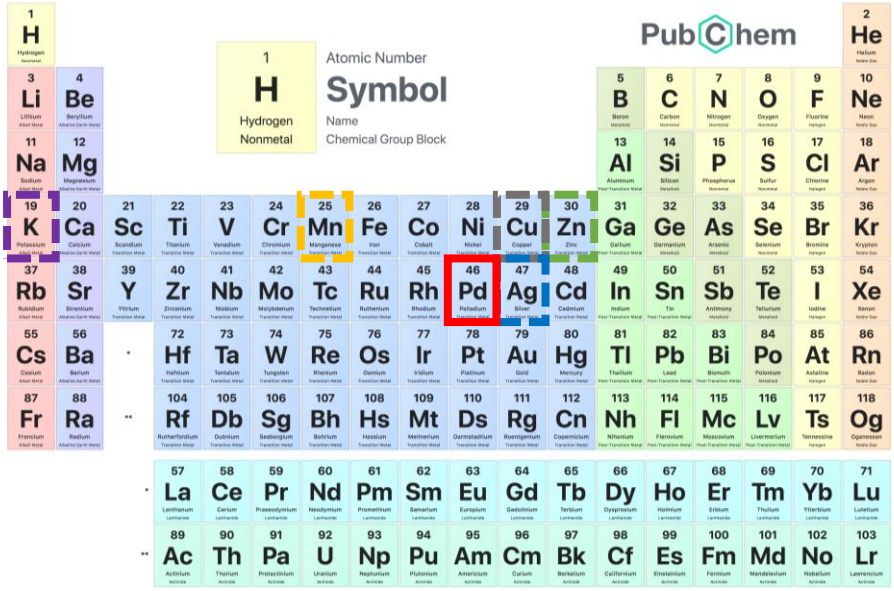

Figure 3: Periodic table of the elements. The Pd and all the promoter metals, K, Mn, Cu, Zn and Ag are highlighted in the figure.[56]

increasing the alkene selectivity. In this research, mainly electronic promoting effects are expected due to the low mol ratio of promoter metal to Pd (1:10).[9]

2.5 Promotional effect of promoter metals

Several studies were already published on the many different possible promoter metals. However, most of the promoted catalysts were studied in the selective hydrogenation of acetylene instead of butadiene. Besides that, many reported promoted catalysts that were studied had different ratios of promoter metal to Pd, most of the times high ratios. By having low promoter metal to Pd ratios, this study will hopefully give more insight into the promoting effects of K, Mn, Cu, Zn and Ag on Pd. The promoter metal's place in the periodic table are displayed in Figure 3.[56] According to the phase diagram, Ag is expected to form an alloy during the reduction treatment conditions and with metal molar ratios of 1 to 10 promoter metal to Pd.[57] Mn and Cu are not expected to form an alloy under these conditions, whereas Zn is believed to have the potential to form an intermetallic alloy with Pd.[15,58–61] No phase diagram was found for K-Pd. Nevertheless, one was found for lithium-Pd, which is not expected to form an alloy.[62] Since the lithium is an alkali metal from the first group like K, it is expected that K also does not form an alloy with Pd.

2.5.1 K

Research showed that 1B group transition metals, such as Cu and Ag, enhance the selectivity of Pd catalyst due to an electron donating character. Alkali metals would have an even stronger electron donating character.[37] Therefore, studying the potential of K as an electronic promoter for Pd might be interesting. A K promoted Pd catalyst has been studied in the selective hydrogenation of acetylene.[37] The 1 wt.% K- 1 wt.% Pd/Al_2O_3 catalyst (molar ratio of approximately 3:1 K:Pd) enhanced both activity and selectivity towards ethylene. However, it was found to increase the oligomer formation as well.[63] The addition of K was found to reduce the ethylene adsorption strength of the Pd due to electronic effects, thereby increasing the ethylene selectivity.[37] Besides this, using a K promoter on a Pt catalyst for the selective hydrogenation of 1,3-butadiene has also been studied and showed an increase in activity and selectivity due to a similar electronic effect as was seen for K promoted Pd catalyst in the selective hydrogenation of acetylene. However, this was only observed for a K surface coverage on Pt up to 0.4 monolayer. With a higher surface coverage, the activity and selectivity drop, possibly due to site blocking effects.[19]

2.5.2 Mn

Mn was studied as a promoter for Pd in Mn-Pd/Al_2O_3 catalysts (molar ratio of approximately 2:1 Mn:Pd) in the selective hydrogenation of acetylene and showed an increase in activity and selectivity. An increase of the

conversion of acetylene of around 20% was reported due to the addition of a Mn promoter. This was probably due to the changed hydrogen chemisorption and desorption properties of the Mn promoted catalysts. Besides this, the promoter will change the chemisorption properties of the Pd catalysts of acetylene, ethylene and ethane, which might also influence the activity and selectivity of the Pd catalyst.[64]

2.5.3 Cu

Monometallic Cu catalysts are decent catalysts for selective hydrogenation reactions.[24,39,65,66] Cu catalysts display high selectivity for the selective hydrogenation of 1,3-butadiene, but they exhibit significantly lower activity compared to Pd catalysts, by approximately 3-4 orders of magnitude. Besides that, the Cu catalysts require higher temperatures to achieve complete conversion. Furthermore, the Cu catalysts displayed poor stability in this reaction due to high oligomer formation.[24] Besides monometallic Cu catalysts, bimetallic Cu-Pd catalysts for selective hydrogenations of acetylene and 1,3-butadiene have been widely explored by many researchers.[10,12,17,22–24,67,68]

Cu-Pd/TiO_2 catalysts with molar ratios between 0.02-0.09 Cu:Pd displayed a higher selectivity compared to monometallic Pd/TiO_2 catalysts in the selective hydrogenation of acetylene. This improved selectivity is attributed to both an electronic and geometric effect. Unfortunately, the activity was decreased for these promoted catalysts.[22] In the selective hydrogenation of butadiene in an excess of 1-butene, Cu-Pd catalysts with a molar ratio of approximately 2 Cu:Pd showed a much higher selectivity towards butenes. This increase seems to be related to a decrease in the amount of hydrogen that is adsorbed onto the surface.[23] In another research it is stated that a higher selectivity is expected for Pd-Cu/Al_2O_3 catalysts (molar ratio of 1:3 Pd:Cu) compared to monometallic Pd catalysts. It was calculated with Density Functional Theory (DFT) that the adsorption energies of hydrogen and butenes over the bimetallic Pd-Cu (111) are lower than over the monometallic Pd (111), which indicates that the surface of the bimetallic catalyst should be more selective to butenes. Their experimental results confirmed these expectations as the bimetallic catalysts showed a higher selectivity to butenes. Besides that, the bimetallic catalysts showed a higher activity to the total of butenes and 1-butene at lower temperatures (<50 °C). They contribute this to both a geometric effect by Pd active site isolation and an electronic effect of an electron transfer of Cu to Pd.[10]

2.5.4 Zn

A PdZn/ZnO (1 wt.% Pd) catalyst of which the molar ratios are unclear (but it seems like an intermetallic 1:1 PdZn alloy has formed) has been reported for the selective hydrogenation of acetylene in an excess of ethylene. The catalyst is reported to reach a selectivity of ~90% at acetylene conversion of nearly 100% at reaction temperatures of 60 °C. The Pd active sites are said to be arranged in Pd-Zn-Pd intermetallic alloy ensembles, which will isolate the Pd active sites, making isolated Pd active sites. These single Pd active sites can easily dissociate hydrogen to active H species. The isolated sites have a weak bonding which promotes the desorption of ethylene of the surface and thereby suppresses the formation of ethane. Besides that, the sites have a moderate bonding mode for acetylene. This combination leads to high activity and selectivity.[28] The formation of PdZn alloys by hydrogenating Pd/ZnO catalysts was studied before by Tew et al.[32] The PdZn alloy started forming around 100 °C already and at 300 °C a crystalline 1:1 PdZn alloy is observed. This catalyst shows a decrease in the activity of 1-pentyne hydrogenation probably due to surface site dilution and increased particle size. However, it does show an increase in pentene selectivity, which is attributed to the changed electronic structure of the PdZn alloy, which is similar to monometallic Cu.[32] For a PdZn/ZnO catalyst (unclear molar ratio) in the selective hydrogenation of 1,3-butadiene in an excess of 1-butene, the surface coverage of hydrogen is reported to be lower. This results in an increase of butene selectivity and less butane formation. Moreover, the concentration of butadiene and butene adsorption sites has changed, which also leaded to a change in selectivity.[69]

2.5.5 Ag

Bimetallic Ag-Pd/Al_2O_3 catalysts have been used in industry since the 1980s. However, these catalysts usually consist of an excess of Ag compared to the Pd. This catalyst has been well studied, but since this research is about using low Ag to Pd ratios, the observed promotional effects might be different. The bimetallic industrially applied catalysts are said to supress the unwanted over hydrogenation to alkanes and also increase process selectivity. The Ag will modify the electronic properties of Pd by increasing the d-band electron density due to a charge

transfer from Ag to Pd. This electronic effect reduces the adsorption strength of ethylene, making is easier for ethylene to desorb from the surface.[9]

Ag-Pd/TiO_2 catalysts with a molar ratio of 0.64 Ag:Pd showed an increase in both activity and selectivity in the selective hydrogenation of acetylene. This was attributed to both an electronic and a geometric effect. More specifically, Ag is able to geometrically block large Pd ensembles on the surface which leads to a higher selectivity.[18] Besides, the use of Ag promote as a promoter was studied for bio-synthesized Ag-Pd/Al_2O_3 catalysts with 1:1 and 1:3 Ag:Pd molar ratios in the selective hydrogenation of butadiene. Both 1:1 and 1:3 Ag-Pd/Al_2O_3 catalysts exhibit a higher selectivity than the monometallic Pd/Al_2O_3 catalyst. This is contributed to a Pd active site dilution, which suppressed the over hydrogenation reaction towards n-butane. Furthermore, the Ag-Pd catalysts showed improved stability; the butadiene conversion decreased from 100% to 90% and the butene selectivity is almost unchanged after 50 hours on stream at 35 °C. This was attributed to an unchanged particle size and metallic state of Pd.[34]

2.6 Pre-treatments effects on a bimetallic system

Some of the promoter metals will form metal oxides in air at room temperature, even after a reduction treatment. To reduce the metal oxide another time just before the catalyst testing, a reducing pre-treatment can be performed. Moreover, the performance of a pre-treatment may lead to restructuring of bimetallic catalyst particles and therefore also lead to a change in the catalytic properties.[41,70,71] One study shows that a pre-treatment with an oxygen containing compound can improve the catalytic performance of bimetallic Pd-Ag catalysts in the selective hydrogenation of acetylene. A pre-treatment with O_2, CO or CO_2 will expose the Pd active sites in the PdAg alloy, which increases the acetylene conversion.[70] The aim of conducting an oxidative pre-treatment on the promoted catalysts utilized in this study, is to surface and expose either Pd or promoter atoms. Reduction-oxidation-reduction treatments are known for redispersion of the active metal to regenerate deactivated catalysts.[52] Therefore, this treatment could also alter the catalyst metal dispersion when performed as a pre-treatment.

Metallic Mn is not stable in air and the surface will oxidize to manganese oxide when being exposed to air after the reduction treatment.[72] That is why the pre-treatment effects will be studied on Mn promoted catalysts in this research, to hopefully see a change in activity or selectivity due to the difference of metallic Mn or Mn oxide in the catalyst. The reduction pre-treatment will (partly) reduce the Mn oxide again. On the other hand, the oxidation pre-treatment might bring the Mn oxide to the surface of the Pd particle. Combining the two might also have different effects on the catalytic properties. Moreover, performing a reducing pre-treatment might increase the amount of Pd hydrides on the surface and in the bulk of the catalyst, which would result in a higher activity. That is why oxidation (O), reduction (R), oxidation-reduction (OR) and reduction-oxidation-reduction (ROR) pre-treatments and their effect on activity and selectivity of the Mn promoted catalyst are investigated.

3. Aim & Approach of the research

The aim of this research is to study the effects of several promoter metals on Pd catalysts in the selective hydrogenation of poly-unsaturated hydrocarbons. In this study, the selective hydrogenation of a 1,3-butadiene impurity in a propylene feed is used as a model reaction. To get more insight into the different promoting effects of metals on Pd, several metals within the d-block and one alkali metal are studied, namely; K, Mn, Cu, Zn and Ag. Literature suggests that all these metals have the potential to promote Pd catalysts in selective hydrogenation reactions in some manner. By correlating changes in catalytic properties like activity and selectivity with metal properties such as electronegativity and atom size, it might be possible to attribute the observed changes to specific promoting effects. A better understanding of the promoting effects that positively or negatively impact the Pd catalyst, can aid in carefully choosing the appropriate promoter metal to optimize these effects.

First, a standard synthesis method has to be determined to prepare all bimetallic catalysts in the same manner and create comparable promoted catalysts. The heat treated catalysts are studied with Temperature Programmed Reduction (TPR) analysis, to study the reduction process and determine if the promoter atoms are in proximity to the Pd particles. The reduced catalysts are characterised using Electron Microscopy (EM) analysis techniques, mainly to determine the particle size of the Pd particles and the particle distribution on the support surface. X-Ray Diffraction (XRD) analysis is used to determine particle size as well, besides, the Pd crystal lattice contraction can be studied. The prepared catalysts are tested in a gas flow set up to compare the catalytic properties of the promoted catalysts in terms of activity and selectivity. Isomerisation tests are performed to study the isomerisation properties of 1-butene of each promoted catalyst. Lastly, the effect of performing a pre-treatment on the monometallic Pd and Mn promoted catalysts before the catalytic test is researched.

4. Experimental details

4.1 Catalyst preparation

4.1.1 Chemicals

The support that is used for the preparation of the catalysts, is Graphene Nanoplatelets (GNP) with a surface area of approximately 500 m^2/g (high purity grade, XG Sciences). The used precursor salts are $Pd(NH_3)_4(NO_3)_2$ (aq) (10 wt.% in H_2O, Sigma Aldrich), KNO_3 (s) (ACS reagent, ≥99.0%), Mn $(NO_3)_2 \cdot 4\ H_2O$ (s) (for analysis, Acros Organics), Cu $(NO_3)_2 \cdot 3\ H_2O$ (s) (99% for analysis, Acros Organics), Zn $(NO_3)_2 \cdot 6\ H_2O$ (s) (98% reagent grade, Sigma Aldrich) and $AgNO_3$ (s) (Laboratory reagent grade, Fisher Scientific).

4.1.2 Synthesis methods

Incipient wetness impregnation (IWI) is used to prepare the monometallic Pd catalysts, this method is depicted in Figure 4. In an IWI method, the carbon support is dried before the impregnation by heating it to 180 °C for 2 hours under vacuum. A 2 mL precursor solution is made by dissolving a Pd precursor salt in purified water (Milli-Q). The volume of precursor solution that is added is calculated to be the same as the pore volume of the support. The Pd precursor solution is added dropwise to the dry support with a needle, while under vacuum and being stirred with a stirring bar. After impregnation, the Pd catalysts are dried under vacuum for 18 ± 1.5 hours at room temperature. Additionally, the dried impregnated catalyst is heat treated to form a Pd pre-catalyst. Finally, this pre-catalyst is reduced to form the monometallic Pd catalyst.

There are two possible routes to prepare the promoted Pd catalysts, one of them is the co-IWI method which is indicated with the red arrow in Figure 4. In this method, first the support is dried as described for the Pd catalyst synthesis. The dried support is then impregnated with a 2 mL precursor solution containing two precursor salts, the Pd precursor salt and the promoter precursor salt. After the impregnation, the sample is dried as described above. Subsequently, the dried catalyst is heat treated and reduced to form a co-impregnated Pr-Pd/C catalyst.

The second method to prepare the promoted Pd catalysts is the sequential IWI method. In this method, the second impregnation is performed on a previously synthesized Pd (pre-)catalyst. The sequentially impregnated promoted catalyst can either be reduced via a conjointly or subsequent reduction method, which are both depicted in Figure 4 as the blue and green arrow, respectively. In the conjointly reduction method, the sequential impregnation is performed on a Pd pre-catalyst. After this second impregnation, the promoted Pd pre-catalyst is dried and heat treated again. Finally, the PdO and the promoter oxide will be reduced conjointly. In the subsequent reduction method, the second impregnation is performed on a reduced Pd catalyst. After which the promoted Pd catalyst is dried, heat treated and reduced once again. In Chapter 5.1, the determination of the best synthesis method for the preparation of the promoted catalysts will be discussed.

The different ratios of the metal salt and metal solution were combined to prepare various weight percentages (wt.%) of the promoters. All catalysts are prepared so that the catalyst would have 2 wt.% Pd and a 1:10 promoter to Pd mol ratio. To determine the heat treatment and reduction temperatures needed to treat the catalysts, literature was consulted and Thermo Gravimetric Analysis – Mass Spectrometry (TGA-MS) and Temperature Programmed Reduction (TPR) were performed to experimentally determine the right treatment temperatures

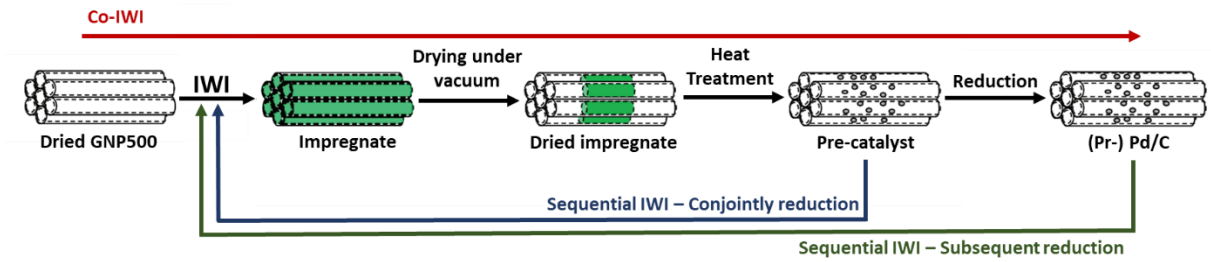

Figure 4: Description of incipient wetness impregnation (IWI) synthesis methods. A Pd/C catalyst is prepared by IWI followed by drying, heat treating and reduction. In the co-IWI method the dried carbon support is impregnated with a precursor solution containing both the Pd and the promoter precursor salt, then dried, heat treated and reduced to from Pr-Pd/C. To synthesize Pr-Pd/C with a sequential impregnation, a Pd pre-catalyst (conjointly reduction method) or a reduced Pd catalyst (subsequent reduction method) is impregnated, dried, heat treated and reduced.

per catalyst. All heat treatments are performed for 2 hours under a gas flow of 100 mL/min N_2. All the reduction treatments are performed under a gas flow of 90:10 mL/min N_2:H_2. In both treatments, the temperature ramp was between 0.5 to 3 °C/min.

4.2 Catalyst characterisation

4.2.1 Nitrogen Physisorption

A micromeritics TriStar II Plus Version 3.01.01 is used to determine the pore volume and BET surface area of the support and reduced Pd catalysts. It is important to know the pore volume of the synthesized Pd catalysts for the sequential incipient wetness impregnation to prepare the promoted catalysts. The samples are first dried at 150˚C under N_2 for 10 minutes before starting the analysis. The micro- and mesopore volumes are determined using the t-plot method.

4.2.2 TGA-MS

Thermo Gravimetric Analysis – Mass Spectrometry (TGA-MS) is performed on a PerkinElmer TGA 8000 coupled to a Hiden Analytical HPR-20 to study the decomposition of the metal precursor salts into metal oxides by analysing mass loss and product gasses that are formed during the heating. The samples are first dried at 100 ˚C for one hour and cooled down again to 30 ˚C before heating to 800 ˚C with a 5 ˚C/min under 100 mL/min argon flow. The following MS components listed with their corresponding mass-to-charge (m/z) ratios are monitored during the TGA-MS experiment: ammonia (17) water (18), nitric oxide (30), carbon dioxide (44) and nitrogen dioxide (46).

4.2.3 TPR

Hydrogen Temperature Programmed Reduction (TPR) is used to analyse the reduction process of heat treated catalysts and to determine the reduction temperature of the promoted catalysts. This is done by studying the hydrogen that is taken up by the sample during the heating program. All TPR measurements are performed on a Micromeritics AutoChem II 2920 apparatus with Thermal Conduction Detector. Approximately 40 mg of >75 µm sieved sample is used to avoid pressure drop. The sieved sample is transferred into a quartz tube reactor and embedded between small pieces of glass wool. First, the samples are dried by heating the oven to 120 °C with a heating ramp of 10 °C/min under an argon flow, for 15 minutes. The samples are then cooled down to room temperature before the measurement starts. The gas flow is switched to 5% hydrogen in argon and is equilibrated for 15 minutes. Subsequently, the temperature is increased to 700 °C with a ramp of 5 °C/min. Finally, the reactor is cooled down to room temperature under an argon flow.

After plotting the data, a TPR peak area (A_{TPR}) is obtained and with this area, the amount of H_2 uptake per gram catalyst is determined with Equation 1. In this calculation, a pressure (p) of 1 atm, room temperature (298.15 K) and a gas constant R = 82.05734 cm^3 atm K^{-1} mol^{-1} are used.[73]

$$Experimental\ value\ of\ H_2\ uptake\ per\ catatlyst\ \left(\frac{\mu mol}{g}\right) = \frac{p\ (atm) * A_{TPR}\ (\frac{cm^3}{g} STP)}{R\ \left(\frac{cm^3 * atm}{K * mol}\right) * T\ (K)}$$

Equation 1: The calculation of the experimental value of H_2 uptake per catalyst.

Besides this, an expected value of H_2 uptake per gram catalyst can be calculated with Equation 2. With the amount of sample used for the TPR experiment, the wt.% of metal (wt.% M) in the sample and the molecular weight of the metal (M_M), the amount of mol metal oxide is calculated. With this and the reaction mol ratios of H_2 to metal oxide, it is determined how much H_2 should be taken up by the metal oxide to fully reduce.

$$Expected\ value\ of\ H_2\ uptake\ per\ catatlyst\ \left(\frac{\mu mol}{g}\right) = \frac{wt.\%\ M}{M_M(\frac{g}{mol})} * molratio \frac{H_2\ (mol)}{metal\ oxide\ (mol)} * 10^6$$

Equation 2: The calculation of the expected value of H_2 uptake per catalyst.

4.2.4 XRD

A Bruker D2 Phaser 2nd Generation diffractometer X-ray diffraction (XRD) apparatus is used to perform powder XRD measurements on most calcined, reduced and in some cases dried catalysts. The apparatus has an X-ray

source of 30 kV and 10 mA, a 1 mm fixed slit, a 141 mm goniometer radius, a scattering screen 2 mm above the sample and a Lynxeye (1D mode) detector. The samples are irradiated with a Co-$K_{\alpha,1,2}$ source with a wavelength (λ) of 1.79026 Å. All samples are measured at room temperature at 2θ ranges 15-85° or 20-80°, while rotating at 15 rotations/min. The increment was set at 0.05 degrees/step and the time of steps between 0.9 and 3 s/step.

The XRD diffractograms are normalised to the peak intensity of the GNP diffraction peak at approximately 30.5 °2θ. The Pd crystallite size is calculated by applying the Scherrer equation (Equation 3)[74] to the Pd diffraction peak around 46.5 °2θ. The full width at half maximum (FWHM) of this Pd peak is used as line broadening (β) and the FWHM is obtained by fitting a Gaussian peak on the Pd peak at around 46.5 °2θ using Origin software. In the calculation, the shape factor of K= 1 for spherical crystals with a cubic symmetry and a X-ray wavelength for Co-$K_{\alpha,1,2}$ of λ = 1.79 Å are used.[74]

$$d_{XRD}(nm) = \frac{K * \lambda\,(m)}{\beta\,(\text{radians}) * \cos(\theta)(radians)} * 10^{-9}$$

Equation 3: The calculation of the Pd crystallite size (d_{XRD}).

The crystal lattice constant (a) of the Pd can also be determined from the XRD diffractograms. These are calculated with Braggs Law[75] (Equation 4):

$$a\,(\text{Å}) = \frac{\lambda\,(\text{Å})}{2\sin\left(\frac{1}{2} * 2\theta\right)(radians)} * \sqrt{h^2 + k^2 + l^2}$$

Equation 4: The calculation of the Pd crystal lattice constant (a) calculation with Braggs Law.

This equation is applied to the main diffraction peak of the Pd peak with a face-centered cubic (FCC) crystal structure with miller indices (hkl) = 111 at approximately 46.5 °2θ. For each promoted catalyst, the lattice contraction or expansion with respect to the monometallic Pd catalysts is determined with the calculated lattice constants.

When the sample is placed inaccurately in the XRD analysis, the X-ray beam does not converge at the right position which results in incorrect peak positions. This error in the data is called sample displacement. The sample displacement can be taken into account by using the following calculation, with Equation 5.[75] With this formula, it can be calculated where the peaks should be positioned instead of the position where they are observed. In this calculation, s is the amount of displacement, Δ2θ is the peak shift and θ is the position of the observed peak. R is the goniometer radius, which is 0.141 m in the used XRD apparatus.

$$\Delta 2\theta\ (^\circ) = \frac{-2s\ (m) * Cos(\theta)(^\circ)}{R\ (m)}$$

Equation 5: The calculation of the XRD peak shift (Δ2θ).

4.2.5 EM

Bright field Transmission Electron Microscopy (TEM) and High Angle Annular Dark Field (HAADF) imaging with Energy Dispersive X-ray (EDX) spectroscopy are used to study the nanoparticle size and distribution of both Pd and promoter on the carbon support. These experiments are performed on a FEI Talos F200X apparatus. The samples for EM measurements are prepared by depositing small amounts of catalyst sample onto a Cu sample grid, coated with holey carbon (Agar Scientific 300 Mesh Copper grid). Using ImageJ computer software, particle diameters are measured in EM images by measuring at least 200 individual particles on different sample areas. With this data the mean surface averaged particle size (d_{SA}) and their standard deviation (σ_{SA}) are calculated with Equation 6.[18] In this equation, n is the total number of measured particles and d_i displays the diameter of the i^{th} particle.

$$d_{SA}(nm) \pm \sigma_{SA}\,(nm) = \frac{\sum_{i=1}^{n} d_i^3\ (nm^3)}{\sum_{i=1}^{n} d_i^2\ (nm^2)} \pm \sqrt{\frac{1}{n}\sum_{i=1}^{n} (d_{SA}(nm) - d_i\,(nm))^2}$$

Equation 6: The calculation of the mean surface averaged particle size (d_{SA}) and their standard deviation (σ_{SA}).

$$N_{monolayer} = \frac{A_{Pr}\ (nm^2)}{A_{Av,Pd}\ (nm^2) * N_{Pd\ atoms}}$$

Equation 7: The calculation of the number of monolayers that a promoter can form on the Pd surface.

Besides that, the number of monolayers that a promoter metal can form on the Pd surface ($N_{monolayer}$) can be calculated with the data (Equation 7). In this formula, the area of each promoter atom (A_{Pr}), the average area of all EM measured Pd atoms ($A_{Av,Pd}$) and the number of Pd atoms in the sample ($N_{pd\ atoms}$) can be calculated with Equation 8, Equation 9 and Equation 10 respectively. The van der Waals radius of each metal ($r_{vdw,Pr}$) used in Equation 8 is calculated using Equation 12. In the calculations with Equation 10, the amount of Pd that is in the catalyst is derived from how much Pd precursor salt is added during the synthesis. The density of Pd (ρ_{Pd})that is used for the calculations is 12.02 g/cm^3.[72] The average volume of all EM measured Pd atoms ($V_{Av,Pd}$) that is used in Equation 10, can be calculated with Equation 11. In Equation 9 and Equation 11, n also displays the total number of particles measured with TEM and $r_{Pd,i}$ is the radius of the ith Pd particle.

$$A_{Pr} = 4\pi * r_{vdw,M}\ (nm^2)$$

Equation 8: The calculation of area of each promoter atom.

$$A_{Av,Pd} = \frac{\sum_{i=1}^{n} 4\pi * r_{Pd,i}^2}{n} (nm^2)$$

Equation 9: The calculation of the average area of all EM measured Pd atoms.

$$N_{Pd\ atoms} = \frac{Amount\ Pd\ in\ catalyst\ (g)}{\frac{\rho_{Pd}\ (\frac{g}{nm^3})}{V_{Av,Pd}(nm^3)}}$$

Equation 10: The calculation of the number of Pd atoms in the catalyst sample.

$$V_{Av,Pd} = \frac{\sum_{i=1}^{n} \frac{4}{3}\pi * r_{Pd,i}^3}{n}\ (nm^3)$$

Equation 11: The calculation of the average volume of all EM measured Pd atoms.

The van der Waals radius of each metal ($r_{vdw,M}$) can be calculated with Equation 12. This calculation changes for each crystal structure due to the shape of the unit cell and the number of atoms in the unit cell. Pd, Ag and Cu exhibit a face-centered cubic (FCC), Mn a body-centered cubic (BCC) and Zn a hexagonal close packed (HCP) crystal structure.[72] For each crystal structure x and y can be filled in from Table 1 and with those, the van der Waals radius of the metal can be calculated. It should be noted that FCC and HCP have the same packing density, so to calculate $r_{vdw,M}$ of a HCP crystal lattice, the FCC parameters can be used. In the formula, the molecular weight of the metal (M_M), density of the metal (ρ_M) and Avogadro's number (N_a) are used.[72] For the K promoted catalysts, the ionic radius is used for the calculation of $N_{monolayer}$, since K is present as KNO_3 or K^+.[72]

$$r_{vdw,M}\ (nm) = x * \sqrt[3]{y * \frac{M_M\ (\frac{g}{mol})}{\rho_M\ \left(\frac{g}{cm^3}\right) * N_a\ (mol^{-1})}}$$

Equation 12: The calculation of the van der Waals radius (r_{vdw}) of each metal.

	FCC	BCC
x	$\frac{1}{\sqrt{8}}$	$\frac{\sqrt{3}}{4}$
y	4	4

Table 1: Variables x and y for Equation 11 for different crystal structures, face-centered cubic (FCC) and body-centered cubic (BCC).

4.3 Catalytic testing

4.3.1 Standard catalytic test

To study catalysts in the selective hydrogenation of poly-unsaturated hydrocarbons, the selective hydrogenation of a 1,3-butadiene impurity in a propylene feed is used as a model reaction. A gas flow set up with a Pyrex plug flow reactor with an internal diameter of 4 mm is used to study the catalytic properties of each (promoted) catalyst. The oven temperature and reactor temperature are measured during the tests.

The reactors are filled with an amount of catalyst that contains approximately 0.6 µg of Pd, but the exact amount of Pd in each reactor can be found in figure descriptions. Every catalyst is hundred times diluted with GNP and sieved at a 38-75 µm fraction to minimize the internal diffusion limitations. Besides the catalyst, around 300 mg Silicon Carbide (SiC) is used as a thermal dilutant to prevent hot spots from developing.

The reactor is placed inside an oven, which allows for a good temperature control. A thermocouple is placed in close proximity to the catalyst bed, which will monitor the temperature of the catalyst bed. The total gas flow is kept constant at 50 mL/min, which corresponds to a Gas Hourly Space Velocity (GHSV) of approximately 20000 h^{-1}. In a standard catalytic test, this gas feed consists of 0.3% 1,3-butadiene, 30% propylene, 20% H_2 and the rest is balanced by helium gas. The gas flows are controlled by EL-FLOW Bronkhorst mass flow controllers. The gas outlet is connected to a Thermo Scientific Trace 1300 gas chromatograph (GC), which analyses the product gas feed and provides a measured signal intensity of each gas. The temperature ramp used is always 0.5°C/min, except for the Mn-Pd/C catalyst, which has a heating temperature ramp of 0.75 °C/min. Before each test, the gas flow is analysed on bypass to obtain a reference for the gas concentration in ppm. This value will be used in calculations to account for the impurities in the gas feed.

Each monometallic promoter catalyst that does not contain any Pd is tested as reference on the catalytic setup to establish that the promoter metal does not show any activity in this reaction without the Pd. For these reference catalysts, the amount of promoter metal is kept roughly the same as in the promoted Pd catalysts.

Activity calculations

The catalyst activity is discussed in terms of conversion and Turnover Frequency (TOF). The conversion is calculated via Equation 13.

$$Butadiene\ Conversion\ (\%) = \left(1 - \frac{C_{t,bd}(ppm)}{C_{0,bd}(ppm)}\right) * 100\%$$

Equation 13: The calculation of the butadiene conversion.

In this equation, $C_{t,\ bd}$ is the concentration of butadiene at a certain time, and $C_{0,\ bd}$ is the bypass analysed concentration of butadiene. This equation calculates the amount of butadiene that is converted with respect to the reference starting butadiene concentration that was measured. The conversion of propylene is calculated in a similar matter, but with propylene concentrations.

The Turnover Frequency (TOF) is defined as the amount of mol butadiene that is converted per mol surface Pd atoms per second and is calculated by Equation 14.[18] By using TOF, the particle size and amount of Pd in the reactor are taken into account, therefore making the comparison between all catalysts more straightforward.

$$TOF\ (s^{-1}) = \frac{Conv.butadiene\ (\%) *\ 0.3\% * Tot.gas\ flow\ (L\ s^{-1}) * p\ (atm) *\ D\ (\%)}{R\ (\mathrm{L\ atm}\ K^{-1}\ mol^{-1}) * T_{room}(K)} * \frac{M_{Pd}(\frac{g}{mol})}{Pd_{in\ reactor}\ (g)}$$

Equation 14: The calculation of the Turnover Frequency (TOF).

$$D\ (\%) = Dispersion\ (\%) = \frac{1.112\ (nm)}{d_{SA}\ (nm)}$$

Equation 15: The calculation of the dispersion (D) of atoms in a Pd particle.

In this calculation, the amount of mol butadiene that is converted, is calculated by multiplying the conversion of butadiene with the total amount of butadiene gas flow. The total amount of butadiene gas flow is calculated with the knowledge that 0.3% of the total gas feed consists of butadiene. It is assumed that the pressure (p) in

the lab is 1 atm and that the temperature is equal to room temperature (293.15 K). A gas constant of R=0.082 057 338 $\mathrm{L\ atm}\ K^{-1}\ mol^{-1}$ and M_{Pd}=106.42 g/mol are used for the calculation. The amount of Pd surface atoms is determined by calculating the dispersion of the catalyst particles. The dispersion (D) calculates the fraction of Pd atoms that are on the surface of the Pd particle and is defined as 1.112 divided by the surface averaged particle size (d_{SA}), see Equation 15. The number 1.112 is derived from a calculation involving the volume occupied by an atom in bulk metal (14.70 $Å^3$ for Pd) and the area occupied by a surface atom (7.93 $Å^2$ for Pd).[76]

Selectivity calculations

The selectivity is explained by three terms, the selectivity of product p, the (total) selectivity of butenes and the C4-selectivity of product p. The selectivity of a product p (S_p) is defined as the fraction of the product p in the product gas stream, see Equation 16. The total gas stream is all of the C4 products plus the product propane. The selectivity of butenes is defined as the sum of the selectivity of all the butenes, as can be seen in Equation 17.

$$Selectivity\ of\ p = S_p(\%) = \left(\frac{C_p\ (ppm)}{C_{c4\ products}(ppm) + C_{propane}(ppm)}\right) * 100\%$$

Equation 16: The calculation of the selectivity of a product p (Sp).

$$Selectivity\ of\ butenes\ (\%) = S_{1-butene} + S_{trans-2-butene} + S_{cis-2-butene}$$

Equation 17: The calculation of the selectivity of butenes.

The C4 selectivity of a product p is defined as the fraction of the product p in the C4 gas stream. The C4 gas stream in this case consists of 1-butene, cis- and trans-2-butene and n-butane. The C4 selectivity to a product p is explained by Equation 18.

$$C4\ selectivity\ of\ p\ (\%) = \left(\frac{C_p\ (ppm)}{C_{c4\ products}(ppm)}\right) * 100\%$$

Equation 18: The calculation of the C4 selectivity of a product p.

4.3.2 Isomerisation testing

Isomerisation tests are performed to study the isomerisation properties of each promoted and monometallic Pd catalyst. The isomerisation activity and selectivity of each promoted catalyst might give us more information on the hydrogenation mechanism of butadiene. The same catalytic gas flow set-up is used, but the gas feed mixture of butadiene and propylene is changed to a 1-butene gas feed. The catalysts will isomerise the 1-butene towards cis-2-butene and trans-2-butene or hydrogenate to n-butane. Here, the total gas flow is kept constant at 50 mL/min. The isomerisation gas feed consists of 0.3% 1-butene, 5% H_2 and a He gas is used as balance. The rest of the isomerisation test is similar to the standard catalytic test that is described above. The conversion of 1-butene is calculated the same as for butadiene as explained in Equation 12 only then with the 1-butene concentrations. The TOF is also calculated in a similar way as Equation 13 describes, but then with the 1-butene conversion instead of the butadiene conversion. The selectivity calculations are also similar and the selectivity of an isomerisation product p is calculated via Equation 15. The fraction of a specific product in the isomerisation products stream is determined with Equation 17.

4.3.3 Pre-treatments

In a standard catalytic test with butadiene, no pre-treatment (PT) is performed before the test. However, the use of different PTs, and especially their effect on a Mn promoted catalyst, is also studied in this research. The pre-treatments are performed by heating the catalyst in the reactor at 300 °C for one hour with a 5 °C/min temperature ramp under either a gas flow of 30 mL/min of either H_2 for reduction or O_2 for oxidation. Four different PTs are researched; oxidation (O), reduction (R), oxidation-reduction (OR) and reduction-oxidation-reduction (ROR) PTs. After the pre-treatments, the sample is cooled down again to 25 °C and is flushed with 30 mL/min N_2 gas before the standard butadiene catalytic test is performed.

5. Results & Discussion

5.1 Determination of synthesis method

To be able to study the promotional effect of several metals, a standard synthesis method has to be determined to prepare all bimetallic catalysts in the same manner. To prevent any particle size effects in catalysis, it is desired to have a similar average particle size in all of the catalysts. Therefore, the goal of studying the synthesis method is to find the synthesis method that can prepare a bimetallic catalyst with average particle size that is comparable to the mono-metallic Pd catalyst. The monometallic Pd catalyst, reduced at 500 °C, had an average particle size of 4.5 ± 1.4 nm (Pd_S/C) .

First, bimetallic Mn-Pd/C catalysts were prepared using both a co- and sequential-impregnation method with a heat treatment and reduction step performed at 600 °C and 450 °C, respectively. These catalysts were characterised with TEM analysis and the mean particle size was determined for both methods, see Table 2. By using the sequential-impregnation method, particles were obtained with an average size of 10.0 ± 3.2 nm. This is much larger than the monometallic Pd catalyst. However, the 13.8 ± 3.8 nm particles of the co-impregnated catalyst was even larger. Hence, the sequential impregnation method is more favourable than the co-impregnation method.

Within the sequential impregnation method, there are also two ways in preparing the catalyst. A conjointly-reduction or a subsequent-reduction may be used to reduce the metal oxides. To study the influence of the reduction method, sequentially impregnated and subsequent reduced catalysts were prepared to compare to the sequentially impregnated and conjointly-reduced catalyst. The subsequent reduction synthesis led to a mean particle size of 6.4 ± 1.8 nm, which is closer to 4.5 nm, the particle size of the monometallic Pd catalyst, than the conjointly reduced sample. However, the heat treatment and reduction temperatures were also different so the differences in particle size will more likely relate to that. But since the sequential impregnation with subsequent reduction method led to more similar particle sizes to the monometallic Pd catalyst, this method was considered as the best synthesis method to prepare bimetallic catalysts in this study.

	IWI method	Reduction method	T_{HT} (°C)	T_{red} (°C)	$d_{SA} \pm \sigma_{SA}$ (nm)
Mn-Pd/C	Co-	Conjointly	600	450	13.8 ±3.8
Mn-Pd/C	Sequential	Conjointly	600	450	10.0 ± 3.2
Mn-Pd/C	Sequential	Subsequent	250	560	6.4 ± 1.8

Table 2: A comparison between two different Incipient Wetness Impregnation (IWI) methods (co and sequential) and two different reduction methods (conjointly and subsequent); the corresponding heat treatment (T_{HT}) and reduction (T_{red}) temperatures used in the synthesis, the TEM obtained surface averaged particle size (d_{SA}) and standard deviation (σ_{SA}).

Nevertheless, during the synthesis of several catalysts, the obtained mean particle size was still much larger than was desired. This was due to the fact that the reduction temperatures used to reduce the promoter metals were higher than the reduction temperature of the monometallic Pd catalyst, which was 500 °C. To overcome this problem, a monometallic Pd catalyst is prepared using a similar reduction temperature as the highest reduction temperature used to prepare a promoted catalyst (600 °C). This yielded a monometallic Pd catalyst with a larger mean particle size (d_{SA} = 10.9 ± 3.1 nm), named Pd/C.

Since the decomposition of KNO_3 only occurs at very high temperatures (~750°C) under oxygen,[77–79] it is decided to not try to decompose the precursor salt with a heat treatment and just study the promotion of the impregnated and dried KNO_3 on Pd. Furthermore, following the usual synthesis steps (in light) when preparing the Ag-Pd catalysts resulted in very large (~50-140 nm) Ag particles due to the silver precursor that is easily reduced by photons. Therefore, the synthesis of the Ag promoted Pd catalyst is performed in the dark as much as possible. Besides this, the Ag precursor salt was impregnated on a oxidized Graphene Nanoplatelets (oxC) supported Pd catalyst (d_{SA} = 4.3 nm). The oxC support is chosen because the extra surface groups[38] decrease the mobility of the silver particles on the support, and thereby result in less sintering of these particles. The carbon support is oxidized at 80°C for 2 hours with 65% HNO_3 (aq) and the Pd catalysts are synthesized with this support. The oxidation and the synthesis of the oxGNP supported Pd catalysts were performed by Oscar Brandt Corstius.

5.2 Characterisation of the prepared catalysts

Two monometallic Pd catalysts were prepared using an incipient wetness impregnation (IWI) method, one with a small (Pd_S/C) and one with a large (Pd/C) surface averaged particle size. With these Pd catalysts, the promoted Pd catalysts were synthesized using a sequential IWI with subsequent reduction method. In Table 3, it is listed on which Pd catalyst each of the prepared promoted catalysts have been impregnated and the amount of Pd and promoter (Pr) that are present in each catalyst. The Mn and Zn promoted catalysts have been sequentially impregnated on the Pd_S/C catalyst (d_{SA} = 4.5 nm), while the K and Cu promoted catalysts have been sequentially impregnated on the Pd/C catalyst (d_{SA} = 10.9 nm). As stated in the previous chapter (5.1), the Ag promoted catalyst has been synthesised on a Pd/oxC catalyst (d_{SA} = 4.3 nm). Besides that, the resulting mol ratio of Pr to Pd per catalyst is listed. The desired mol ratio of Pr to Pd was 0.1, and as can be seen in Table 4, this mol ratio was accomplished for each catalyst. The heat treatment and reduction temperatures that were used in the preparation of the catalysts is specified.

All catalysts were characterised with TEM, see Figure 5a-f. These images show that the particles are distributed uniformly over the carbon support. Besides that, the particle size distributions were also determined from these TEM images. As can be seen, all catalysts show a good particle size distribution with a low standard deviation. Only the Ag-Pd/C catalyst displays a little larger standard deviation, which might be the result of the facile reducibility of the Ag nitrate by light. However, even for this catalyst, the particle size distribution is still decent with only a few outliers. The calculated surface averaged particle size of every catalyst was determined from these images and is listed in Table 3. Most of the catalysts have a comparable particle size to the monometallic Pd/C catalyst, except for the Mn-Pd/C catalyst. Therefore, each bimetallic catalyst will be compared to the monometallic Pd/C catalyst (d_{SA} = 10.9 nm) in the catalytic data. It is not expected that the difference in the particle sizes will have a significant influence on the activity or selectivity of the catalysts. A TEM image of the Pd_S/C catalyst and its particle size distribution can be found in Appendix Figure A1.

Catalyst	IWI on	Wt.% Pd	Wt.% Pr	Mol ratio Pr:Pd	T_{HT} (°C)	T_{red} (°C)	$d_{SA} \pm \sigma_{SA}$ (nm)	d_{XRD} (nm)	$N_{monolayer}$
Pd_S/C	GNP	1.88	-	-	250	500	4.5 ± 1.4	4.5	-
Pd/C	GNP	2.53	-	-	250	600	10.9 ± 3.1	8.6	-
K-Pd/C	Pd/C	2.53	0.10	0.11	-	-	10.4 ± 3.2	7.9	1.5
Mn-Pd/C	Pd_S/C	1.88	0.12	0.12	250	560	6.4 ± 1.8	6.9	2.9
Cu-Pd/C	Pd/C	2.53	0.17	0.11	500	450	10.8 ± 3.3	8.9	2.8
Zn-Pd/C	Pd_S/C	1.88	0.14	0.12	350	600	8.6 ± 2.4	8.4	2.8
Ag-Pd/C	Pd/oxC	2.54	0.28	0.11	400	590	9.8 ± 4.4	7.1	3.3

Table 3: A comparison between the monometallic and promoted Pd catalysts; An indication on which monometallic Pd catalysts each of the promoted Pd catalysts have been impregnated, the amount of metal in each catalyst as weight percentage (wt.%) of Pd and promoter (Pr), the corresponding mol ratio of Pr to Pd, the heat treatment (T_{HT}) and reduction (T_{red}) temperatures used in the synthesis, the TEM obtained surface averaged particle size (d_{SA}) and the corresponding standard deviation (σ_{SA}), the Scherrer calculated average particle size (d_{XRD}) and the calculated number of monolayers that the promoter metal could form on the Pd particles surface ($N_{monolayer}$).

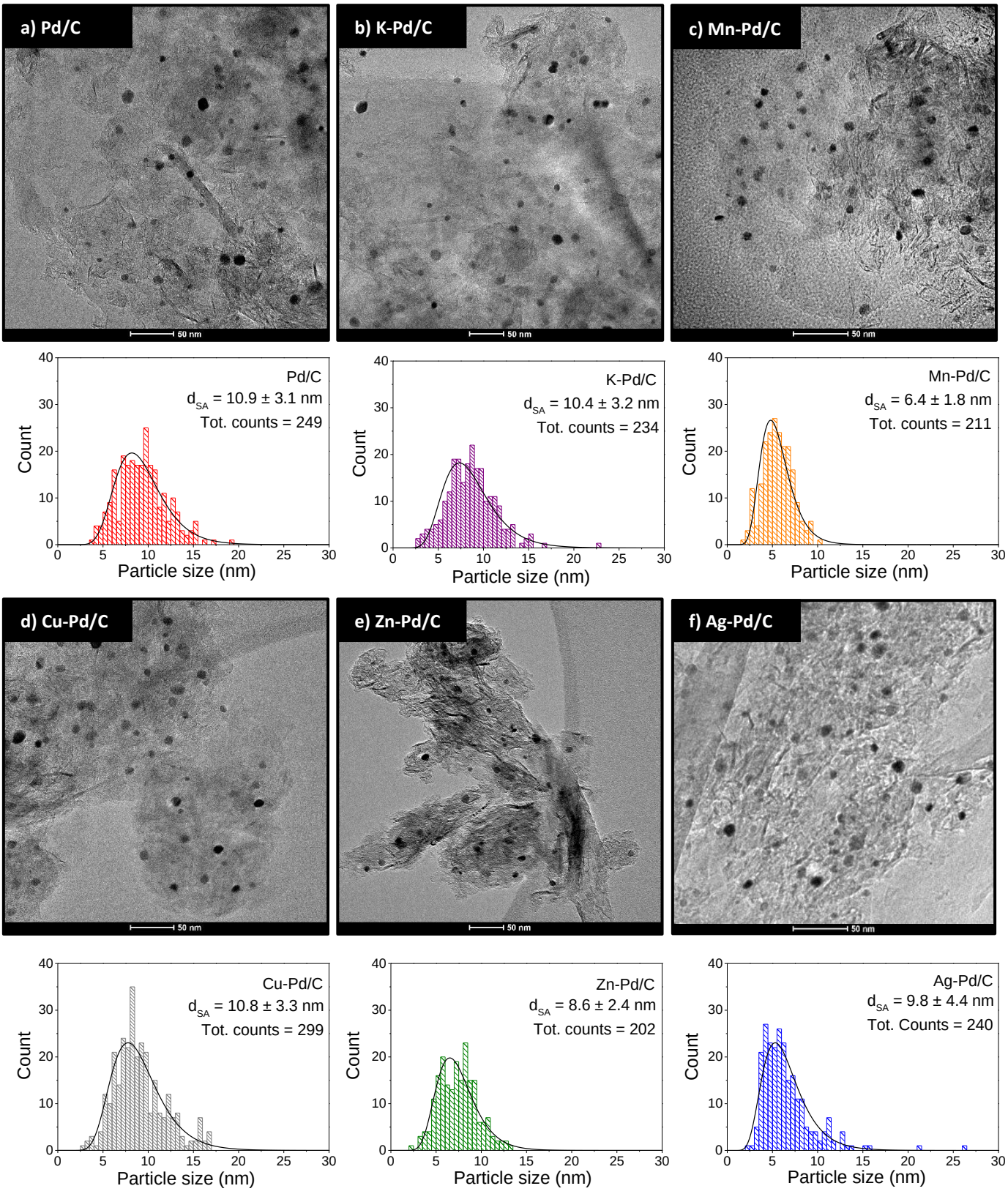

Figure 5: a-f) TEM images of monometallic and promoted Pd catalysts and the obtained particle size distribution per catalyst, the surface averaged particle size and standard deviation and the total counts in the analysis.

Per catalyst, the number of monolayers that the promoter metal would be able to form on the Pd surface was calculated and are listed in Table 3. All promoters are able to form approximately 2 or 3 monolayers on the Pd surface. This is high, since it is unwanted to cover the whole surface of all Pd particles. However, it is unknown if the promoter metals will only be found on/in the Pd particles or if the promoter metals are also/only to be found on the carbon support. If the promoter metals exists on the support, it might not cover the whole Pd surface. If the promoter metals would only attach onto the carbon support, the surface coverage of all promoter metals on the carbon support is calculated to be around 0.1-0.3%. With EDX, images were made of some of the promoted catalysts. The images made from the Mn, Zn and Ag promoted catalysts are shown in Figure 6. For the Mn and Ag promoted sample, it is unclear if the promoter metal signal is actually higher in the Pd particles than in the background/on the support. For the Zn promoted samples, it seems like the promoter metal signal is higher on the Pd particles than in the background, but the background also shows promoter metal signal. This could mean that Zn can be found on both the support and on/in the Pd particles.

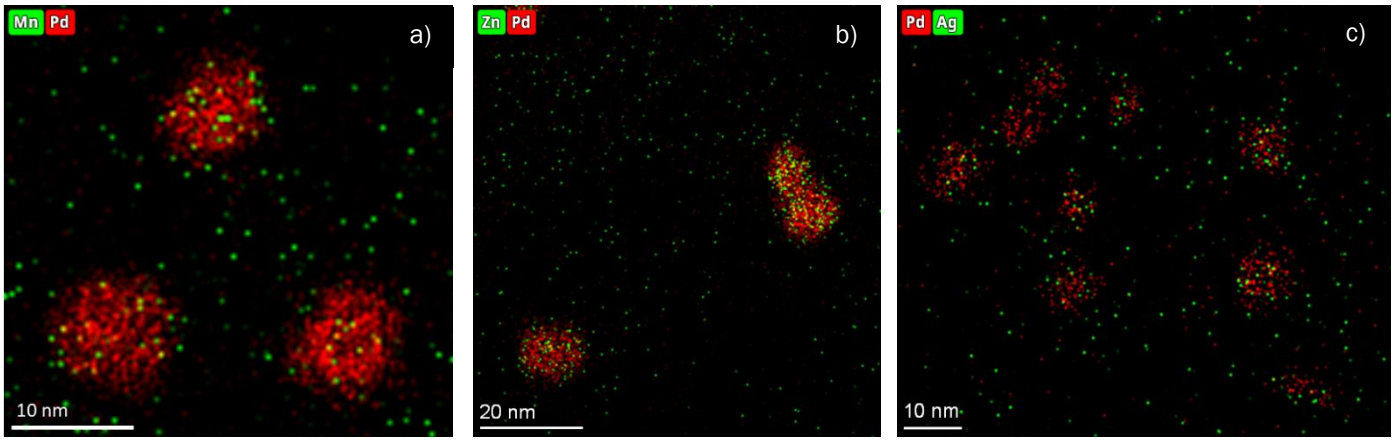

Figure 6: STEM-EDX images of **a)** Mn-, **b)** Zn- and **c)** Ag-Pd/C catalysts. Pd signal is indicated by a red dot and the promoter metals are indicates with a green dot.

For the Ag-Pd/C catalyst, 13 particles divided over 2 images (Appendix Figure A2 and Figure A3) were quantified by measuring the amount of signal in specific areas created over the particles. The results are shown in Figure 7. The results from the particles in Image 1 indicate that the ratio of Pd to Pr is approximately 0.1 for smaller particles, which was the desired mol ratio. However, the results from the particles in Image 2 show that with larger particle sizes (>12 nm), the ratio of Ag:Pd increases. This might be the result of the unstable Ag nitrates that reduce easily under light. When the Ag nitrates are reduced, the metallic Ag might sinter onto Pd particles, which would explain why the ratio of Ag:Pd increases linearly with increasing the particle size. The quantification of both images indicates that Ag is somehow present on or in the Pd particles.

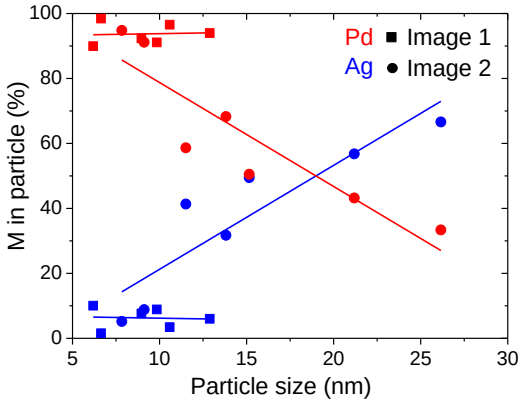

Figure 7: EDX metal signal intensity which gives the percentage of metal in the particle as a function of the particle size for 13 particles, divided over 2 images. Pd is indicated in red and Ag is indicated in blue. The data points obtained from image 1 are squares and the data points obtained from image 2 are dots.

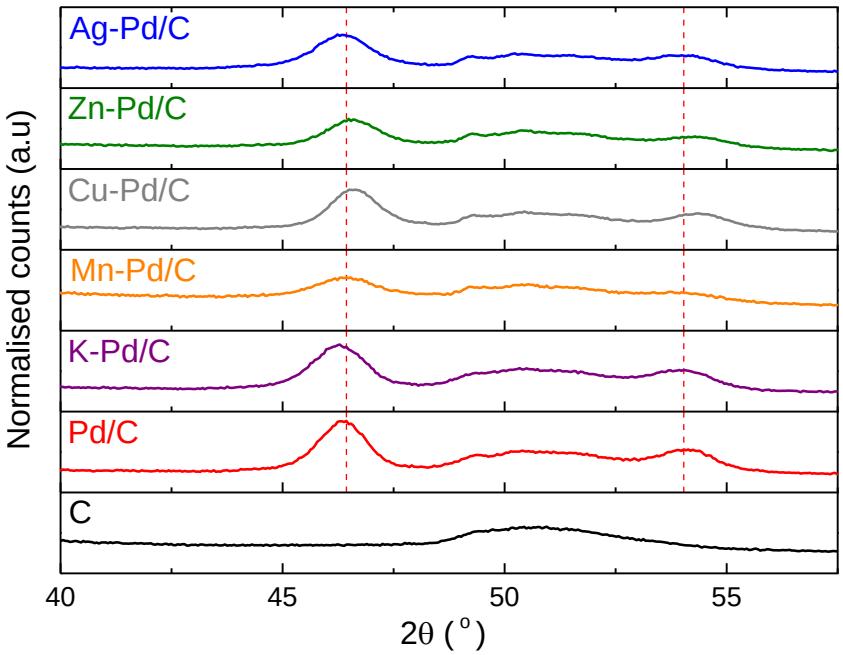

Figure 8: XRD plots of the carbon support (C), the monometallic Pd catalyst and all promoted catalysts between 40 and 57.5 °2θ. The two Pd diffractions are indicated by the dotted red lines, Pd(111) around 46.4 °2θ and Pd(200) around 50.9 °2θ. The carbon diffraction peak around 31 °2θ is normalised to the same peak in the carbon reference with respect to its position (°2θ) and intensity. In the plotted data, sample displacement is not taken into account.

All prepared promoted catalysts and the monometallic Pd/C catalyst were analysed with XRD and the diffractograms between 40 and 57.5 °2θ are shown in Figure 8. The full diffractograms between 20 and 80 °2θ can be found in Appendix Figure A4. The Pd peaks, indicated by the dotted red lines, are clearly visible in all samples. The main diffraction peak of Pd(111) at approximately 46.4 °2θ is used to calculated the particle sizes listed in Table 3 with the Scherrer equation. The metals used for promotion are not visible in these diffractograms due to the low weight loading in the samples. Something that does indicate the presence of the promotion metals, is the main diffraction peak of Pd at 46.4 °2θ, which shifts a little bit for the promoted samples. When atoms with a different atomic radii are added to the Pd crystal lattice, lattice defects are created. As a result, the lattice might expand or contract. This lattice expansion or contraction will lead to a shift in the Pd diffraction. The lattice constants are calculated using Brags Law. Additionally, the peak shifts are calculated in terms of lattice contraction in % compared to the Pd(111) peak in the monometallic Pd catalysts with the most comparable surface averaged particle size. This is the Pd/C catalyst for each promoted catalyst, except for the Mn-Pd/C catalyst. Both the calculated lattice constants and peak shifts are specified in Table 4. In these calculations, sample displacement is taken into account.

Catalyst	Calculated r_{vdw} (Å)	a (Å)	Lattice contraction (%)
Pd_S /C	1.38	3.925	-
Pd /C	1.38	3.927	-
Mn-Pd/C	1.16	3.907	0.46
Cu-Pd/C	1.28	3.889	0.97
Zn-Pd/C	1.39	3.891	0.91
Ag-Pd/C	1.44	3.906	0.51

Table 4: A comparison between the monometallic and the Mn, Cu, Zn and Ag promoted Pd catalysts in terms of the calculated atomic radius of the metal. For the monometallic Pd catalysts this metal is Pd, for the promoted catalysts it is the promoter metal. The lattice constants (a) are calculated for each Pd crystal with the main Pd diffraction around 46.4°2θ and with Brags Law. In this calculation, sample displacement is taken into account. With these lattice constants, the lattice contraction in percentage is calculated and listed here. The lattice contraction is calculated for each promoted catalysts with respect to the Pd/C catalyst, except for the Mn-Pd/C catalyst which was compared to the Pd_S/C catalyst because their particle sizes are more comparable.

Recent research has shown that K^+ ions are small enough to be intercalated into the graphite lattice.[80,81] This will lead to peak shifts of the carbon support diffractions, which is used as a reference to determine if the Pd(111) peak has shifted. For that reason, it is not reliable to do a similar lattice contraction analysis of the K-Pd/C XRD data. Therefore, the K-Pd/C catalyst is not listed in Table 4. To overcome this issue, another crystalline substance could be added to the sample to use as a reference for the XRD data.

When adding a metal atom with a larger atomic radius to the Pd lattice, it is expected for the lattice to expand, while it is expected to contract when a smaller atom is added to the Pd lattice. However, a lattice contraction is observed for each promoted catalyst while some of the promoter metal atoms have a larger calculated atomic radius. The addition of Mn, Cu, Zn and Ag does lead to a lattice contraction, 0.46, 0.97, 0.91 and 0.51% respectively. The lattice contraction could indicate that these promoter metals are incorporated into the Pd lattice. Nevertheless, only Ag and Zn are expected to form an (intermetallic) alloy with Pd according to their phase diagrams.[15,57,58,60,61] So it could be that this lattice contraction is a result of the incorporation of the Ag and Zn in the Pd lattice. At least, the contraction indicates that the addition of the promoter metals lead to some kind of lattice defect. Still, it is hard to say whether a lattice contraction smaller than 1% are actually meaningful or if they fall into the margin of error within the XRD analysis technique or calculations that were made.

Most of the prepared catalysts were also studied with TPR and these results are shown in Figure 9, except for the K and Ag promoted samples. A zoom at the CuO/C and CuO-Pd/C plots is provided in the figure. The K promoted catalysts was never heat treated due to very extreme heat treatment conditions to form potassium oxides and was therefore not studied with TPR. The Ag promoted catalyst was reduced directly after the heat treatment to minimize light exposure and thereby preventing sintering as much as possible, thus no TPR analysis is performed on this catalyst before reduction. No monometallic MnO_2/C catalyst was prepared and is therefore also missing from these TPR results. The calculated amounts of hydrogen needed to reduce the sample and the reduction temperatures of the carbon support are shown in Table 5. In Figure 9, it is hard to find any reduction peaks of metal oxides other than PdO and possibly CuO, this is probably due to low weight loadings of the promoter metals. Nevertheless, we can still explore the influence of the promoter metals on the reduction of the carbon support.

Pd_S/C is used as a reference for the TPR analysis instead of the Pd/C catalyst, but this should not be a problem for the comparison with the promoted Pd catalysts. That is because during the reduction of the metal oxide in the Pd_SO/C catalyst in the TPR measurement, reduced metal nanoparticles will form and grow. Because the analysis temperature is rising to 700 °C, the metal nanoparticles will sinter at higher temperatures and therefore increase in particle size during the analysis. The Pd/C catalyst has a larger average particle size than Pd_S/C, 10.9 nm vs 4.5 nm respectively (Table 3). The Pd particles in the Pd/C, that has been previously reduced at 600 °C, will not grow much in particle size until the TPR measurement has reached a temperature higher than 600 °C. However, the Pd particles in the Pd_S/C catalyst, which has been previously reduced at 500 °C, will sinter and grow at temperatures higher than 500 °C. At the TPR measurement temperature of 600 °C, the Pd particles in the Pd_S/C catalyst should have similar particle sizes to the Pd particles in the Pd/C catalyst. Therefore, it is assumed that particle sizes are similar for the Pd_S/C and Pd/C catalyst at 600 °C during the TPR measurement. This allows us to study the carbon reduction peak around 600 °C and compare the prepared promoted Pd catalysts to the Pd_S/C catalyst instead of the Pd/C catalyst. Unfortunately, the CuO-Pd/C catalyst does contain another wt.% of Pd compared to Pd_S/C, 2.53 wt.% and 1.88 wt.%, respectively (Table 3). This will most likely have an influence on the amount of hydrogen needed for the carbon support reduction.

In Figure 9, the PdO reduction peak around 175 °C is clear and the area is close to the calculated expected value of 177 µmol H_2/ g cat that is needed to hydrogenate the amount of PdO that is present in the Pd_SO/C catalyst (188 µmol H_2/ g cat, see Table 5). Moreover, after PdO reduction, the freshly reduced Pd also seems to promote the carbon support reduction. This can be seen because the amount of hydrogen that is used for the support reduction is higher. For the Pd_S/C catalyst, the reduction of PdO to metallic Pd took place before the TPR analysis. In this catalyst, the Pd does increase the amount of hydrogen that is consumed to hydrogenate the carbon support with the same amount as PdO did (22 µmol H_2/ g cat). Furthermore, a small hydrogen release can be seen around 60 °C for the previously reduced Pd_S/C catalyst. This hydrogen release is the result of the decomposition of PdH_x species.

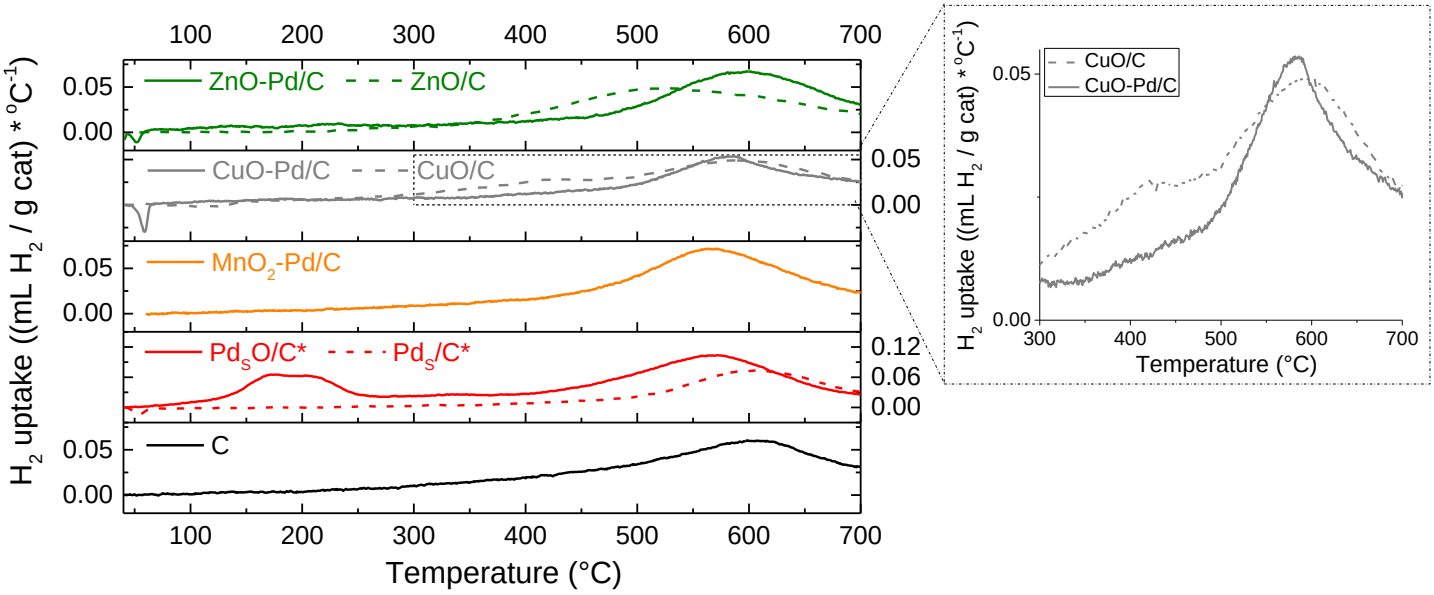

Figure 9: TPR plots of the carbon support (C), the monometallic heat treated and reduced Pd catalyst, Mn, Cu and Zn promoted and monometallic Cu and Zn heat treated catalysts. The hydrogen uptake is expressed as a function of temperature. By calculating the area of a peak (with Origin software), the amount of hydrogen that is taken up by the sample (µmol H_2/ g cat) is determined. *The named Pd_S/C (and Pd_SO/C) catalyst in this figure is not the same as the Pd_S/C catalyst listed in Table 4. The impregnated batch of catalyst was split in two batches and heat treated and reduced separately. However, the heat treatment and reduction conditions were exactly the same, resulting in very similar catalysts. The difference in the calculated d_{XRD} of both catalysts is 0.12 nm.

a)	$T_{C,red}$ (°C)	H_2 uptake (µmol H_2/ g cat)
C	599	212
Pd_S/C*	599	234
Pd_SO/C*	572	234

b)	$T_{C,red}$ (°C)	H_2 uptake C (µmol H_2/ g cat)	H_2 uptake C (µmol H_2/ g cat) relative to C (1) or Pd_S/C (2)
MnO_2-Pd/C	562	304	70 (2)
CuO-Pd/C	582	149	-85 (2)
CuO	589	208	-4 (1)
ZnO-Pd/C	597	246	11 (2)
ZnO	511	291	79 (1)

c)	$T_{M,red}$ (°C)	H_2 uptake metal oxide (µmol H_2/ g cat)	Expected H_2 uptake (µmol H_2/ g cat)
Pd_SO/C*	173	188	177
CuO/C	420	13	19

Table 5: a) The reduction temperature of the carbon support and the calculated hydrogen uptake for this carbon reduction peak of the C support reference, Pd_S/C and Pd_SO/C. **b)** The reduction temperature of the carbon support, the calculated hydrogen uptake for this carbon reduction peak and the relative hydrogen uptake for this carbon reduction peak compared to the hydrogen uptake of the carbon support (1) or Pd_S/C (2), of several Pd promoted and monometallic promoter metal oxides. **c)** The reduction temperature of the Pd_SO and CuO reduction peak, the calculated hydrogen uptake for this metal oxide reduction peak and the calculated expected hydrogen uptake value of the reduction of the metal oxides. *The named Pd_S/C catalyst in this table is not the same as the Pd_S/C catalyst listed in Table 4. The impregnated batch of catalyst was split in two batches and heat treated and reduced separately. However, the heat treatment and reduction conditions were exactly the same, resulting in very similar catalysts. The difference in the calculated d_{XRD} of both catalysts is 0.12 nm.

The MnO_2-Pd/C catalyst does increase the amount of hydrogen that is consumed to reduce the carbon support, by 70 µmol H_2/ g cat, compared to the monometallic Pd_S/C catalyst. Additionally, This could mean that MnO_2 has a promoting effect on the support reduction. The MnO_2-Pd/C catalysts does not shown a hydrogen release because the analysis started after the typical hydride release temperatures (between 50 and 60 °C).

When the CuO/C catalyst is studied in Figure 9, the carbon reduction peak appears to have a small shoulder peak. This peak is better visible in the zoom of the CuO/C and CuO-Pd/C graphs, which is also shown in this figure. The H_2 uptake of this peak, 13 µmol H_2/ g cat, is close to the expected H_2 uptake value for the reduction of CuO that was calculated, 19 µmol H_2/ g cat. Therefore, this small peak could be ascribed to the CuO reduction. However, CuO usually reduces at much lower temperatures (300 °C).[65,82] Consequently, it is questionable if this shoulder peak is a result of CuO reduction. In the CuO-Pd/C catalyst, this shoulder disappears A possible explanation for the disappearance of the shoulder peak for the TPR analysis of the Cu-Pd/C catalyst, is that Pd may have promoted the reduction of CuO, resulting in the peak being reduced at much lower temperatures. This would indicate that Pd and the CuO are in close proximity. Since it is unclear whether the shoulder peak can be ascribed to CuO reduction, not many conclusions can be made.

When we look at the carbon reduction peak around 585 °C of the CuO/C catalyst, the addition of CuO to the carbon support does not seem to lead to a promotion of the support reduction like was observed for the PdO/C catalyst. The amount of hydrogen that is used for the carbon support reduction is approximately the same for the carbon support (212 µmol H_2/ g cat) and the CuO/C catalyst (208 µmol H_2/ g cat). However, the combination of CuO and metallic Pd seems to limit the carbon support reduction considering it has a lower hydrogen uptake of 85 µmol H_2/ g cat. This is unexpected since the CuO-Pd/C catalyst has a higher wt.% of Pd, which should lead to a higher amount of carbon reduction. It could indicate that Pd has some kind of influence on the CuO or vice versa, leading to a different carbon reduction.

On the contrary, the ZnO seems to have a promoting effect on the carbon support reduction, since the peak shifts from 599 °C to 511 °C. Furthermore, the amount of hydrogen that is taken up is increased by 80 µmol H_2/ g cat. For the ZnO-Pd/C catalyst, this promoting effect on the support reduction disappears and no other reduction peaks are visible in the plot. This could indicate that the reduced Pd metal already reduces ZnO before the TPR analysis is even started and therefore leads to a different carbon reduction as well. This would indicate that Pd and ZnO are in close proximity. Since the Pd probably promotes reduction of ZnO, it might be worth to try to reduce the K promoted Pd samples in future work. High temperatures are needed to reduce KNO_3, but maybe the Pd is able to promote the reduction and make it possible to reduce KNO_3 at lower temperatures. This would allow for a better comparison of results with the K-Pd/C catalyst.

To conclude, the addition of metal oxides to the carbon surface lead to a higher hydrogen uptake by the carbon support reduction and sometimes also lower reduction temperatures. Moreover, Pd probably promotes the reduction of ZnO and possibly CuO, and this is also expected for the promoter metals Mn and Ag.

5.3 Catalysis

5.3.1 Activity

In this chapter, catalytic performance in terms of activity of all promoted catalysts will be discussed. In each test, approximately 0.6-0.7 µg Pd is loaded in the reactor. As stated in the experimental section, each monometallic promoter catalyst that does not contain any Pd is tested as reference on the catalytic setup. This is done to establish that the promoter metal does not show any activity in this reaction without the Pd. For these reference catalysts, the amount of promoter metal is kept roughly the same as in the promoted Pd catalysts. The results of the reference tests can be found in Appendix Figure A5 and, it is clear that the catalytic activity for the selective hydrogenation of butadiene or propylene of the promoter metals is negligible compared to Pd catalysts.

In Figure 10a the conversion of butadiene as a function of the temperature is shown for the monometallic and all promoted Pd catalysts. Already at room temperature, the Pd catalyst converts more than 10% of the butadiene feed and reaches full conversion already around 80 °C. None of the promoted catalysts reach full conversion at this temperature, they all required higher temperatures, ranging from 90 °C for the Mn-Pd/C catalyst to 140 °C for the Zn- and Ag-Pd/C catalysts. However, some promoted catalysts did display an even higher conversion at room temperature than the Pd only catalyst. The Mn- and K-Pd/C promoted catalysts convert about 20% of the butadiene at room temperature.

The calculated Turnover Frequency (TOF) per temperature is plotted in Figure 10b. As explained in the experimental details section, the particle size and amount of Pd in each catalyst will be taken into account in the TOF calculations, making it a fair way to compare the activity of the catalysts. One thing that stands out is that most of the curves resemble the curves Figure 10a, only the curve of the Mn-Pd/C catalyst has changed extensively. This is because all catalysts have comparable particle sizes, except for the Mn-Pd/C one, which has a much smaller particle size (see Table 3) and therefore also a lower TOF compared to the others at similar activity per gram Pd. The Cu-, Zn-, Ag-Pd/C and monometallic Pd/C all show an exponential curve for the activity, which is expected. However, the K- and Mn-Pd/C catalysts do not display an exponential curve, which could indicate that there are mass transfer limitations. Smaller particles lead to more mass transfer limitations than larger particles. This is a possible explanation why the Mn-Pd/C displays mass transfer limitation, since the particles in the Mn-Pd/C catalyst are smaller than all the particles in all other catalysts (d_{SA} = 6.4 nm). It could also be due to a bad mixing of the catalytic bed, but this is not likely since all catalyst reactors are prepared in a similar way.

As expected from the results of Figure 10a, Pd/C displays the highest TOF values in the higher temperature range. Only the K-Pd/C catalyst shows higher TOF values at temperatures lower than 45 °C. The Cu-Pd/C and Mn-Pd/C catalyst show similar TOF values as the monometallic Pd catalyst at 25 °C, but yield lower TOF values at higher temperatures. The Ag-Pd/C and Zn-Pd/C catalysts both show lower TOF values than the monometallic catalyst in the whole temperature range. However, all promoted catalysts still have a relatively high TOF for the

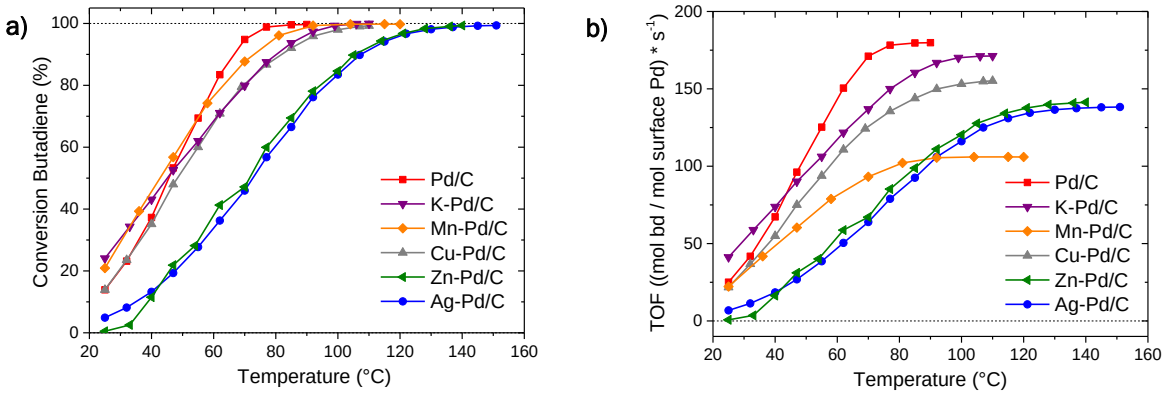

Figure 10: Catalytic performance of the monometallic Pd and all promoted Pd catalysts; **a)** Conversion of butadiene as a function of temperature. **b)** Turnover frequency as a function of temperature. Amount of Pd loaded in each reactor (µg): 0.598 Pd/C; 0.601 K-Pd/C; 0.600 Mn-Pd/C; 0.685 Cu-Pd/C; 0.598 Zn-Pd/C; 0.703 Ag-Pd/C.

hydrogenation of butadiene. With TOF values higher than 100 mol butadiene per mol surface Pd per second at T=90 °C, all catalysts are still very active compared to non-Pd catalysts.[7,24,39] To conclude, all promoted catalysts have a lower activity than the monometallic Pd catalyst at higher temperatures near full conversion, but the promoted catalysts still have a reasonable high activity for the hydrogenation of butadiene.

5.3.2 Selectivity

As mentioned in the introduction, the bottle neck of Pd catalysts is the selectivity, especially at high conversion levels. Therefore, it is important to also study the influence of the promoters on the selectivity. The selectivity as a function of the butadiene conversion of all catalysts are shown in Figure 11a. The monometallic Pd catalyst exhibits the highest selectivity to butenes at higher conversion. The Ag-Pd/C catalyst displays the highest selectivity of the promoted catalysts, which is just a bit lower than the Pd catalyst. The Cu-Pd/C catalyst shows comparable selectivity to the monometallic Pd catalyst at lower conversion levels (~14-24%). Unfortunately, the selectivity goes down almost immediately, yielding less butenes than the Pd/C and Ag-Pd/C catalyst at higher conversion. The steep decrease in the selectivity curves of the K- and Mn-Pd/C catalysts indicate once again that mass transfer limitations might be present for these catalysts.

The fraction of 1-butene in the C4 stream is expressed in Figure 11b at two different levels of butadiene conversion, namely around 22% and 86% butadiene conversion. Around 22% conversion, the fraction of 1-butene in the stream is much higher for the Ag-Pd/C catalyst than for the Pd/C catalyst, respectively 61% and 56%. Besides the Ag promoted catalyst, the Cu, Mn and Zn promoted samples have a slightly higher fraction of 1-butene in the gas stream at low conversion. The K promoted sample has approximately the same selectivity to 1-butene at low conversion. At higher conversion, the differences in 1-butene selectivity become more apparent. The Pd/C and Ag-Pd/C catalyst stay stable at around the same fraction. However, the Zn-Pd/C catalyst increases

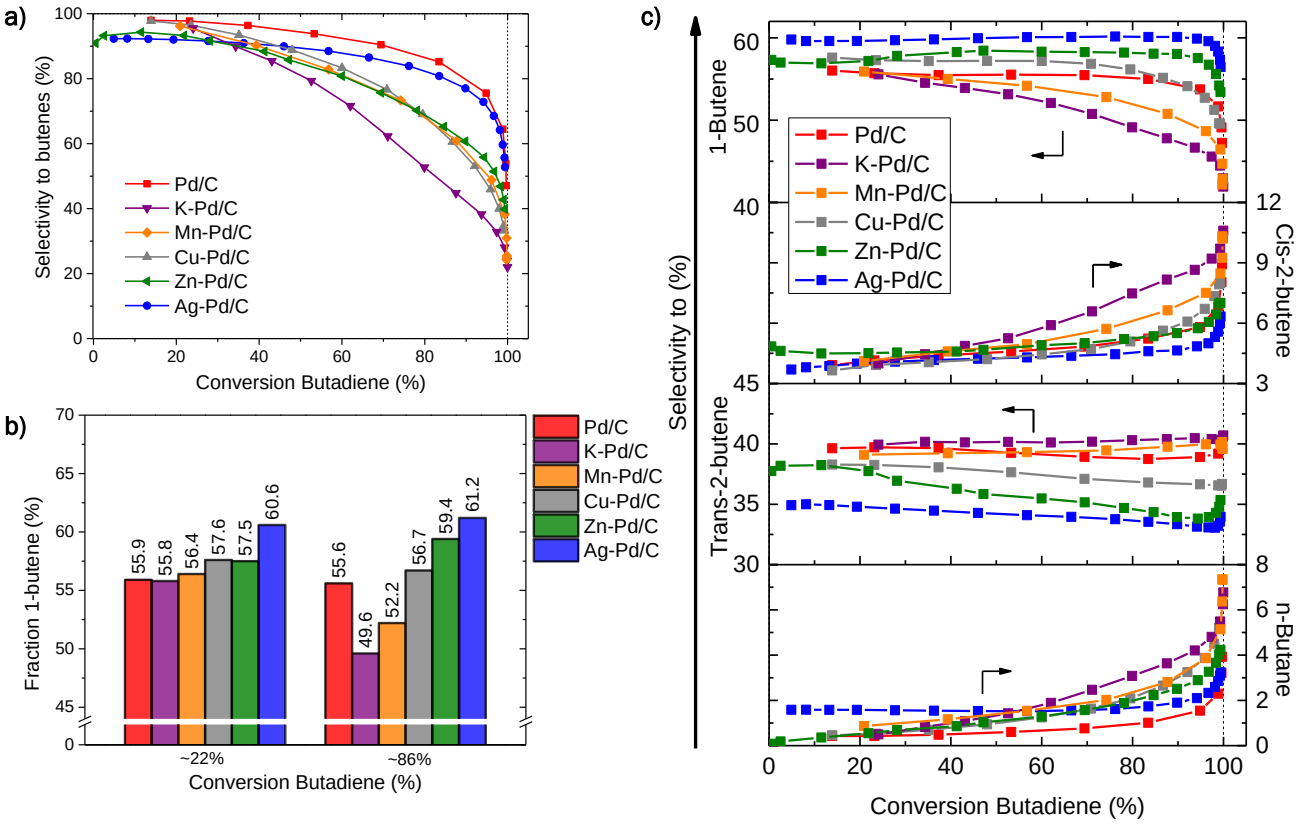

Figure 11: Catalytic performance of the monometallic Pd and all promoted Pd catalysts; **a)** Selectivity towards all butenes as a function of butadiene conversion. **b)** Fraction of 1-butene in the C4 product stream at conversion levels around 22% (19-24%) and 86% (83-88%). The exact fraction of 1-butene of each catalyst is displayed above the column. **c)** The C4 selectivity towards all butenes and n-butane as a function of the butadiene conversion. Amount of Pd loaded in each reactor (µg): 0.598 Pd/C; 0.703 Ag-Pd/C; 0.685 Cu-Pd/C; 0.601 K-Pd/C; 0.600 Mn-Pd/C; 0.598 Zn-Pd/C.

a bit and the K- and Mn-Pd/C decrease with 6% and 4%, respectively. The reason why the Ag-Pd/C catalyst has such high fractions of 1-butene might be due to an isomerisation effect, which will be discussed further in Chapter 5.3.3.

The selectivity towards all butenes and n-butane as a function of conversion are displayed in Figure 11c. The Ag-Pd/C catalyst shows the highest selectivity towards n-butane at low conversion as can be seen in this figure. But as the conversion increases, the selectivity to n-butane of all other promoted catalysts gradually increases, while the n-butane level for the Ag promoted catalyst stays rather stable until 95% conversion is reached. This gradual increase finally results in a higher n-butane formation for every other promoted catalyst at 80% conversion and higher. Only the Pd/C catalyst has a lower formation in the whole conversion range, but is also less constant than the Ag promoted sample. Additionally, it stands out that the Ag-Pd/C catalyst not only has the highest selectivity towards 1-butene, it displays the lowest for cis-2-butene and trans-2-butene as well. This could be explained by different isomerisation properties of Ag-Pd/C compared to the monometallic Pd/C catalyst. Therefore, more research is performed on the 1-butene isomerisation properties of all promoted samples and the monometallic Pd catalyst, which is discussed in the next section.

5.3.3 Isomerisation

As mentioned in the previous chapter, the Ag, Zn and Cu promoted catalysts showed a higher selectivity towards 1-butene than the monometallic Pd catalyst and this may be the result of a isomerisation effect. To study this isomerisation effect, catalytic experiments are performed with a 1-butene gas flow instead of a butadiene gas flow. With a 0.3% 1-butene and 5% hydrogen gas feed, the catalyst can isomerise the 1-butene towards cis-2-butene or trans-2-butene, or fully hydrogenate the 1-butene to n-butane. Each catalyst is tested until temperatures are reached where the same catalyst would have reached a 100% butadiene conversion.

The monometallic and all promoted catalysts are tested and the results are shown in Figure 12a,b. In Figure 12a, the 1-butene conversion is plotted as a function of temperature. The figure indicates that none of the catalysts reach full conversion of 1-butene, even at the temperature where the catalyst would have reached a 100% butadiene conversion. Besides that, the curves seems to reach a plateau at higher temperatures. Some catalysts even exhibit a slight decrease in 1-butene conversion at higher temperatures (K-Pd/C, Mn-Pd/C and Pd/C). The data that were measured during cooling down slope of the catalyst, is shown in Appendix Figure A6. Here it can be seen that all catalysts seem to deactivate after reaching the highest temperature, except for Ag-Pd/C, which seems to activate. The deactivation characteristics were not observed for the butadiene tests for all promoted and monometallic Pd catalysts, except for Mn-Pd/C, which can be seen in Appendix Figure A7. This indicates that the deactivation is not temperature related. It could also be the result of a catalyst reshaping, which might change the binding sites of the catalysts. This could change the catalysts' activity for the isomerisation of 1-butene, but not for butadiene.

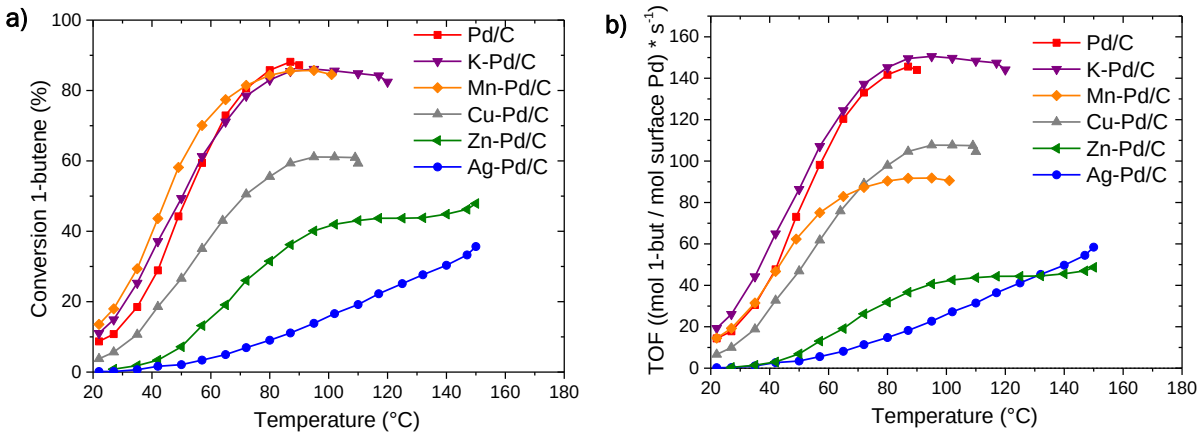

Figure 12: Catalytic performance of the monometallic Pd and all promoted Pd catalysts; **a)** The 1-butene conversion as a function of temperature. **b)** Turnover frequency as a function of temperature. Amount of Pd loaded in each reactor (µg): 0.658 Pd/C; 0.594 K-Pd/C; 0.600 Mn-Pd/C; 0.612 Cu-Pd/C; 0.607 Zn-Pd/C; 0.602 Ag-Pd/C.

For the isomerisation reaction, the activity is also expressed in terms of Turnover Frequency (TOF). However, the TOF is now defined as the amount of mol 1-butene that is converted per mol Pd surface atom per second. It is clear that the monometallic Pd and K promoted catalysts have a very high TOF for 1-butene, especially compared to the Zn and Ag promoted samples. The TOF of 1-butene of the monometallic Pd catalyst is around 140 s^{-1} at the temperature where the catalyst would reach full butadiene conversion (90 °C, see Figure 10a), while all promoted samples, except for K-Pd/C, show a lower TOF (approximately 50-110 s^{-1}) at their corresponding full conversion temperatures. This gives an explanation for the higher selectivity of Zn and Ag towards 1-butene during butadiene hydrogenation: the 1-butene simply gets converted with slower rates by the Zn- and Ag-Pd/C than by the monometallic Pd catalyst.

By comparing the temperatures of the isomerisation test with the results of standard catalytic butadiene tests, corresponding butadiene conversion levels are determined. With this comparison, the selectivity towards the 1- and 2-butenes can be represented as a function of selected low and high butadiene conversion values, as depicted in Figure 13a. This figure shows that at temperatures corresponding to low and especially at high butadiene conversion the Cu, Zn and Ag promoted samples isomerise less 1-butene to cis- or trans-2-butene than the monometallic Pd catalyst. On the other hand, the K- and Mn-Pd/C catalysts display an even higher isomerisation of 1-butene at high butadiene conversion. This is the same conclusion as was drawn from the isomerisation activity results, only here it is compared to the butadiene conversion instead of the temperature. This gives more insight in what is happening in the butadiene hydrogenation at low and high butadiene conversion. The trend that was observed for the selectivity to 1-butene at high conversion in Figure 11b, is very similar to the trend that can be seen in amount of 1-butene that is left in the stream at high conversion in Figure 13a.

In Figure 13a, the ratio of trans- to cis-2-butene seems to be very similar for each catalyst. The ratio of trans- to cis-2-butene is expressed at low and high corresponding butadiene conversion in Appendix Figure A8. At low butadiene conversion, this ratio is approximately 1:1 for every catalyst. At higher conversion, the selectivity shifts a little bit towards trans-2-butene. Still, this ratio is quite comparable for each catalyst. The 1:1 ratio of trans- to cis-2-butene in the isomerisation test indicates that the isomerisation of 1-butene to cis-2-butene is as favourable as the isomerisation to trans-2-butene.

The selectivity to n-butane as a function of temperature is shown in Figure 13b. The figure seems to resemble Figure 12a, which makes sense, since the more 1-butene is converted at a certain temperature, the more n-butane is formed. Furthermore, in the butadiene test, the Pd/C catalyst displayed the lowest selectivity towards n-butane at almost the whole temperature range. While for the 1-butene isomerisation, several catalysts show a lower selectivity towards n-butane than Pd/C at all temperatures, namely Cu-, Zn- and Ag-Pd/C. The Ag-Pd/C catalyst displays the lowest formation of n-butane at the whole temperature range, which is quite surprising since the Ag promoted catalyst showed the highest selectivity of n-butane in the standard butadiene catalyst tests at lower conversion levels, see Figure 11c. Moreover, the monometallic Pd had a lower n-butane

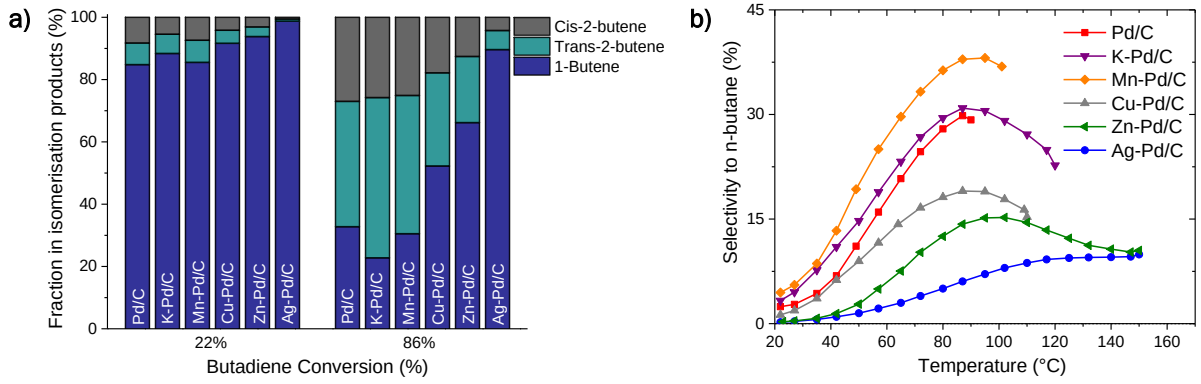

Figure 13: Catalytic performance of the monometallic Pd and all promoted Pd catalysts; **a)** Selectivity towards all butenes as a function of the estimation of the corresponding butadiene conversion. **b)** Selectivity towards n-butane as a function of temperature. Amount of Pd loaded in each reactor (µg): 0.658 Pd/C; 0.594 K-Pd/C; 0.600 Mn-Pd/C; 0.612 Cu-Pd/C; 0.607 Zn-Pd/C; 0.602 Ag-Pd/C.

selectivity than Ag-Pd/C at the whole temperature range, which can also be seen in Figure 11c. One explanation for this result could be that the Ag-Pd/C catalyst forms n-butane out of butadiene without releasing 1-butene from the catalyst surface. This would indicate that the Ag-Pd/C catalyst has a higher adsorbing strength to 1-butene. But if this is true, 1-butene should not desorb from the surface easily, resulting in more n-butane formation compared to the Pd catalyst in the isomerisation test as well as in the butadiene test. Surprisingly, this was not observed in the results. The obtained results are puzzling and challenging to explain.

To conclude, Ag addition to a Pd catalyst limits the activity for 1-butene isomerisation. The catalyst also exhibited the lowest formation of n-butane with a 1-butene feed.

5.3.4 Trends in results

It would be valuable if a correlation could be made with the catalysts' activity and selectivity compared to certain metal properties. This would make it easier to attribute the improved or regressed catalytic results that are observed to a type of promoting effect such as electronic, geometric or kinetic. Since an electronic effect is mainly expected, the electronegativity (EN)[83] of the promoter metals might give more insight. The EN of each promoter metal and Pd itself is listed in Table 6. Besides the EN of the promoter metals, the van der Waals radius (r_{vdw}) might also have an influence on the catalytic properties of Pd. When an alloy is formed and a smaller or larger atom enters the Pd lattice, the lattice might expand or contract. This adapted lattice might have different catalytic properties due to for instance a change in adsorption and desorption properties. The r_{vdw} and the difference in van der Waals radius (Δr_{vdw}) compared to Pd are calculated and listed in Table 6 together with the XRD obtained lattice contraction. It has been decided to leave the K-Pd/C data points out of the linear fit for the comparison of activity and selectivity to Δr_{vdw}, as the Δr_{vdw} value that is listed in Table is probably not fit to use for the data comparison. That is because the K promoted catalyst is not heat treated and reduced and most likely still consists of KNO_3. However, the data points of the K-Pd/C catalysts are still shown in each r_{vdw} comparison plot.

	Pd	K	Mn	Cu	Zn	Ag
EN	2.2	0.82	1.55	1.9	1.65	1.93
ΔEN		-1.38	-0.65	-0.3	-0.55	-0.27
r_{vdw} (pm)	138	133*	116	128	139	144
Δr_{vdw} (pm)		-5	-22	-10	+1	+6
Lattice contraction (%)			0.46	0.97	0.91	0.51

Table 6: Pauling electronegativity (EN) for Pd and each promoter metal and the difference in electronegativity between Pd and promoter metals (ΔEN). A darker yellow indicates a larger difference. The calculated van der Waals radius (r_{vdw}) of Pd and each promoter metal, the difference in the van der Waals radius between Pd and the promoter metals (Δr_{vdw}) and the corresponding lattice contraction expressed in percentage.*The literature derived ionic radius of K^+.[72] A darker colour indicates a larger difference, where red indicates a smaller and blue a larger r_{vdw} than Pd. For the lattice contraction, a darker green indicates a larger lattice contraction.

It immediately stands out that Pd has the highest EN, thus all the added promoter metals will act as an electron donor to Pd. The activity in terms of butadiene TOF at 25 °C of the promoted samples is plotted as a function of the difference in EN (ΔEN), see Figure 14a. The K promoted sample is the only promoted catalyst that shows an increase in TOF at lower temperatures compared to the Pd catalyst. This might be due to the fact that K is the least electronegative and could therefore have a larger electronic effect than the other metals. However, when looking at the other catalysts, Mn and Cu promoted samples show a comparable TOF as the Pd catalyst, while Ag and Zn show a decrease in TOF. Yet, the Cu and Ag have a similar EN, so if the Pd is promoted by an electronic effect, it would be expected that Ag and Cu show similar values of TOF as well. Likewise, the Zn and Mn have a similar EN, but show totally different TOF values at 25 °C. Therefore, it is concluded that no distinct trend is observed for the activity in butadiene hydrogenation compared to the EN.

The activity in terms of TOF expressed as a function of both Δr_{vdw} and the lattice contraction is shown in Figure 14. There seems to be a relation between the Δr_{vdw} and the TOF. The promoter metals with a more similar r_{vdw}

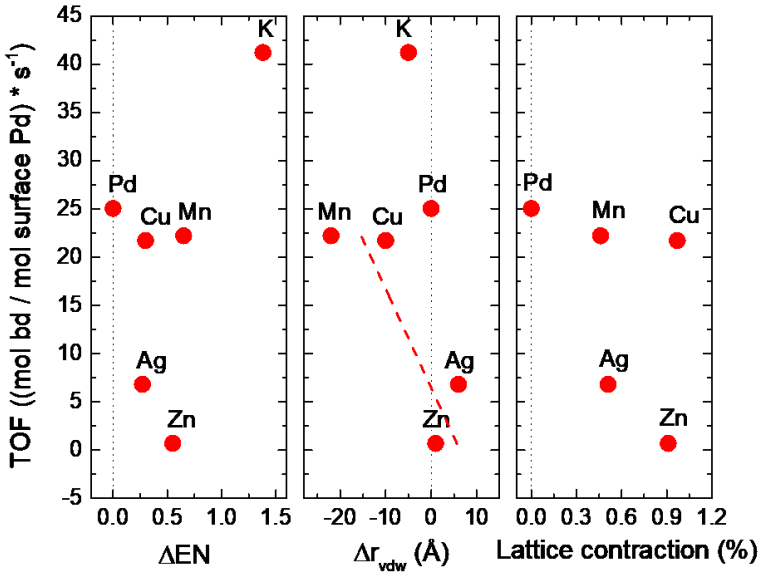

Figure 14: Butadiene (bd) TOF values of all promoted and monometallic Pd catalysts in the butadiene experiments at 25˚C as a function of the difference in the difference in EN (ΔEN) and van der Waals radius (Δr_{vdw}) compared to Pd, and the calculated lattice contraction. The red dotted line indicates a linear fit between all data points except K-Pd/C and Pd/C.

to the r_{vdw} of Pd lead to a lower TOF, while the promoter metals with a smaller r_{vdw} than Pd lead to a higher TOF. However, none of the promoted catalysts reach a higher TOF than Pd (except for the K promoted catalyst which was left out of the correlation assessment). Two pairs of promoted catalysts showed a comparable lattice contraction, namely Mn and Ag, and Zn and Cu. Despite that, the catalysts with similar lattice contraction show a totally different TOF value at 25 °C. It could be concluded that the activity of the catalyst may depend on the size of the promoter metal atom, but not on the measured lattice contraction. Nevertheless, if the r_{vdw} of the promoter metal is influencing the Pd catalyst, it will probably be the result of incorporation into the Pd lattice. This incorporation could lead to a change in the active sites of Pd, leading to different catalytic properties. However, if this is indeed the case, then a similar correlation with the lattice contractions would be expected. Moreover, none of the promoter metals are actually expected to be incorporated into the Pd lattice according to their phase diagrams, except for Ag and possibly Zn.[15,57–61]

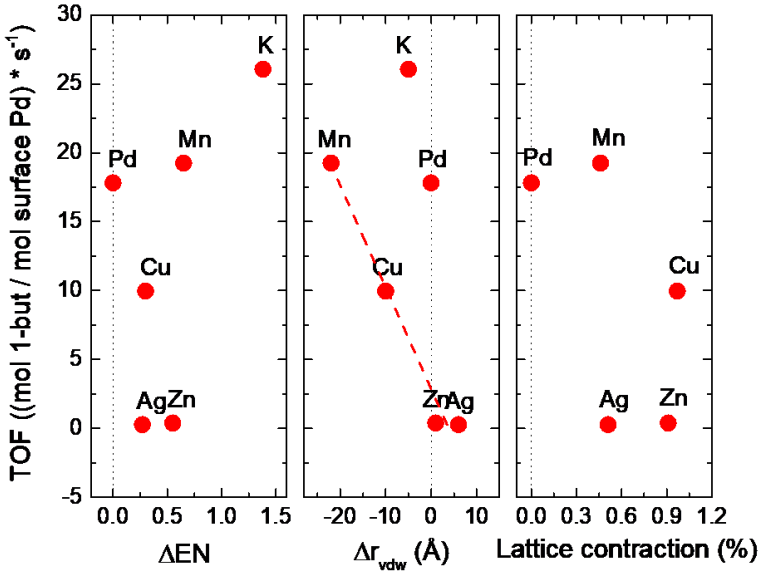

Figure 15: 1-Butene (1-but) TOF values of all promoted and monometallic Pd catalysts in the isomerisation experiments at 27˚C as a function of the difference in the difference in EN (ΔEN) and van der Waals radius (Δr_{vdw}) compared to Pd, and the calculated lattice contraction. The red dotted line indicates a linear fit between all data points except K-Pd/C and Pd/C.

The isomerisation activity is also plotted as a function of the EN, Δr_{vdw} and lattice contraction and can be found in Figure 15. Similar to the results that were obtained for the butadiene TOF and EN correlation, no distinct trend is observed. Cu and Ag, and Mn and Zn have a very comparable ΔEN, but their 1-butene TOF values are not alike.

In the correlation of Δr_{vdw} and the TOF of 1-butene, a clear correlation can be distinguished. It seems that a promoter metal with a r_{vdw} that is smaller than the r_{vdw} of Pd increases the isomerisation activity of 1-butene, which is similar to the observed results for the butadiene TOF. Unfortunately, it is desired to have a catalyst with a high butadiene TOF and a low 1-butene TOF, because a high 1-butene TOF will lead to a lower 1-butene selectivity in the selective hydrogenation of butadiene. For the correlation of the lattice contraction and the TOF of 1-butene, there is no trend observed. This raises the same concerns as was stated earlier regarding the correlation of Δr_{vdw} and the lattice contraction with the TOF of butadiene.

As stated in the background information, besides the activity, it is known that electronic effects could also affect the selectivity. At lower conversion, the differences in selectivity of all catalysts are small, this makes it hard to find any trends at lower conversion. At higher conversion levels (~86% butadiene conversion), the differences in selectivity become more apparent, therefore the selectivity at higher butadiene conversion levels is used for the correlations. However, it is good to keep in mind that at higher conversion, more mass transfer limitations will come into play. Two types of selectivity will be studied, the total selectivity towards all butenes and the fraction of 1-butene in the C4 gas stream. In the total selectivity, the fraction of all butenes divided by all butenes, n-butane and propane is used. In the fraction of 1-butene in the C4 gas stream, the fraction of 1-butene divided by all butenes and n-butane is used. The hydrogenation of propylene is not taken into account in this second calculation.

In Figure 16b, the total selectivity and fraction of 1-butene in the C4 gas stream of all catalysts at approximately 86% conversion are displayed as a function of ΔEN compared to Pd. The total selectivity of Pd is the highest. The Ag shows a bit lower selectivity, Mn, Cu and Zn show similar selectivity and K shows the lowest selectivity. The K promoted sample might exhibit the lowest selectivity due to the biggest difference in EN, in which case the electronic effect has had a negative influence on the selectivity. A trend might be present, in which the promoter metals with the smallest difference in EN display a higher total selectivity. However, then it would be expected that the Cu promoted sample exhibits a similar selectivity compared to the Ag, since they also have comparable

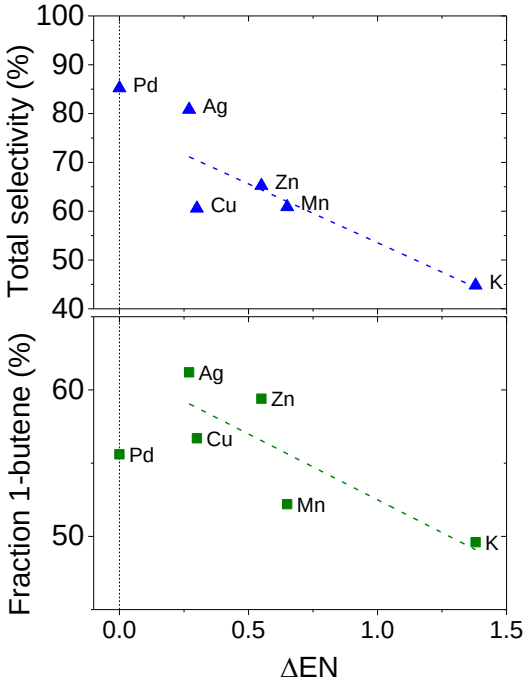

Figure 16: Total selectivity and fraction of 1-butene in the gas stream of all promoted and monometallic Pd catalysts at approximately 86% conversion as a function of the difference in electronegativity (ΔEN). The coloured dotted lines indicate a linear fit between all data points except Pd/C.

ENs. Moreover, the Mn, Cu and Zn sample show comparable selectivity, even though their EN is different. Therefore, it is hard to say if the trend is really there. A trend might also exist as the promoters with a EN closer to Pd show a higher 1-butene selectivity and the ones that have a larger difference in EN show a decrease in 1-butene selectivity. However, again, not all the promoters fall into the trend perfectly. The Cu should be closer to the Ag value and Mn should also exhibit slightly higher selectivity to fit in the curve.

To conclude, it is hard to find a clear correlation in the comparison of EN to selectivity and it is not clear if the difference in selectivity for the promoted catalysts are caused by an electronic effect. A correlation might be observed, indicating that the promoter metals with a smaller difference in electronegativity tend to have a higher total selectivity.

The relation of the Δr_{vdw} and the lattice contraction to the total selectivity and 1-butene selectivity are also studied and displayed in Figure 17. For both the total and the 1-butene selectivity, the larger the promoter metal atom is, the higher the selectivity. Still, if this is the reason why selectivity is increased, then it would also be expected that adding an atom that is of similar size of Pd, would not have a large influence. When looking at the Zn promoted catalysts, which has a comparable size to Pd, it shows much lower overall selectivity and much higher 1-butene selectivity. Therefore, it is unclear if this observed trend is correct. If it is true that the atom size of the promoter metals influences the selectivity, then this would most likely also be seen when comparing the selectivity to lattice contraction. However, this is not the case. No trend is observed when comparing the total selectivity to the lattice contraction. The Zn and Cu promoted catalysts have a similar lattice contraction and also a similar total selectivity. On the other hand, the Ag- and Mn-Pd/C catalysts have a similar lattice contraction as well, but show a large difference in total selectivity (about 20%). For the fraction of 1-butene, there is also no observed trend. Here, it is also the case that Ag- and Mn-Pd/C catalysts have a similar lattice contraction, but at the same time display a large difference in selectivity. Again, this raises the concerns that were stated before regarding the correlation of Δr_{vdw} and the lattice contraction with the TOF of butadiene.

To conclude, it might be that adding larger promoter metal atoms to Pd will lead to a higher total selectivity, but not higher than Pd itself. Furthermore, the addition of larger promoter metal atoms to Pd may lead to a higher 1-butene selectivity, which may exceed the 1-butene selectivity of Pd. Besides, no trends are observed for the comparison with the selectivity and the XRD derived lattice contraction.

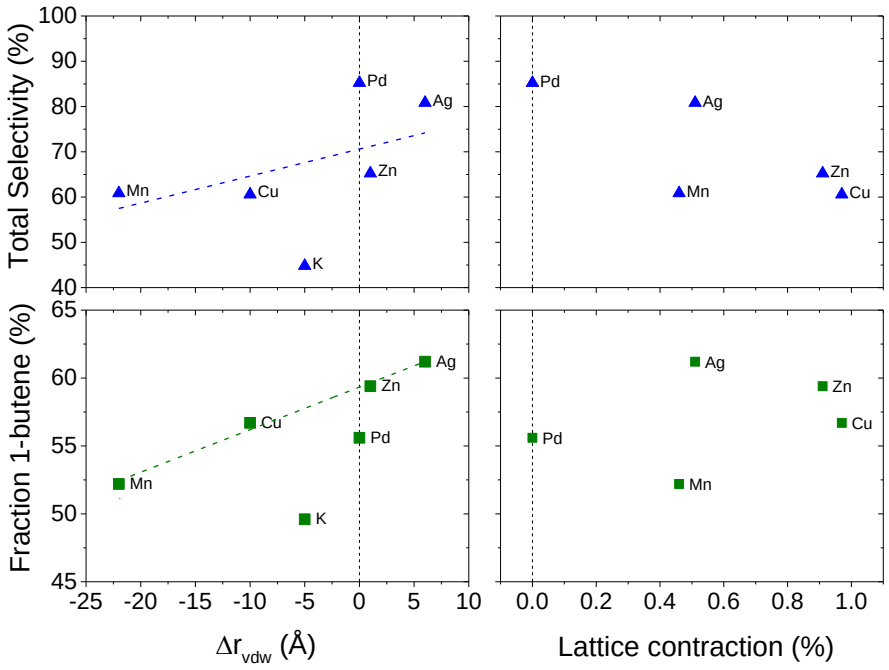

Figure 17: Total selectivity and fraction of 1-butene in the C4 gas stream of all promoted and monometallic Pd catalysts at approximately 86% conversion as a function of the difference in the van der Waals radius (Δr_{vdw}) and the calculated lattice contraction. The coloured dotted lines indicate a linear fit between all data points except K-Pd/C and Pd/C.

5.4 Pre-treatments

5.4.1 Pre-treatments on monometallic Pd catalyst

The effect of performing pre-treatments (PTs) before a catalytic test is studied on a monometallic Pd catalyst. Oxidizing the monometallic Pd catalyst will most likely not have any positive effects on the catalytic properties of the catalyst because metallic Pd has a better catalytic performance than PdO. Therefore, a reduction PT (PT_R) at 300 °C is studied for the monometallic Pd catalyst. The results are shown in Figure 18a-c. In Figure 18a, the conversion of butadiene is expressed as a function of temperature. This figure shows that the pre-treated catalyst reaches full conversion at lower temperatures (~70 °C) than the Pd/C catalyst without any PT (~80 °C). This might be due to the reduction of some oxidized Pd particles to metallic Pd during the PT. The total selectivity towards all butenes is plotted against the butadiene conversion in Figure 18b. The two catalysts exhibit comparable total selectivity and only differ a little bit at higher conversion levels (Figure 18c). Nevertheless, the fraction of 1-butene is reasonably higher at lower conversion levels for the pre-treated Pd catalyst. At higher conversion, this difference becomes smaller (~1%) because the fraction of 1-butene in the C4 product stream lowers significantly for the pre-treated catalyst.

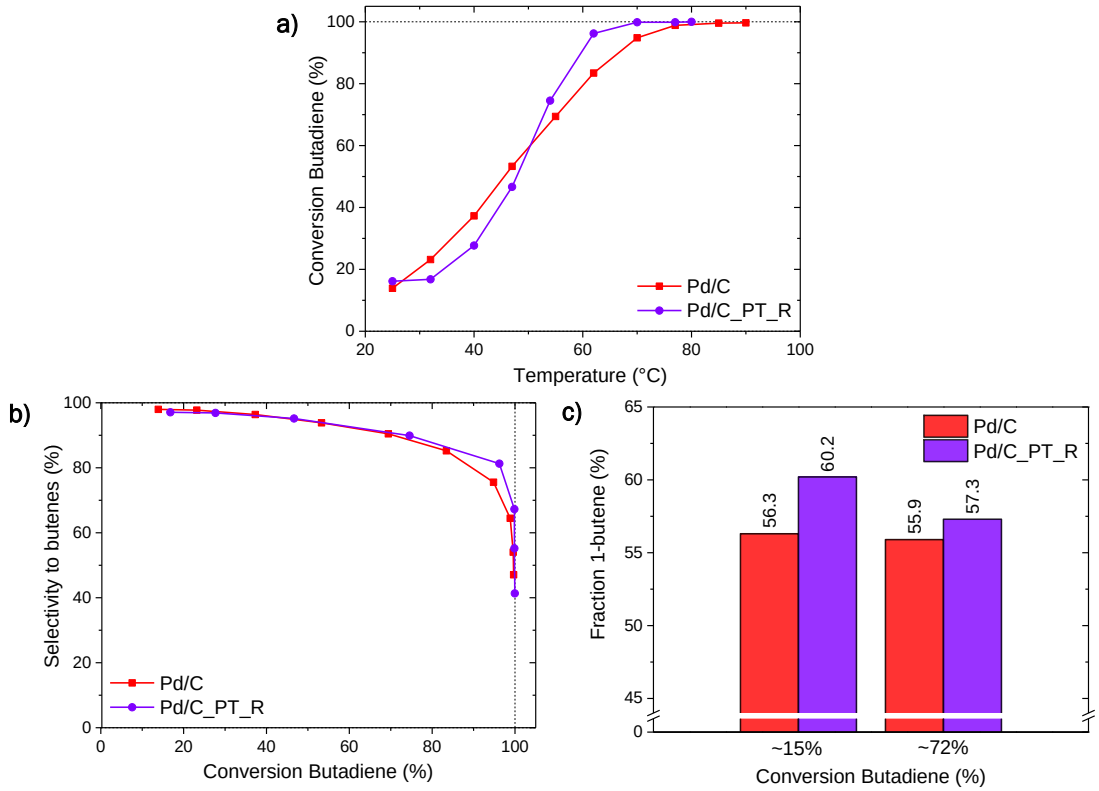

Figure 18: Catalytic performance of the Pd/C catalyst with and without reducing pre-treatment (PT_R); **a)** Turnover frequency as a function of temperature. **b)** Selectivity towards all butenes as a function of butadiene conversion. **c)** Fraction of 1-butene in the C4 product stream at conversion levels around 15% (14-17%) and 72% (69-75%). Amount of Pd loaded in each reactor (µg): 0.598 Pd/C; 0.595 Pd/C_PT_R.

5.4.2 Pre-treatments on Mn promoted Pd catalyst

The effect of doing a PT before performing the catalytic test with a Mn promoted catalyst is investigated. This study is performed on the Mn promoted catalyst, since Mn is easily oxidized back to manganese oxide in air. This would probably result in mainly Mn oxide species in the Mn-Pd/C catalyst in the standard catalytic tests. Therefore, the Mn promoted sample is expected to show the greatest differences in catalytic properties after performing PTs. The oxidation PT might bring the Mn oxide to the surface of the Pd particle. On the other hand, the reduction PT could (partly) reduce the metal oxides again. Combining the two might also have different

effects on catalytic properties. That is why oxidation (O), reduction (R), oxidation-reduction (OR) and reduction-oxidation-reduction (ROR) PTs at 300 °C and their effect on activity and selectivity of the Mn promoted catalyst are researched.

The effect of all these different PTs on the activity are shown in Figure 19a-c. Figure 19a shows that all PTs result in the catalysts needing lower temperatures to reach full conversion. The catalyst without PT needs a temperature of approximately 95 °C, while the catalysts with a O or ROR PT only need temperatures of 70 °C and R and OR approximately 85-90 °C. Besides this, the ROR PT catalyst already has a butadiene conversion of approximately 50% at RT, while the catalyst without PT starts at 20% butadiene conversion at RT. The Pd catalyst starts at a butadiene conversion of around 15%, thus the ROR PT catalyst shows increased conversion levels at RT. It also stands out that the R, OR and ROR PT have different curves, but they all reach full conversion around the same temperatures (80-90°C). For example, this might be an indication that there is a loss of active sites or that mass transfer limitations are influencing the catalysis.

One more thing that stood out in the plot with the conversion as a function of temperature, is displayed in Figure 19b. The oxidation and reduction PT catalysts exhibit a different ramp during the heating (H) and during the cooling (C). For the O PT and R PT, the cooling ramps end at room temperature at approximately 55% and 30% butadiene conversion, while the heating ramp started around 25% and 10% butadiene conversion at room temperature, respectively. This could indicate the activation of a catalyst during the catalytic test. For the O PT, this activation could be due to reduction of the oxidized catalyst in the reducing conditions of the catalytic test at higher temperatures. However, if the reduction of the catalyst after the oxidation PT resulted in the higher butadiene conversion at room temperature, then it is also expected that the OR PT would start at the same conversion level at room temperature as the ending of the oxidated cooling ramp. Yet, this is not the case. As can be seen in Figure 19b, the OR PT catalyst starts with even lower butadiene conversion at room temperature as the heating ramp of the O PT catalyst did. One thing that catches the eye in this plot is that the ROR treated catalyst does show a similar starting level of butadiene conversion (~50%) as the activated O PT catalyst. The activation during catalysis might also be a result of particle resizing. To study that, the spent catalyst that was pre-treated with an O PT, was studied with TEM analysis. Since the catalyst is 100 times diluted with GNP, it was very hard to find actual catalyst particles. However, some were found and analysed and the mean particle size of the spent catalyst was determined. The Mn-Pd/C catalyst before catalysis had an average particle size of 6.4 nm with a standard deviation of 1.8 nm. The spent Mn-Pd/C PT_O catalyst had an average particle size of 6.8 ± 1.6 nm. No substantial change in particle size was observed, so this is probably not the reason for the observed activation of the catalyst during catalysis.

It might also be a result of the presence or absence of PdC_x or β-PdH_x species in the catalyst. As stated in chapter 2.2, it is known that the presence of β-PdH_x species can increase the catalyst activity and decrease the catalyst selectivity. It could be that the O PT removes β-PdH_x species and that these species form again during the catalysis at higher temperatures. After catalysis, the reformed β-PdH_x species in the catalyst could increase catalyst activity in the cooling ramp. This would explain why the catalyst diplays higher activity at room temperature in the cooling slope than in the heating slope. In that case, it is also expected that the selectivity decreases in the cooling slope. However, this is not observed for the catalyst, see Figure 19c. On the contrary, the total selectivity is higher in the cooling ramp than in the heating ramp.

For the R PT, the activity is also increased during the heating and cooling cycle, but the selectivity is pretty similar for the heating and cooling ramp, see Figure 19b and c. This is hard to explain, since an increase in activation might mean a higher amount of β-PdH_x species that are formed during the catalysis. But after a reducing pre-treatment, we do not expect this value to increase by much during the catalysis. It would even make more sense if the activity would decrease during catalysis after a hydrogenation treatment, as the formation of PdC_x species that can be formed during the catalysis conditions, will prevent more formation of β-PdH_x species.

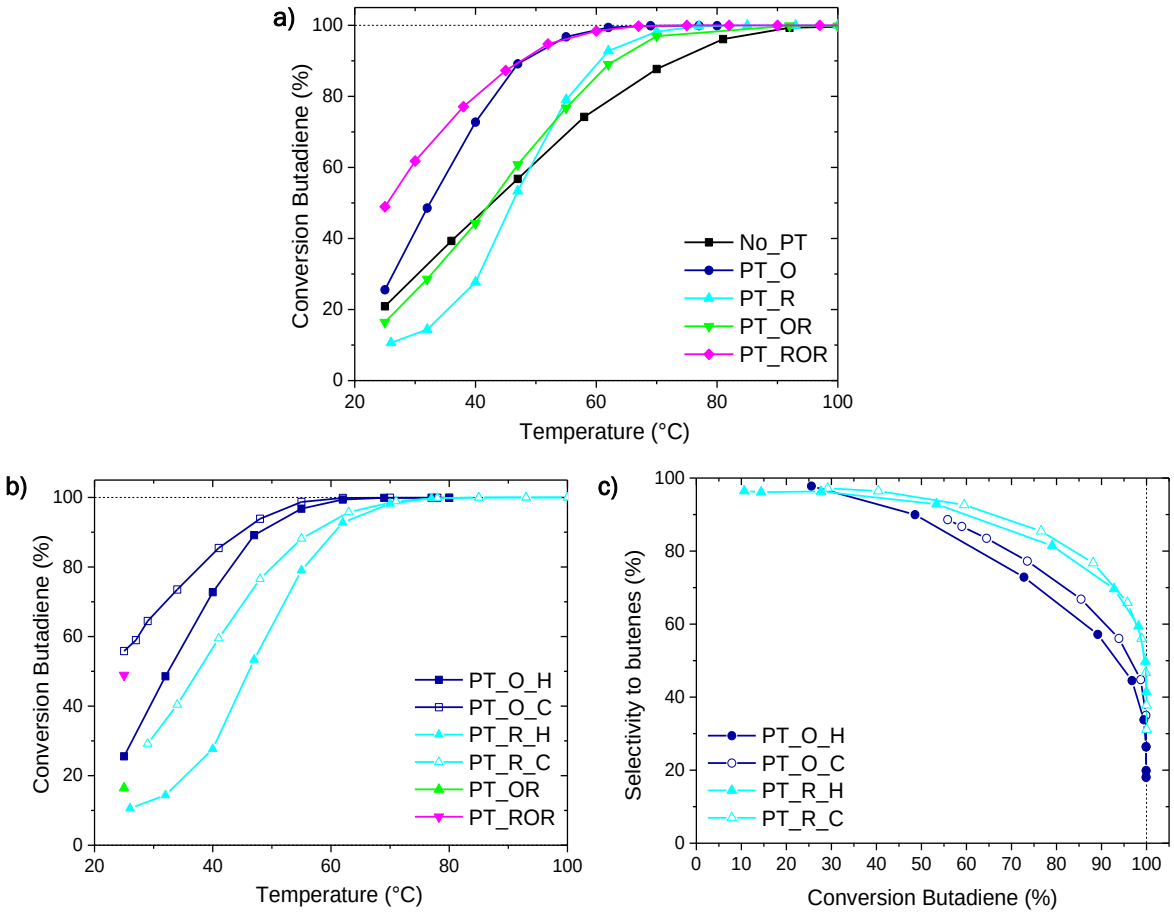

Figure 19 Catalytic performance of the Mn-Pd/C catalyst with and without PTs. The four different PT's are oxidation (O), reduction (R), oxidation-reduction (OR) and reduction-oxidation-reduction (ROR); **a)** Conversion of butadiene as a function of temperature of all PTs. **b)** Conversion of butadiene as a function of temperature for the O and R PT, the heating (H) and cooling (C) ramps of these PTs are shown. The conversion of butadiene at room temperature is shown for the OR and ROR PT.**c)** Selectivity towards all butenes as a function of butadiene conversion of the heating (H) and cooling (O) ramp the PT_O and PT_R. Amount of Pd loaded in each reactor (µg): 0.600 No_PT; 0.602 PT_O; 0.593 PT_R; 0.606 PT_OR; 0.611 PT_ROR.

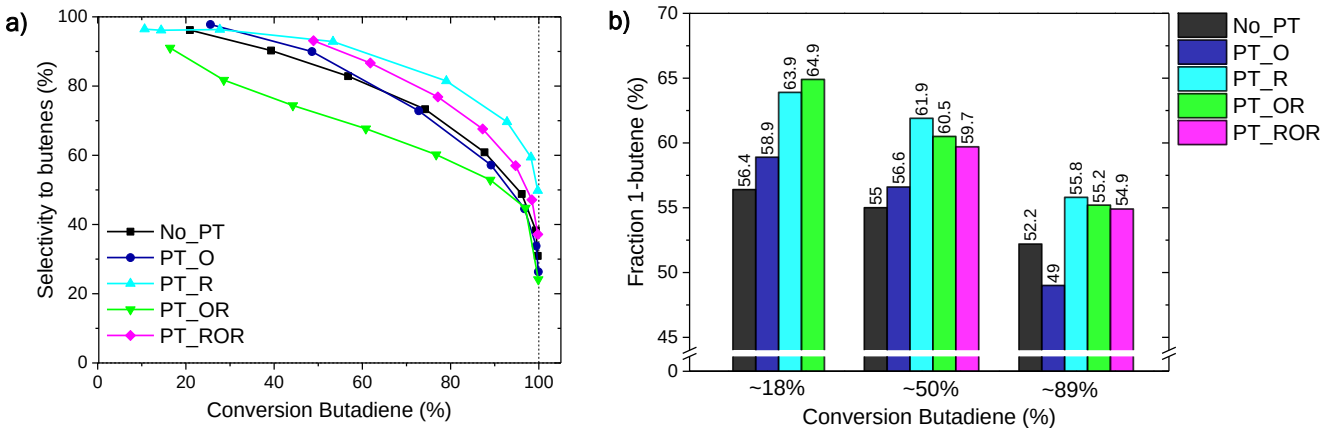

Figure 20: Catalytic performance of the Mn-Pd/C catalyst with and without PTs. The four different PT's are oxidation (O), reduction (R), oxidation-reduction (OR) and reduction-oxidation-reduction (ROR); **a)** Selectivity towards all butenes as a function of butadiene conversion. **b)** Fraction of 1-butene in the C4 product stream at conversion levels around 18% (14-21%), 50% (44-57%) and 89% (87-93%). The exact fraction of 1-butene of each catalyst is displayed above the column. Amount of Pd loaded in each reactor (µg): 0.600 No_PT; 0.602 PT_O; 0.593 PT_R; 0.606 PT_OR; 0.611 PT_ROR.

The selectivity towards all butenes and the fraction of 1-butene in the C4 product stream at certain butadiene conversion levels are shown in Figure 20a and b, respectively. The R and ROR PTs seem to increase the total selectivity towards all butenes. This might suggest that having a reduction as the last PT is the reason why the total selectivity increases. On the contrary; the OR PT results in a lower total selectivity. When looking at the fraction of 1-butene in the C4 product stream in Figure 20b, the selectivity towards 1-butene is higher for every PT catalyst at low butadiene conversion. Only the O PT catalyst has a lower fraction of 1-butene in the stream at high conversion, compared to the not pre-treated catalyst. With these results we can conclude that having a reducing step as last PT step will increase the selectivity towards 1-butene. This could be due to the reduction of the Pd in the catalyst, since these results were also observed for the monometallic Pd catalyst. However, a R PT for the monometallic Pd catalyst didn't influence the selectivity towards the total of butenes much, whereas a influence of PTs is observed when performed on the Mn-Pd/C catalysts.

Even though the obtained results are fascinating, they are hard to explain. To gain more insight into the effects of performing a PT, a suggestion for further research is to study the PTs on a different bimetallic promoted Pd catalyst. For example on the Ag-Pd/C catalyst. This catalyst already shows an increase in 1-butene selectivity compared to the monometallic Pd. It will be of particular interest to investigate if the performance of a R PT will improve the 1-butene selectivity of that promoted Pd catalyst even more. Besides that, the Ag-Pd/C catalyst has the best total selectivity of the promoted catalysts, even though it is still lower than the monometallic Pd. It will be interesting to see whether a R PT will increase the total selectivity of the Ag-Pd/C, maybe even to similar values as the monometallic Pd with a R PT.

6. Conclusions

A synthesis method has been established to prepare promoted catalysts of comparable size, namely sequential incipient wetness impregnation with a subsequent reduction. This method leads to promoted Pd catalysts with the desired mol ratio of promoter metal to Pd of 1:10. Moreover, the catalysts all displayed an uniform particle distribution over the support as determined by TEM. Analysis of TEM images showed a narrow particle size distribution for each catalyst, with surface averaged particle sizes of approximately 6-11 nm. From characterisation with XRD, a lattice contraction was calculated for the Pd(111) lattice. A lattice contraction was observed for the Mn, Cu, Zn and Ag promoted Pd catalysts. Mn and Ag exhibited comparable lattice contractions, as did Cu and Zn, which were respectively 0.46% and 0.51%, and 0.97% and 0.91%. However, it is unclear if these values fall into the margin of error or if they are really due to the lattice contraction of Pd. TPR analysis shows that the addition of metal oxides to the carbon surface leads to a higher hydrogen uptake for the reduction of the carbon support and sometimes also leads to lower reduction temperatures. Moreover, Pd probably promotes the reduction of ZnO and possibly CuO too. This is also expected for the promoter metals Mn and Ag, but this could not be investigated since the AgO_2(-Pd)/C and MnO_2/C catalysts were not measured with TPR.

During the selective hydrogenation of butadiene, all promoted Pd catalysts needed higher temperatures (90-140 °C) to reach full conversion compared to the monometallic Pd catalyst (80 °C). The K promoted catalyst is the only promoted catalyst that shows a higher TOF than the monometallic Pd catalyst at lower temperatures. At 25 °C the K-Pd/C catalyst exhibits a TOF of approximately 40 $mol_{bd}/mol_{surface\ Pd}\ s^{-1}$and retains its higher TOF values until around 45 °C. At higher temperatures, the monometallic Pd/C catalyst shows the highest TOF. The Cu and Mn promoted samples show similar TOF values at 25 °C but have a lower TOF than Pd/C at full conversion. The Ag and Zn promoted catalysts show lower activity in the whole temperature range. Nevertheless, all catalysts have a high activity for the hydrogenation of butadiene compared to other transition metals.

The monometallic Pd catalyst does exhibit the highest selectivity towards the sum of all butenes in the selective hydrogenation reaction of butadiene. Ag-Pd/C displays slightly lower total butene selectivity compared to Pd/C. The Mn-,Cu-, Zn- and especially K-Pd/C catalysts have a much lower total selectivity. Besides a reasonably high total selectivity, the Ag promoted catalyst shows a higher 1-butene fraction in the C4-product stream than Pd/C, both at low and high conversion levels. The Zn and Cu promoted samples also exhibit a higher 1-butene selectivity. The K and Mn promoted samples display similar 1-butene selectivity at lower conversion, but this 1-butene selectivity decreases at higher conversion. This can be explained by the different 1-butene isomerisation properties of the catalysts. None of the catalysts reach a full conversion of 1-butene, even at higher temperatures. Furthermore, the K promoted and monometallic Pd catalyst exhibit a much higher isomerisation rate than the other catalysts, with the Ag and Zn promoted catalyst displaying the lowest isomerisation activity. At 90 °C, the Ag and Zn promoted catalysts displayed 1-butene TOF values lower than 40 $mol_{1\text{-}but}/mol_{surface\ Pd}\ s^{-1}$, while the K-Pd/C and Pd/C reached 1-butene TOF values of around 140 $mol_{1\text{-}but}/mol_{surface\ Pd}\ s^{-1}$. Therefore, we can conclude that the Ag and Zn catalysts convert less 1-butene to form cis- and trans-2-butene and consequently have a higher selectivity towards 1-butene. This could indicate that 1-butene is more easily desorbed from the Ag promoted Pd surface than from a monometallic Pd surface, however the higher n-butane formation of Ag-Pd/C in the selective hydrogenation of butadiene refutes this explanation.

A few possible trends are observed by comparing (isomerisation) activity and selectivity of all catalysts to the relative electronegativity, van der Waals radius (r_{vdw}) of each promoter metal and the XRD derived lattice contraction. For the activity in the selective hydrogenation of butadiene and in the isomerisation of 1-butene, there is no dependence found related to electronegativity or observed lattice contraction. However, the r_{vdw} of the promoter metal does seem to influence the butadiene and isomerisation activity of the Pd catalyst. When a promoter metal with a smaller r_{vdw} is added to the Pd catalyst, both the butadiene and 1-butene TOF seem to increase. The r_{vdw} does also seem to influence the selectivity to all butenes and 1-butene; the larger the promoter atom is, the higher the selectivity. Furthermore, the addition of a metal with a lower electronegativity, and thus more electron donating, seems to decrease the total and 1-butene selectivity. For the XRD derived lattice contraction, no distinct relation is observed between either the (isomerisation) activity or selectivity. Nevertheless, for each trend it is hard to say if the observation is reliable, because in each trend one or more data points do not agree with the observed trend.

Oxidation (O), reduction (R), oxidation-reduction (OR) and reduction-oxidation-reduction (ROR) pre-treatments (PTs) are performed before the catalytic test and the results are studied for the Mn promoted Pd catalysts. All PTs decrease the temperature needed to reach full conversion compared to the non-pre-treated catalyst. The ROR PT increases the butadiene conversion at 25 °C from 20% to 50%. The catalysts that were pre-treated with an O or R PT seemed to get activated during the selective hydrogenation reaction conditions and it is unclear what caused the deactivation in these catalysts. Additionally, performing a R or ROR PT increases the total selectivity and a reducing PT as last step increases the selectivity towards 1-butene. Although the obtained results are difficult to explain, they do provide valuable insights into the potential effects of certain PT conditions on bimetallic Pd catalysts.

7. Outlook

First of all, some adjustments can be made to prepare more comparable catalysts. For instance, it might be rewarding to experiment with the heat treatment and reduction of the K promoted catalysts. Due to the presence of Pd, the KNO_3 might decompose and reduce at lower temperatures than the harsh conditions that were stated in literature for the decomposition of KNO_3. Furthermore, it will be useful to prepare monometallic Mn catalysts, for example to use as a reference for TPR and to study the catalytic activity of a monometallic Mn catalyst. Moreover, the Zn and Mn promoted catalysts can be synthesized using the larger monometallic Pd catalyst, as was done for the other promoted catalysts. In this way, more similar particle sizes might be obtained, which is favourable for the comparison between all catalytic properties. Besides that, the number of monolayers that a promoter metal can form on Pd could be taken into account in the synthesis of the catalysts. It is undesired that the promoter metal is able to cover the whole Pd surface and block all active sites. To accomplish this, the wt.% of promoter metals could be lowered.

Secondly, the exact weight percentage of metals in each catalyst can be studied with inductively coupled plasma optical emission spectroscopy (ICP-OES). In this research, the expected wt.% of metals in the catalysts is calculated based on the assumption that all precursor solution is deposited on the support. Nevertheless, the actual wt.% of metals in the catalysts has not been experimentally determined. However, the wt.% of metal are important in the analysis of the catalytic data. For example, the wt.% of Pd is used to calculate the amount of Pd in each reactor. The amount of Pd in each reactor will influence the activity and selectivity greatly and therefore in this research the amount of Pd in each catalytic test was kept constant at approximately 0.6 ug. If the actual amount differs from the amounts we expect, this would have had a big influence on the catalytic properties. Besides, the amount of Pd in each test is also used for the TOF calculations. Therefore, determining the exact wt.% of metals in each catalyst will be useful.

Furthermore, a monometallic Mn and K reference catalyst and the K and Ag promoted Pd catalysts have not been studied with TPR. This might give more insight into the reduction of the promoter metal oxides and proximity of Pd to those promoter metals.

Besides, TEM analysis can be performed on the spent catalysts that were used to perform the catalytic tests. This analysis could give more insight into possible particle resize effects. This was only done for the oxidation pre-treatment (PT), but not for any of the other catalysts. Besides the oxidation PT, the reduction PT catalyst also showed an increase in activity after catalysis, but this spent catalyst was not analysed with TEM. Moreover, EDX quantification can be performed on more bimetallic catalyst particles to study the composition of the particles. This was only done for the Ag-Pd/C catalyst and this gave the insight that the Ag could be found in/on the Pd particles and that the ratio of Ag to Pd was approximately 0.1 for the average sized particles (9.8 ± 4.4 nm). Extending the same conclusions to the other bimetallic catalysts would be advantageous.

In addition, it is recommended to conduct a more elaborate research on the effects of PTs on bimetallic Pd catalysts by examining other bimetallic promoted Pd catalysts, such as Ag-Pd/C. This catalyst has already demonstrated an increase in 1-butene selectivity compared to the monometallic Pd catalyst. It would be particularly valuable to investigate whether the application of an R PT would further improve the 1-butene selectivity of the promoted Pd catalyst. Furthermore, despite having a lower total selectivity than the monometallic Pd, the Ag-Pd/C catalyst has the best total selectivity among the promoted catalysts. It would be intriguing to see if the implementation of an R PT would enhance the total selectivity of the Ag-Pd/C catalyst, potentially even reaching similar values as the monometallic Pd with an R PT.

Besides, since all the promoter metals that are studied in this research have a lower electronegativity than Pd, it might be beneficial to study the promoting effect of another promoter metal that has a higher electronegativity than Pd. For example, Au might be used as a promoter. Au is also known to be active and highly selective in the hydrogenation reaction of butadiene.[39] Using Au as a promoter will hopefully give more insight into the electronic effects of the promoter metals to Pd and confirm or disprove the trends observed for the activity and 1-butene selectivity.

Additionally, studying the promoted catalysts with Extended X-ray Absorption Fine Structure (EXAFS) might give more insight into the position of the promoter metals in the catalyst. For instance, if they are mainly deposited

on the support or on the Pd nanoparticles. By performing XAS, coordination numbers will be obtained from Pd and promoter metals, which can give more insight on the proximity of the promoter and Pd atoms. This is important for this research, since it is now unclear if and how the promoter metals interact with the Pd atoms. Besides this, it might give insight into the possible formation of Pd active site ensembles which would lead to a geometric promotional effect.

Moreover, by changing the partial pressures of reaction gasses in the catalytic tests, reaction-order calculations can be performed with the data obtained. The reaction orders could improve the understanding of the reaction mechanism that the promoted Pd particles follow to hydrogenate butadiene.

Furthermore, catalytic tests to study the stability of the promoted catalysts can be performed to get an even better insight into the promoting effects of the promoter metals on the catalytic properties. To study the stability in a catalytic test, the test can be run for several hours on the same temperature. The results will show if the activity and selectivity of the catalyst is stable over a longer period of time.

Finally, the promoted catalysts can be studied in different selective hydrogenation reactions to research its catalytic properties in other reactions. A reaction that could be of interest, is the selective hydrogenation of acetylene, which has similar applications as butadiene.[9] Besides, this might be interesting because the selective hydrogenation of acetylene involves the partial hydrogenation of a triple bond instead of a diene. Secondly, the selective hydrogenation of cinnamaldehyde also involves another type of partial hydrogenation, namely the selective hydrogenation of an alkene, bonded to a ketone. Additionally, this reaction is widely studied and has a large number of applications in industry.[84]

8. Acknowledgements

Since rejoining the Materials Chemistry & Catalysis (MCC) group almost a year ago, I have gained new knowledge and insights into research, synthesis, characterisation techniques, and particularly catalysis. During my thesis, I received help and got advice from so many people. Everyone was always willing to help me out or discuss about research. I would like to thank all these people. Besides that, I would like to acknowledge some specific people for their help during my thesis:

First and foremost, I would like to thank **Oscar Brandt Corstius** for being my daily supervisor and guiding me through this project. You have always supported me when I needed it, but gave me the freedom to conduct and form my own research as well. Furthermore, I enjoyed all of our discussions and I appreciate it that you gave me a lot of constructive feedback during my thesis. Besides, I am grateful for all the TEM measurements that you have performed for me. Finally, I want to thank you again for helping me with my internship interview and giving me feedback on all my presentations and on my poster.

Secondly, I would like to thank **Prof. Petra de Jongh** and **Dr. Jessi van der Hoeven** for giving me the opportunity of doing this research and being my examinators. Besides that, thank you for providing me with advice and new ideas to try during my research.

I thank **Hidde Nolten** for the nice discussions on my project and his help with performing the pre-treatment experiments.
I thank **Kristiaan Helfferich** for lending me some lab equipment and performing TEM measurements for me.
I thank **Kristiaan Helfferich, Suzan Schoemaker** and **Claudia Keijzer** for stepping in multiple times as supervisor in Oscar's absence.
I thank **Matt Peerlings** for letting me use his Zn precursor salt.
I thank **Claudia Keijzer** for letting me use her Mn precursor salt.
I thank **Laura Barberis** for discussing the reduction process of Zn with me.
I thank **Francesco Mattarozzi** for advising me about the Ag promoted catalyst synthesis.
I thank **Marta Perxés** for discussing and sharing literature on the restructuring of bimetallic particles with me.
I thank **Jan Willem de Rijk** for his help with the selective hydrogenation setup.
I thank **Remco Dalebout** for training me to do TPR measurements.
I thank **Dennie Wezendonk** for performing TGA measurements for me and training me to use the XRD apparatus.
I thank **Joren Dorresteijn**, **Suzan Schoemake**r and **Tom Welling** for performing nitrogen physisorption measurements for me.

I thank my **fellow master students** for their fruitful discussions, for keeping the spirit high and creating such a nice ambience during my research and all the coffee and lunch breaks.

I thank everyone in the **MCC group** for teaching me so many things. Moreover, for creating such a pleasant working environment and organising many awesome events, drinks and activities that I always loved joining.

9. Layman's abstract

Plastics are produced out of alkenes and therefore, the demand for alkenes is very large and still growing. An alkene, is a molecule consisting entirely of hydrogen and carbon, with only one double bond. To produce alkenes more purely, we need to remove small amounts of molecules with two double bonds from the gas stream. This can be done by selective hydrogenation, which is the addition of hydrogen to one of the two double bonds, creating an alkene. It is however unwanted to remove both double bonds which would lead to the formation of alkanes.

A catalyst will improve this reaction. A catalyst is a compound which makes a reaction go faster, without it being consumed or changed during the reaction. In this research, we will study Palladium (Pd) as a catalyst. Pd is a metal, which has a very high activity for this reaction, but not a high selectivity. The activity of a reaction means how much of the product is made every second. In this reaction it is desired to only produce the alkenes as a product, and not any by-products such as the alkanes. The selectivity expresses a ratio of how much products are made versus the by-products. The higher this ratio is, the better. To improve the selectivity of the catalyst, another metal can be added to the Pd catalyst. This metal is called a promoter to Pd.

The aim of this research is to study the effects of several promoter metals: Potassium (K), Manganese (Mn), Copper (Cu), Zinc (Zn) and Silver (Ag) on a Pd catalyst. The exact reaction that was studied is displayed in Figure 21. It is the selective hydrogenation of 1,3-butadiene in an excess of propene. We want to remove 1,3-butadiene by adding hydrogen to one of its double bonds. This will form 1-butene, our desired product. Moreover, 1-butene is able to change its shape to form trans-2-butene and cis-2-butene. We also wish to keep propene the same as it is in the starting gas stream. We do not want to hydrogenate to form the alkane by-products, butane and propane.

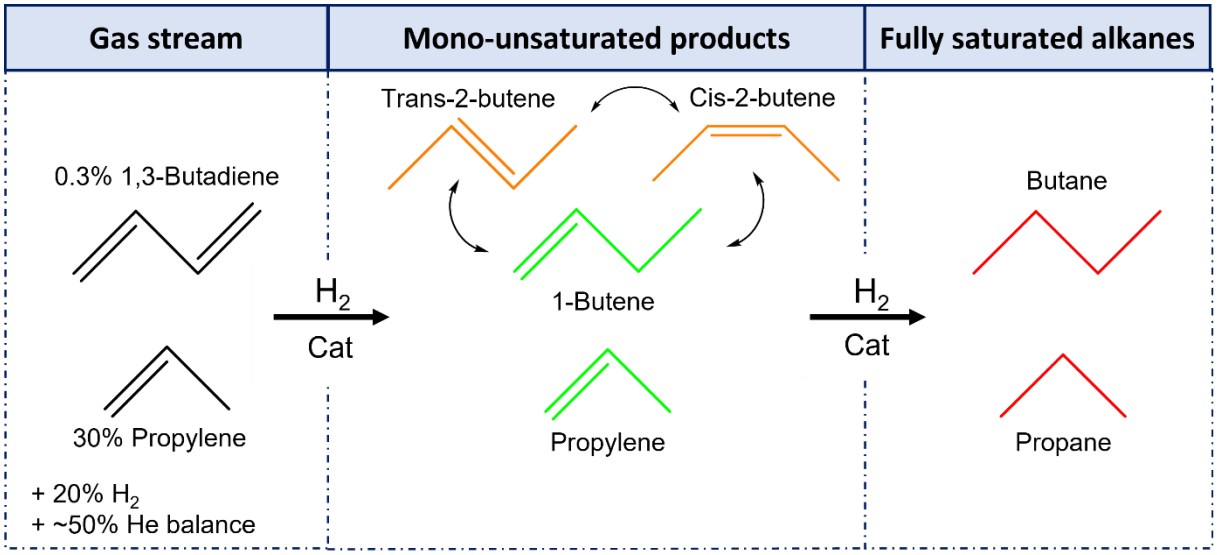

Figure 21: The selective hydrogenation of 1,3-butadiene to butenes in an excess of propylene. H_2 means hydrogen and cat means catalyst. The gas stream consists of a small impurity of 1,3-butadiene, propylene, hydrogen and a helium balance. It is desired to produce the following alkenes; 1-butene (green), trans-2-butene and cis-2-butene (both orange). It is unwanted to form the alkanes, butane and propane, indicated in red.

A method has been established to prepare the catalysts. In this method, we first make a Pd catalyst by mixing the support and a carefully chosen amount solution of a Pd salt and water. A support is a compound that is needed to keep the metals stable, in this research a Carbon support (C) is used. After the mixing, the catalyst is dried and heat treated to remove the salt and the water and form Pd particles. Subsequently, a salt of the promoter metal is added and the catalyst is again dried and heat treated. This resulted in catalysts with a ratio of promoter metal to Pd of 1:10, which was also desired. Analysis showed that the catalysts are distributed evenly over the support and the particle sizes are approximately 6 to 11 nanometer, which is approximately 20 million times smaller than a usual soccer ball. It was also determined that Cu and possibly Zn could be in close proximity to Pd.

Overall, the catalyst with only Pd yielded the highest activity and selectivity. Only at lower temperatures, the Pd catalyst with K added exhibited a higher activity. Nevertheless, all catalysts still showed a higher activity compared to other metals. The Pd with Ag promoted catalyst had the highest selectivity towards the sum of all butenes of all the promoted catalysts, which was just a little bit lower than the Pd catalyst itsself. The Pd catalyst with Ag added displayed a higher selectivity to specifically 1-butene, which is favourable. The Pd catalysts with Zn and Cu also showed this increase in 1-butene selectivity. By contrast, the K and Mn promoted Pd catalysts decreased this selectivity at higher conversion.

These results can be explained by the isomerisation process, which was also studied here. The isomerisation process is the change that 1-butene can make to cis-2-butene and trans-2-butene. The catalyst can improve this process, which results in more 1-butene that is converted to cis-2-butene and trans-2-butene. The catalyst with only Pd, is a lot better at improving this process, than the Pd catalyst with Ag, Zn or Cu on it. Because the Pd catalyst converts more 1-butene, the ratio of 1-butene will decrease in the product composition, which explains the lower 1-butene selectivity that was observed for the Pd catalyst.

Every metal has certain properties, for instance, how big the metal atom is. Besides this, a property of metals is the electronegativity. The electronegativity is a way to express whether the metal would rather attract an electron or donate some of its electrons. If the electronegativity of a metal is larger than another metal, it will steal a part of its electrons. In this research, it was studied if these metal properties could explain the results that were obtained for the activity and selectivity. The activity only seemed to depend on the atom size of a metal; the smaller the atom, the higher the activity. The selectivity was influences by two things: the electronegativity and the promoter atom size. The selectivity increases when the electronegativity is small. Besides, when a larger atom is used as a promoter, the selectivity increases.

Lastly, a study was conducted on the effect of pre-treatments. When a pre-treatment (PT) is performed, the catalyst will be heated to 300 °C in a certain gas just before the reaction experiments. Several PT types were studied by using two different types of gas in the PT; oxygen and hydrogen. When using oxygen, the PT is called an oxidation. When using hydrogen, the PT is called a reduction. Oxidation (O), reduction (R), oxidation-reduction (OR) and reduction-oxidation-reduction (ROR) PTs were performed and studied. The PTs were all performed on the Pd catalyst with Mn added to it. All the PTs decreased the temperature which is needed to convert all the 1,3-butadiene in the stream, compared to the catalyst that had no PT. Furthermore, performing a R or ROR PT increased the total selectivity. Finally, when the last step of the PT was a R, the selectivity towards 1-butene increased.

10. Appendices

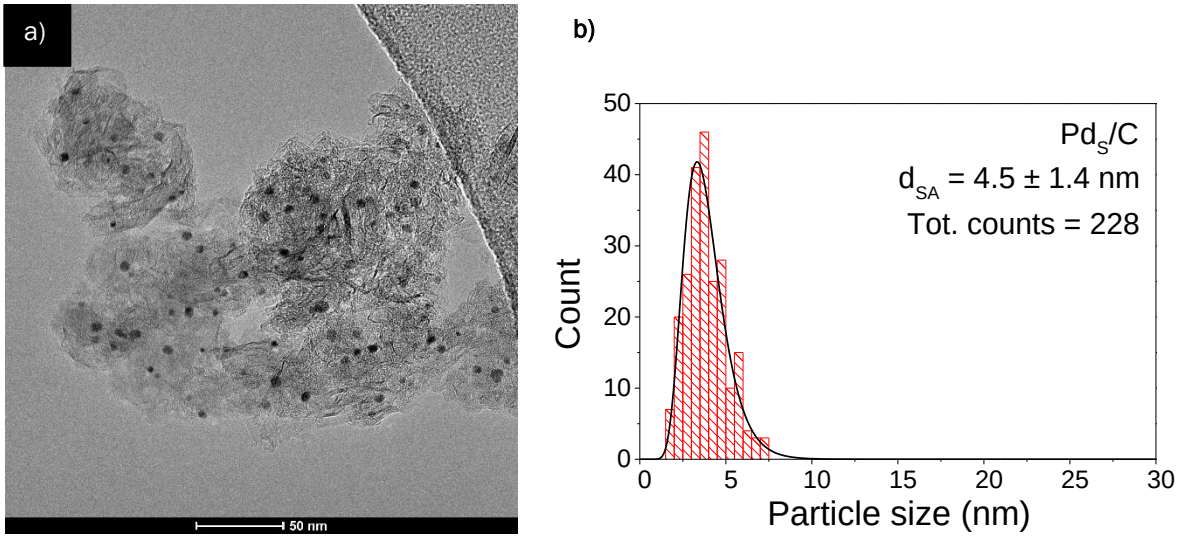

Figure A1: a) TEM image of Pd catalyst with smaller particle size (Pd_S/C) than Pd/C and **b)** the obtained particle size distribution. The surface averaged particle size and standard deviation and the total counts in the analysis are displayed in the figure.

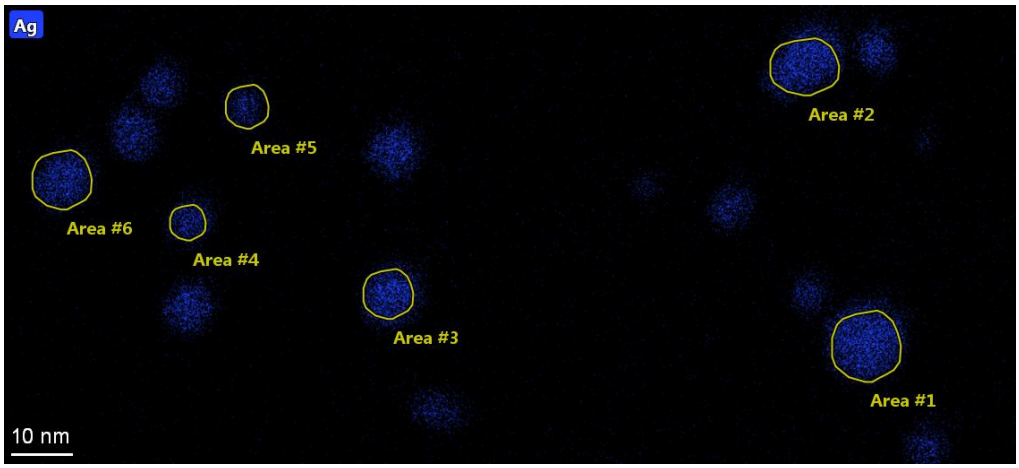

Figure A2: EDX image 1 of the particles that were quantified in the Ag-Pd/C sample.

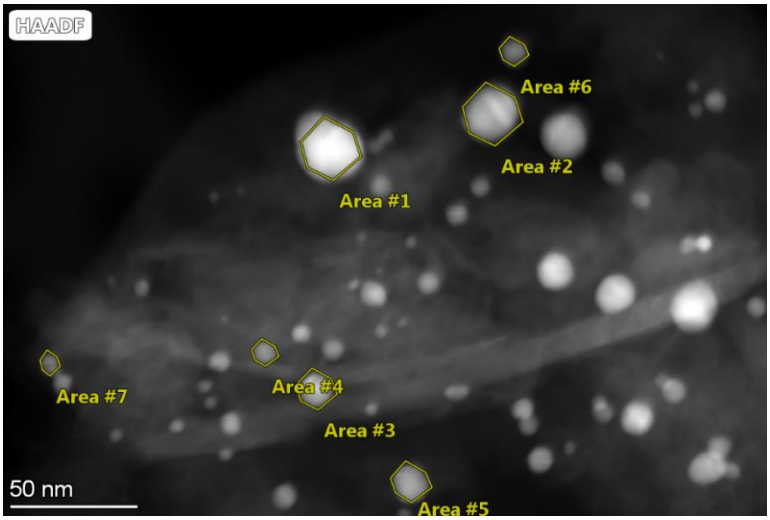

Figure A3: EDX image 2 of the particles that were quantified in the Ag-Pd/C sample

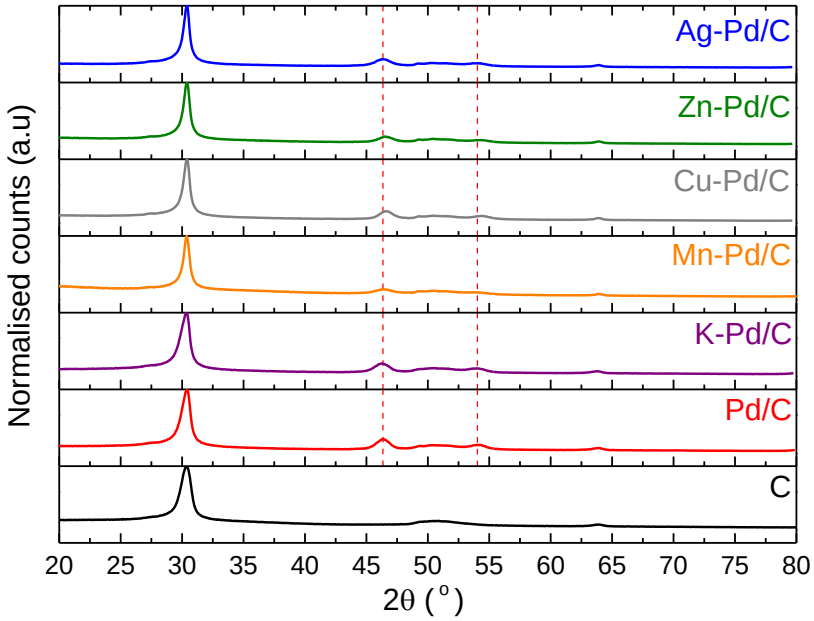

Figure A4: XRD plots of all promoted and monometallic Pd catalysts from 20-80 °2θ.

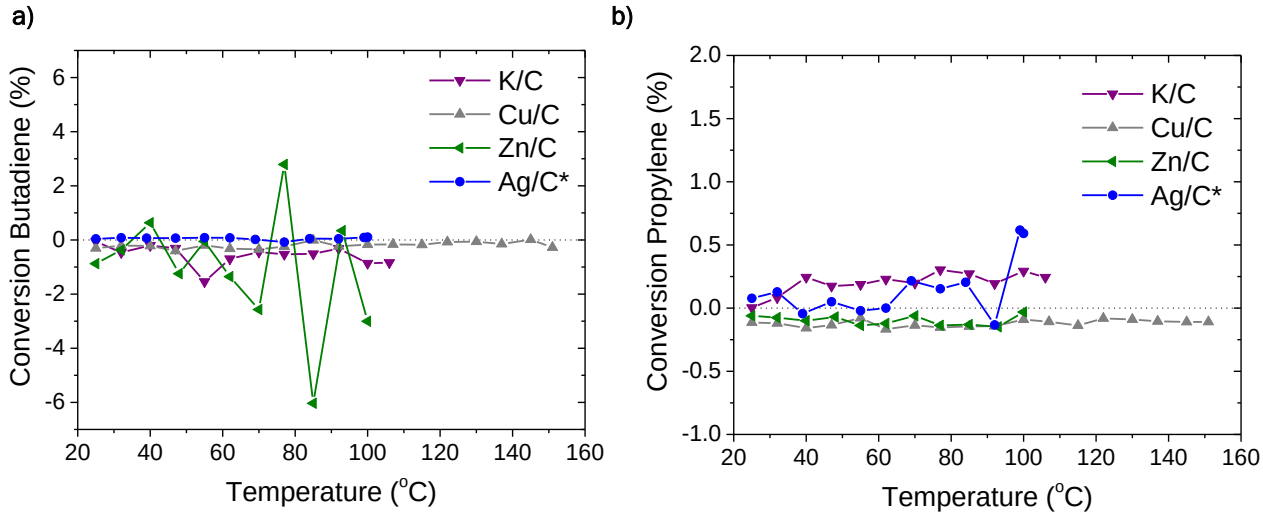

Figure A5: Plots of monometallic K, Cu, Zn and Ag/C reference catalysts. **a)** Conversion of butadiene and **b)** conversion of propylene as a function of temperature. *Ag catalyst was synthesized in light and thus has large Ag particles (±100 nm).

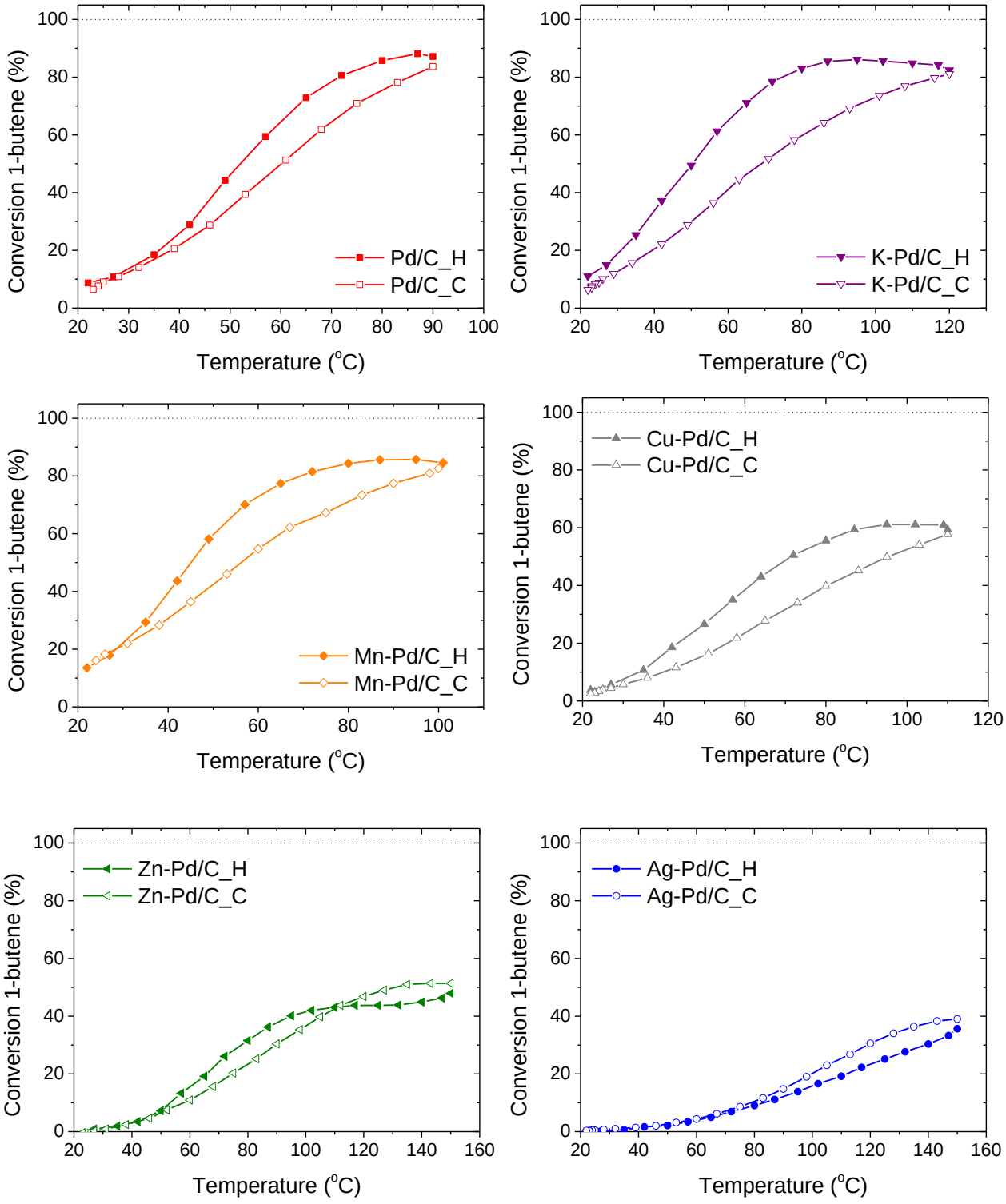

Figure A6: The conversion of 1-butene as a function of temperature in the isomerisation tests, the heating (_H) and cooling (_C) curves of all promoted and monometallic Pd catalysts are displayed.

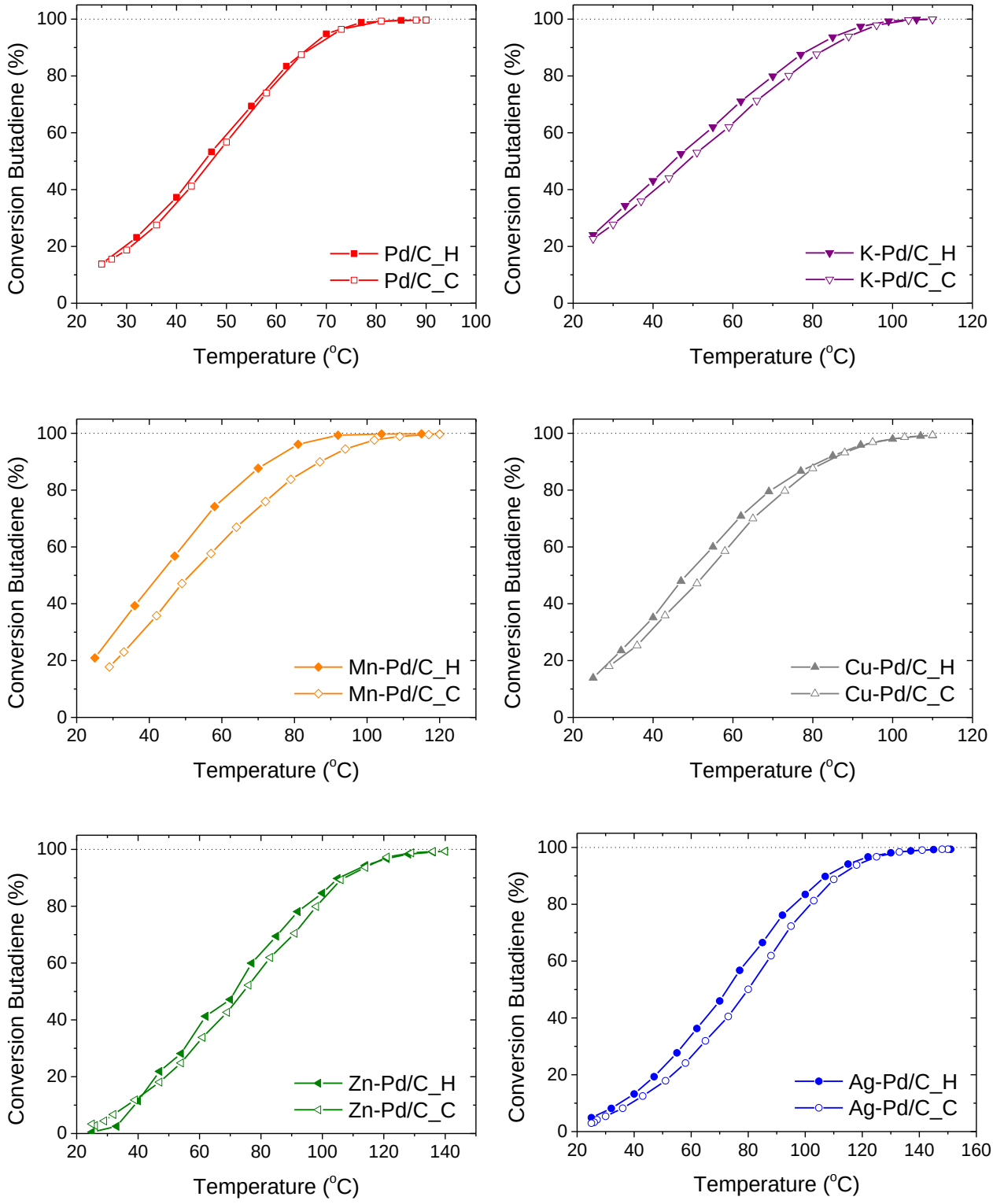

Figure A7: The conversion of butadiene as a function of temperature in the isomerisation tests, the heating (_H) and cooling (_C) curves of all promoted and monometallic Pd catalysts are displayed.

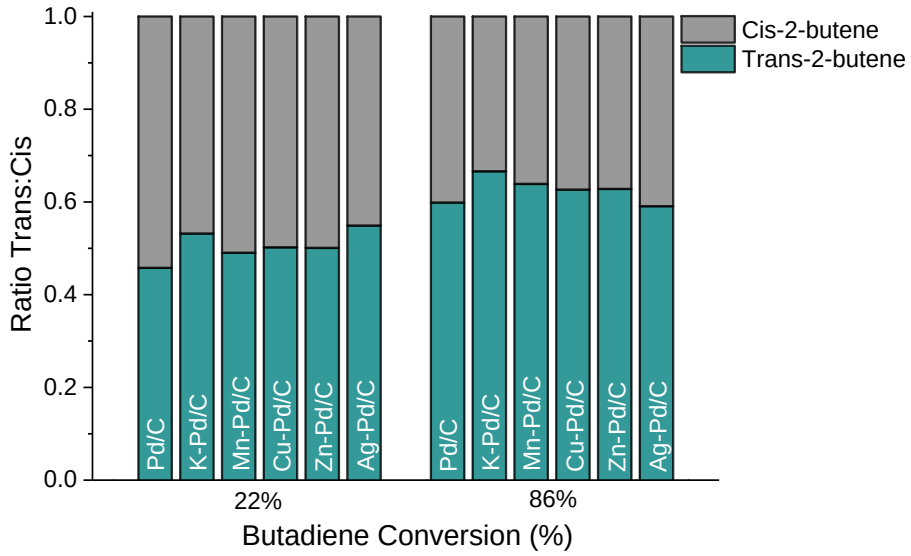

Figure A8: The ratio of trans-2-butene to cis-2-butene in the isomerisation tests at low and high corresponding butadiene conversion for all the promoted and monometallic Pd catalysts.

11. Bibliography

11.1 References

(1) Ertl, G.; Knozinger, H.; Weitkamp, J. *Handbook of Heterogeneous Catalysis*; 1997.

(2) Fechete, I.; Wang, Y.; Védrine, J. C. The Past, Present and Future of Heterogeneous Catalysis. *Catal. Today* **2012**, *189* (1), 2–27. https://doi.org/10.1016/j.cattod.2012.04.003.

(3) Védrine, J. C. Importance, Features and Uses of Metal Oxide Catalysts in Heterogeneous Catalysis. *Chinese J. Catal.* **2019**, *40* (11), 1627–1636. https://doi.org/10.1016/S1872-2067(18)63162-6.

(4) Friend, C. M.; Xu, B. Heterogeneous Catalysis: A Central Science for a Sustainable Future. *Acc. Chem. Res.* **2017**, *50* (3), 517–521. https://doi.org/10.1021/acs.accounts.6b00510.

(5) Yentekakis, I. V.; Chu, W. Advances in Heterocatalysis by Nanomaterials. *Nanomaterials* **2020**, *10* (4), 3–8. https://doi.org/10.3390/nano10040609.

(6) Molnár, Á.; Sárkány, A.; Varga, M. Hydrogenation of Carbon-Carbon Multiple Bonds: Chemo-, Regio- and Stereo-Selectivity. *J. Mol. Catal. A Chem.* **2001**, *173* (1–2), 185–221. https://doi.org/10.1016/S1381-1169(01)00150-9.

(7) Wang, Z. Selective Hydrogenation of Butadiene over Non-Noble Bimetallic Catalysts. **2018**.

(8) Phung, T. K.; Pham, T. L. M.; Vu, K. B.; Busca, G. (Bio)Propylene Production Processes: A Critical Review. *J. Environ. Chem. Eng.* **2021**, *9* (4), 105673. https://doi.org/10.1016/J.JECE.2021.105673.

(9) Takht Ravanchi, M.; Sahebdelfar, S.; Komeili, S. Acetylene Selective Hydrogenation: A Technical Review on Catalytic Aspects. *Rev. Chem. Eng.* **2018**, *34* (2), 215–237. https://doi.org/10.1515/revce-2016-0036.

(10) Yang, Q.; Hou, R.; Sun, K. Tuning Butene Selectivities by Cu Modification on Pd-Based Catalyst for the Selective Hydrogenation of 1,3-Butadiene. *J. Catal.* **2019**, *374*, 12–23. https://doi.org/10.1016/J.JCAT.2019.04.018.

(11) Hou, R. Catalytic and Process Study of the Selective Hydrogenation of Acetylene and 1,3-Butadiene; 2011; Vol. 53.

(12) Cooper, A.; Bachiller-Baeza, B.; Anderson, J. A.; Rodríguez-Ramos, I.; Guerrero-Ruiz, A. Design of Surface Sites for the Selective Hydrogenation of 1,3-Butadiene on Pd Nanoparticles: Cu Bimetallic Formation and Sulfur Poisoning †. *Cite this Catal. Sci. Technol* **2014**, *4*, 1446. https://doi.org/10.1039/c3cy01076g.

(13) Nikolaev, S. A.; Zanaveskin, L. N.; Smirnov, V. V; Averyanov, V. A.; Zanaveskin, K. L. Catalytic Hydrogenation of Alkyne and Alkadiene Impurities from Alkenes. Practical and Theoretical Aspects. *Russ. Chem. Rev.* **2009**, *78* (3), 231–247. https://doi.org/10.1070/rc2009v078n03abeh003893.

(14) Gao, X.; Zhou, Y.; Jing, F.; Luo, J.; Huang, Q.; Chu, W. Layered Double Hydroxides Derived ZnO-Al2O3 Supported Pd-Ag Catalysts for Selective Hydrogenation of Acetylene. *Chinese J. Chem.* **2017**, *35* (6), 1009–1015. https://doi.org/10.1002/cjoc.201600865.

(15) Zhang, L.; Zhou, M.; Wang, A.; Zhang, T. Selective Hydrogenation over Supported Metal Catalysts: From Nanoparticles to Single Atoms. *Chem. Rev.* **2020**, *120* (2), 683–733. https://doi.org/10.1021/acs.chemrev.9b00230.

(16) Hisham A. Maddah. Polypropylene as a Promising Plastic: A Review. *Am. J. Polym. Sci.* **2016**, *6* (1), 1–11. https://doi.org/10.5923/j.ajps.20160601.01.

(17) Kim, W. J.; Moon, S. H. Modified Pd Catalysts for the Selective Hydrogenation of Acetylene. *Catal. Today* **2012**, *185* (1), 2–16. https://doi.org/10.1016/J.CATTOD.2011.09.037.

(18) Beerthuis, R.; de Jongh, P.; de Jong Krijn. *PhD Thesis: Carbon-Supported Copper for Gas-Phase Hydrogenation Catalysis*; 2020.

(19) Massardier, J.; Bertolini, J. C.; Ruiz, P.; Delichère, P. Platinum Single Crystals: The Effect of Surface Structure and the Influence of K and Na on the Activity and the Selectivity for 1,3-Butadiene Hydrogenation. *J. Catal.* **1988**, *112* (1), 21–33. https://doi.org/10.1016/0021-9517(88)90117-0.

(20) Masoud, N.; Delannoy, L.; Calers, C.; Gallet, J. J.; Bournel, F.; de Jong, K. P.; Louis, C.; de Jongh, P. E. Silica-

Supported Au–Ag Catalysts for the Selective Hydrogenation of Butadiene. *ChemCatChem* **2017**, *9* (12), 2418–2425. https://doi.org/10.1002/cctc.201700127.

(21) Méndez, F. J.; Solano, R.; Villasana, Y.; Guerra, J.; Curbelo, S.; Inojosa, M.; Olivera-Fuentes, C.; Brito, J. L. Selective Hydrogenation of 1,3-Butadiene in Presence of 1-Butene under Liquid Phase Conditions with NiPd/Al2O3 Catalysts. *Appl. Petrochemical Res.* **2016**, *6* (4), 379–387. https://doi.org/10.1007/s13203-016-0149-y.

(22) Ball, M. R.; Rivera-Dones, K. R.; Gilcher, E. B.; Ausman, S. F.; Hullfish, C. W.; Lebrón, E. A. L.; Dumesic, J. A. AgPd and CuPd Catalysts for Selective Hydrogenation of Acetylene. **2020**. https://doi.org/10.1021/acscatal.0c01536.

(23) Furlong, B. K.; Hightower, J. W.; Chan, T. Y. L.; Sarkany, A.; Guczi, L. 1,3-Butadiene Selective Hydrogenation over Pd/Alumina and CuPd/Alumina Catalysts. *Appl. Catal. A Gen.* **1994**, *117* (1), 41–51. https://doi.org/10.1016/0926-860X(94)80157-6.

(24) Totarella, G.; Beerthuis, R.; Masoud, N.; Louis, C.; Delannoy, L.; de Jongh, P. E. Supported Cu Nanoparticles as Selective and Stable Catalysts for the Gas Phase Hydrogenation of 1,3-Butadiene in Alkene-Rich Feeds. *J. Phys. Chem. C* **2021**, *125* (1), 366–375. https://doi.org/10.1021/acs.jpcc.0c08077.

(25) Chinayon, S.; Mekasuwandumrong, O.; Praserthdam, P.; Panpranot, J. Selective Hydrogenation of Acetylene over Pd Catalysts Supported on Nanocrystalline α-Al2O3 and Zn-Modified α-Al2O3. *Catal. Commun.* **2008**, *9* (14), 2297–2302. https://doi.org/10.1016/j.catcom.2008.03.032.

(26) Delgado, J. A.; Benkirane, O.; Claver, C.; Curulla-Ferré, D.; Godard, C. Advances in the Preparation of Highly Selective Nanocatalysts for the Semi-Hydrogenation of Alkynes Using Colloidal Approaches. *Dalt. Trans.* **2017**, *46* (37), 12381–12403. https://doi.org/10.1039/c7dt01607g.

(27) Borodziński, A.; Bond, G. C. Selective Hydrogenation of Ethyne in Ethene-Rich Streams on Palladium Catalysts, Part 2: Steady-State Kinetics and Effects of Palladium Particle Size, Carbon Monoxide, and Promoters. *Catal. Rev.* **2008**, *50* (3), 379–469. https://doi.org/10.1080/01614940802142102.

(28) Zhou, H.; Yang, X.; Li, L.; Liu, X.; Huang, Y.; Pan, X.; Wang, A.; Li, J.; Zhang, T. PdZn Intermetallic Nanostructure with Pd − Zn − Pd Ensembles for Highly Active and Chemoselective Semi-Hydrogenation of Acetylene. **2016**. https://doi.org/10.1021/acscatal.5b01933.

(29) Massard, R.; Uzio, D.; Thomazeau, C.; Pichon, C.; Rousset, J. L.; Bertolini, J. C. Strained Pd Overlayers on Ni Nanoparticles Supported on Alumina and Catalytic Activity for Buta-1,3-Diene Selective Hydrogenation. *J. Catal.* **2007**, *245* (1), 133–143. https://doi.org/10.1016/j.jcat.2006.09.014.

(30) Borodziński, A.; Bond, G. C.; Bond, G. C. Selective Hydrogenation of Ethyne in Ethene - Rich Streams on Palladium Catalysts . Part 1 . Effect of Changes to the Catalyst During Reaction Selective Hydrogenation of Ethyne in Ethene-Rich Streams on Palladium Catalysts . Part 1 . Effect of Changes To. **2006**, *4940*. https://doi.org/10.1080/01614940500364909.

(31) Chanerika, R.; Shozi, M. L.; Prato, M.; Friedrich, H. B. The Effect of Coating Pd/Al2O3 and PdAg/Al2O3 Catalysts with [BMIM][DCA] for the Selective Hydrogenation of 1-Octyne in 1-Octene. *ChemCatChem* **2022**. https://doi.org/10.1002/cctc.202201043.

(32) Tew, M. W.; Emerich, H.; Van Bokhoven, J. A. Formation and Characterization of PdZn Alloy: A Very Selective Catalyst for Alkyne Semihydrogenation. *J. Phys. Chem. C* **2011**, *115* (17), 8457–8465. https://doi.org/10.1021/jp1103164.

(33) Cao, Y.; Sui, Z.; Zhu, Y.; Zhou, X.; Chen, D. Selective Hydrogenation of Acetylene over Pd-In/Al2O3 Catalyst: Promotional Effect of Indium and Composition-Dependent Performance. *ACS Catal.* **2017**, *7* (11), 7835–7846. https://doi.org/10.1021/acscatal.7b01745.

(34) Lu, F.; Sun, D.; Jiang, X. Plant-Mediated Synthesis of AgPd/γ-Al2O3 Catalysts for Selective Hydrogenation of 1,3-Butadiene at Low Temperature. *New J. Chem.* **2019**, *43* (35), 13891–13898. https://doi.org/10.1039/c9nj01733j.

(35) Guczi, L.; Schay, Z.; Stefler, G.; Liotta, L. F.; Deganello, G.; Venezia, A. M. Pumice-Supported Cu–Pd Catalysts: Influence of Copper on the Activity and Selectivity of Palladium in the Hydrogenation of Phenylacetylene and But-1-Ene. *J. Catal.* **1999**, *182* (2), 456–462.

https://doi.org/10.1006/JCAT.1998.2344.

(36) Renouprez, A.; Faudon, J. F.; Massardier, J.; Rousset, J. L.; Delichère, P.; Bergeret, G. Properties of Supported Pd–Ni Catalysts Prepared by Coexchange and Organometallic Chemistry. *J. Catal.* **1997**, *170* (1), 181–190. https://doi.org/10.1006/jcat.1997.1729.

(37) Park, Y. H.; Price, G. L. Promotional Effects of Potassium on Pd/Al2O3 Selective Hydrogenation Catalysts. *Ind. Eng. Chem. Res.* **1992**, *31* (2), 469–474. https://doi.org/10.1021/ie00002a003.

(38) Beerthuis, R.; Visser, N. L.; van der Hoeven, J. E. S.; Ngene, P.; Deeley, J. M. S.; Sunley, G. J.; de Jong, K. P.; de Jongh, P. E. Manganese Oxide Promoter Effects in the Copper-Catalyzed Hydrogenation of Ethyl Acetate. *J. Catal.* **2021**, *394*, 307–315. https://doi.org/10.1016/J.JCAT.2020.11.003.

(39) Masoud, N.; Delannoy, L.; Schaink, H.; van der Eerden, A.; de Rijk, J. W.; Silva, T. A. G.; Banerjee, D.; Meeldijk, J. D.; de Jong, K. P.; Louis, C.; de Jongh, P. E. Superior Stability of Au/SiO2 Compared to Au/TiO2 Catalysts for the Selective Hydrogenation of Butadiene. *ACS Catal.* **2017**, *7* (9), 5594–5603. https://doi.org/10.1021/acscatal.7b01424.

(40) Totarella, G.; Rijk, W. De; Delannoy, L.; Jongh, P. E. De. Particle Size Effects in the Selective Hydrogenation of Alkadienes over Supported Cu Nanoparticles. *Chem.Cat.Chem.* **2022**, No. e202200348. https://doi.org/10.1002/cctc.202200348.

(41) van der Hoeven, J. E. S.; Jelic, J.; Olthof, L. A.; Totarella, G.; van Dijk-Moes, R. J. A.; Krafft, J.-M.; Louis, C.; Studt, F.; van Blaaderen, A.; de Jongh, P. E. Unlocking Synergy in Bimetallic Catalysts by Core–Shell Design. *Nat. Mater.* **2021**, *20* (9), 1216–1220. https://doi.org/10.1038/s41563-021-00996-3.

(42) Huang, J.; Reque Odoom-Wubah, T.; Jing, X.; Sun, D.; Gu, Z.; Li, Q. Plant-Mediated Synthesis of Zinc Oxide Supported Nickel-Palladium Alloy Catalyst for the Selective Hydrogenation of 1,3-Butadiene. **2017**. https://doi.org/10.1002/cctc.201601178.

(43) Bond, G. C. Hydrogenation of Alkadienes and Poly-Enes. *Met. React. Hydrocarb.* **2006**, 357–394. https://doi.org/10.1007/0-387-26111-7_8.

(44) Bond, B. G. C.; Webb, G.; Wells, P. B.; Winterbottom, J. M. Bond, Webb, Wells, and TVinterbottom : 587. The Hydrogenation of Alkadienes. Part I. **1963**, No. 3218, 3218–3227.

(45) Bates, B. A. J.; Phillipson, J. J.; Wells, P. B. Inorg. Phys. Theor. 2435. **1969**.

(46) Moyes, R. B.; Wells, P. B.; Grant, J.; Salman, N. Y. Electronic Effects in Butadiene Hydrogenation Catalysed by the Transition Metals. *Appl. Catal. A Gen.* **2002**, *229* (1–2), 251–259. https://doi.org/10.1016/S0926-860X(02)00033-9.

(47) H. Lindlar, R. D. Palladium Catalyst for Partial Reduction of Acetylenes. *Org. Synth.* **1966**, *46* (September), 89. https://doi.org/10.15227/orgsyn.046.0089.

(48) Tew, M. W.; Janousch, M.; Huthwelker, T.; Van Bokhoven, J. A. The Roles of Carbide and Hydride in Oxide-Supported Palladium Nanoparticles for Alkyne Hydrogenation. *J. Catal.* **2011**, *283* (1), 45–54. https://doi.org/10.1016/j.jcat.2011.06.025.

(49) Bugaev, A. L.; Guda, A. A.; Pankin, I. A.; Groppo, E.; Pellegrini, R.; Longo, A.; Soldatov, A. V; Lamberti, C. The Role of Palladium Carbides in the Catalytic Hydrogenation of Ethylene over Supported Palladium Nanoparticles. *Catal. Today* **2019**, *336* (January), 40–44. https://doi.org/10.1016/j.cattod.2019.02.068.

(50) Bugaev, A. L.; Usoltsev, O. A.; Guda, A. A.; Lomachenko, K. A.; Pankin, I. A.; Rusalev, Y. V.; Emerich, H.; Groppo, E.; Pellegrini, R.; Soldatov, A. V.; Van Bokhoven, J. A.; Lamberti, C. Palladium Carbide and Hydride Formation in the Bulk and at the Surface of Palladium Nanoparticles. *J. Phys. Chem. C* **2018**, *122* (22), 12029–12037. https://doi.org/10.1021/acs.jpcc.7b11473.

(51) Zhao, X.; Chang, Y.; Chen, W. J.; Wu, Q.; Pan, X.; Chen, K.; Weng, B. Recent Progress in Pd-Based Nanocatalysts for Selective Hydrogenation. *ACS Omega* **2022**, *7* (1), 17–31. https://doi.org/10.1021/acsomega.1c06244.

(52) Mejía, C. H.; Van Deelen, T. W.; De Jong, K. P. Activity Enhancement of Cobalt Catalysts by Tuning Metal-Support Interactions. *Commun. Chem.* **2018**. https://doi.org/10.1038/s41467-018-06903-w.

(53) Monguchi, Y.; Ichikawa, T.; Sajiki, H. Recent Development of Palladium-Supported Catalysts for

Chemoselective Hydrogenation. *Chem. Pharm. Bull.* **2017**, *65* (1), 2–9. https://doi.org/10.1248/cpb.c16-00153.

(54) Kuan, C.; Chiang, C.; Lin, S.; Huang, W. Characterization and Properties of Graphene Nanoplatelets / XNBR Nanocomposites. **2018**, *26* (1), 59–68. https://doi.org/10.1177/096739111802600107.

(55) Dobrezberger, K.; Bosters, J.; Moser, N.; Yigit, N.; Nagl, A.; Fo, K.; Lennon, D.; Rupprechter, G. Hydrogenation on Palladium Nanoparticles Supported by Graphene Nanoplatelets. **2020**. https://doi.org/10.1021/acs.jpcc.0c06636.

(56) National Center for Biotechnology Information (2022). PubChem Periodic Table of Elements https://pubchem.ncbi.nlm.nih.gov/periodic-table/#property=GroupBlock (accessed Dec 18, 2022).

(57) Okamoto, H. Supplemental Literature Review of Binary Phase Diagrams: Ag-Co, Ag-Er, Ag-Pd, B-Ce, Bi-La, Bi-Mn, Cu-Ge, Cu-Tm, Er-Y, Gd-Tl, H-La, and Hg-Te. *Journal of Phase Equilibria and Diffusion*. 2015, pp 10–21. https://doi.org/10.1007/s11669-014-0341-7.

(58) Okamoto, H. Supplemental Literature Review of Binary Phase. *J. Phase Equilibria Diffus.* **2016**, *37* (6), 726–737. https://doi.org/10.1007/s11669-016-0487-6.

(59) Povoden-Karadeniz, E.; Lang, P.; Moszner, F.; Pogatscher, S.; Ruban, A. V.; Uggowitzer, P. J.; Kozeschnik, E. Thermodynamics of Pd-Mn Phases and Extension to the Fe-Mn-Pd System. *Calphad Comput. Coupling Phase Diagrams Thermochem.* **2015**, *51*, 314–333. https://doi.org/10.1016/j.calphad.2015.09.003.

(60) Li, M.; Du, Z.; Guo, C.; Li, C. A Thermodynamic Modeling of the Cu-Pd System. *Calphad Comput. Coupling Phase Diagrams Thermochem.* **2008**, *32* (2), 439–446. https://doi.org/10.1016/j.calphad.2008.04.004.

(61) Vizdal, J.; Kroupa, A.; Popovic, J.; Zemanova, A. The Experimental and Theoretical Study of Phase Equilibria in the Pd-Zn (-Sn) System. *Adv. Eng. Mater.* **2006**, *8* (3), 164–176. https://doi.org/10.1002/adem.200500248.

(62) Okamoto, H. Li-Pd (Lithium-Palladium). *J. Phase Equilibria* **1993**, *14* (5), 653. https://doi.org/10.1007/BF02669164.

(63) Park, Y. H.; Price, G. L. Potassium Promoter for Palladium on Alumina Selective Hydrogenation Catalysts. *J. Chem. Soc. Chem. Commun.* **1991**, No. 17, 1188–1189. https://doi.org/10.1039/C39910001188.

(64) Melnikov, D.; Stytsenko, V.; Saveleva, E.; Kotelev, M.; Lyubimenko, V.; Ivanov, E.; Glotov, A.; Vinokurov, V. Selective Hydrogenation of Acetylene over Pd-Mn/Al2O3 Catalysts. *Catalysts* **2020**, *10* (6). https://doi.org/10.3390/catal10060624.

(65) Nolten, H. Master Thesis: Synthesis , Characterization and Testing of Supported Bimetallic CuPd Catalysts for Selective Hydrogenation of 1,3-Butadiene. **2022**.

(66) Kim, S. K.; Lee, J. H.; Ahn, I. Y.; Kim, W. J.; Moon, S. H. Performance of Cu-Promoted Pd Catalysts Prepared by Adding Cu Using a Surface Redox Method in Acetylene Hydrogenation. *Appl. Catal. A Gen.* **2011**, *401* (1–2), 12–19. https://doi.org/10.1016/J.APCATA.2011.04.048.

(67) Leviness, S.; Nair, V.; Weiss, A. H.; Schay, Z.; Guczi, L. Acetylene Hydrogenation Selectivity Control on PdCu/Al2O3 Catalysts. *J. Mol. Catal.* **1984**, *25* (1–3), 131–140. https://doi.org/10.1016/0304-5102(84)80037-1.

(68) Yuan, D.; Cai, L.; Xie, T.; Liao, H.; Hu, W. Selective Hydrogenation of Acetylene on Cu-Pd Intermetallic Compounds and Pd Atoms Substituted Cu(111) Surfaces. *Phys. Chem. Chem. Phys* **2021**, *23*, 8653. https://doi.org/10.1039/d0cp05285j.

(69) Sarkany, A.; Zsoldos, Z.; Furlong, B.; Hightower, J. W.; Guczi, L. Hydrogenation of 1-Butene and 1,3-Butadiene Mixtures over Pd/ZnO Catalysts. *J. Catal.* **1993**, *141* (2), 566–582. https://doi.org/10.1006/JCAT.1993.1164.

(70) Praserthdam, P.; Ngamsom, B.; Bogdanchikova, N.; Phatanasri, S.; Pramotthana, M. Effect of the Pretreatment with Oxygen and/or Oxygen-Containing Compounds on the Catalytic Performance of Pd-Ag/Al2O3 for Acetylene Hydrogenation. *Appl. Catal. A Gen.* **2002**, *230* (1–2), 41–51. https://doi.org/10.1016/S0926-860X(01)00993-0.

(71) Zugic, B.; Wang, L.; Heine, C.; Zakharov, D. N.; Lechner, B. A. J.; Stach, E. A.; Biener, J.; Salmeron, M.;

Madix, R. J.; Friend, C. M. Dynamic Restructuring Drives Catalytic Activity on Nanoporous Gold-Silver Alloy Catalysts. *Nat. Mater.* **2017**, *16* (5), 558–564. https://doi.org/10.1038/nmat4824.

(72) Palladium, Silver, Copper, Zinc, Potassium, Manganese compound summary https://pubchem.ncbi.nlm.nih.gov/compound/ (accessed Dec 17, 2022).

(73) Gas constant https://www.chemeurope.com/en/encyclopedia/Gas_constant.html (accessed Feb 1, 2023).

(74) Patterson, A. L. The Scherrer Formula for X-Ray Particle Size Determination. *Phys. Rev.* **1939**, *56* (10), 978–982. https://doi.org/10.1103/PhysRev.56.978.

(75) Ali, A.; Chiang, Y. W.; Santos, R. M. X-Ray Diffraction Techniques for Mineral Characterization: A Review for Engineers of the Fundamentals, Applications, and Research Directions. *Minerals* **2022**, *12* (2). https://doi.org/10.3390/min12020205.

(76) Bergeret, G.; Gallezot, P. Characterization of Solid Catalysts: Sections 3.1.2. In *Handbook of Heterogeneous Catalysis*; Wiley-VCH Verlag GmbH: Weinheim, Germany, 2008; Vol. 1–5, pp 427–582. https://doi.org/10.1002/9783527619474.ch3a.

(77) Udupa, M. R. Thermal Decomposition of Potassium Nitrate in the Presence of Chromium(III) Oxide. *Thermochim. Acta* **1976**, *6* (16), 231–235.

(78) Wu, C. Y.; Chen, Y. C.; Wang, T. H.; Lin, C. I.; Huang, C. W.; Zhou, S. R. Effect of Fe-Based Organic Metal Framework on the Thermal Decomposition of Potassium Nitrate and Its Application to the Composite Solid Propellants. *Combust. Flame* **2021**, *232*, 111556. https://doi.org/10.1016/J.COMBUSTFLAME.2021.111556.

(79) Ravanbod, M.; Hamid; Pouretedal, R. Catalytic Effect of Fe2O3, Mn2O3 and TiO2 Nanoparticles on Thermal Decomposition of Potassium Nitrate. https://doi.org/10.1007/s10973-015-5167-y.

(80) Gotoh, Y.; Tamada, K.; Akuzawa, N.; Fujishige, M. Journal of Physics and Chemistry of Solids Preparation of Air-Stable and Highly Conductive Potassium-Intercalated Graphite Sheet. **2013**, *74*, 1482–1486.

(81) BESENHARD, J. 0. THE ELECTROCHEMICAL PREPARATION AND PROPERTIES OF IONIC ALKALI METAL- AND NR , GRAPHITE INTERCALATION COMPOUNDS IN ORGANIC ELECTROLYTES. *Carbon N. Y.* **1976**, *14* (1), 111–115.

(82) Fedorov, A. V.; Kukushkin, R. G.; Yeletsky, P. M.; Bulavchenko, O. A.; Chesalov, Y. A.; Yakovlev, V. A. Temperature-Programmed Reduction of Model CuO, NiO and Mixed CuO–NiO Catalysts with Hydrogen. *J. Alloys Compd.* **2020**, *844*, 156135. https://doi.org/10.1016/j.jallcom.2020.156135.

(83) A. Louis Allred. Electronegativity Values from Thermochemical Data. *J. Inorg. Nucl. Chem.* **1961**, *17* (1949), 215–221.

(84) Wang, X.; Liang, X.; Geng, P.; Li, Q. Recent Advances in Selective Hydrogenation of Cinnamaldehyde over Supported Metal-Based Catalysts. *ACS Catal.* **2020**, *10* (4), 2395–2412. https://doi.org/10.1021/acscatal.9b05031.

11.2 List of Abbreviations

Abbreviation	Definition
(S)TEM	(Scanning) Transmission Electron Microscopy
(Δ)EN	(Difference in) Electronegativity
(Δ)r_{vdw}	(Difference in) Van der Waals radius
1-but	1-butene
Butadiene / bd	1,3-butadiene
A_{TPR}	Temperature-Programmed Reduction peak area
BCC	Body-centered cubic
BET	Brunauer–Emmett–Teller
DFT	Density Functional Theory
d_{SA}	The surface averaged particle size
d_{XRD}	The Scherrer calculated particle size
E_a	Activation energy
EDX	Energy Dispersive X-ray spectroscopy
FCC	Face-centered cubic
FWHM	Full Width at Half Maximum
GC	Gas chromatograph
GHSV	Gas Hourly Space Velocity
GNP	Graphene Nanoplatelets
HAADF	High Angle Annular Dark Field
HCP	Hexagonal close packed
IWI	Incipient Wetness Impregnation
m/z ratio	Mass-to-charge ratio
Milli-Q	(Deionized) ultra-pure water
M_M	Molecular weight of a metal
N_a	Avogadro's number
$N_{monolayer}$	Number of monolayers
O PT	Oxidation Pre-treatment
OR PT	Oxidation-reduction Pre-treatment
oxGNP	oxidized Graphene Nanoplatelets
PdC_x	Pd carbides
PdH_x	Pd hydrides
Pr	promoter
PT	Pre-treatment
R PT	Reduction Pre-treatment
r_M	Calculated (van der Waals) Radius of a metal
ROR PT	Reduction-oxidation-reduction Pre-treatment
$S_{iso,p}$	Selectivity of a product p in a isomerisation test
S_p	Selectivity of a product p
STP	Standard Temperature of 273.15 K and Pressure of 1 bar
T	Temperature
TEM	Transmission Electron Microscopy
TGA-MS	Thermo Gravimetric Analysis – Mass Spectrometry
T_{HT}	The heat treatment temperature
TOF	Turnover Frequency
TPR	Temperature-Programmed Reduction

T_{red}	The reduction temperature
wt.%	Weight percentage
XRD	X-ray Diffraction
β	Line broadening
λ	Wavelength
ρ_M	Density of a metal
σ_{SA}	The surface averaged standard deviation

11.3 List of Figures

11.4 List of Tables

11.5 List of Equations